CESPU
INSTITUTO UNIVERSITÁRIO
DE CIÊNCIAS DA SAÚDE

Wear behavior of materials for standard and anatomical condyles on temporomandibular joint total joint replacement.

Henrique André Oliveira Tavares Pinto Borges

Tese conducente ao **Grau de Doutor** em **Ciências Biomédicas**

Gandra, maio 2023

CESPU
INSTITUTO UNIVERSITÁRIO
DE CIÊNCIAS DA SAÚDE

Henrique André Oliveira Tavares Pinto Borges

Tese conducente ao **Grau de Doutor** em **Ciências Biomédicas**

Wear behaviour of materials for standard and anatomical condyles on temporomandibular joint total joint replacement

Trabalho realizado sob a Orientação de

Professor Doutor Júlio C. M. Souza e Co-orientação do Professor Doutor António M. A. Ramos

Declaração de Integridade

Eu, **Henrique André Oliveira Tavares Pinto Borges**, declaro ter atuado com absoluta integridade na elaboração deste trabalho, confirmo que em todo o trabalho conducente à sua elaboração não recorri a qualquer forma de falsificação de resultados ou à prática de plágio (ato pelo qual um indivíduo, mesmo por omissão, assume a autoria do trabalho intelectual pertencente a outrem, na sua totalidade ou em partes dele). Mais declaro que todas as frases que retirei de trabalhos anteriores pertencentes a outros autores foram referenciadas ou redigidas com novas palavras, tendo neste caso colocado a citação da fonte bibliográfica.

CESPU
INSTITUTO UNIVERSITÁRIO
DE CIÊNCIAS DA SAÚDE

Acknowledgements

I would like to take this opportunity to thank my advisor **Professor Júlio Souza** for giving me the opportunity to pursue my doctoral thesis at CESPU, giving his valuable suggestions and fruitful discussions throughout my thesis work. I cannot forget to recognize that his involvement with other research groups was essential for the accomplishment of this project.

I would also like to thank specially to my co-advisor from the Department of Mechanic Engineering in Aveiro, **Antonio Ramos** for his enthusiasm and expertise in prosthetic devices.

A special thank you to **Professor Filipe Samuel** from the Department of Mechanical engineering (UMinho) who enlighted me since the beginning of my work. **Professor José Gomes** for his valuable suggestions and giving permission for running some experiments at the tribo-lab in Guimarães (UMinho). Researcher engineer **Oscar Carvalho** for all his support and involvement in order to produce several components for my work. **Professor Bruno Henriques** (USFC) who helped me with mathematical issues. **João Pinto** (UMinho) for his collaboration and involvement in the finite element simulations. I would like to also express my deepest appreciation to **Sérgio Carvalho** (UMinho) who was a very important person during the tribological assays of this project. **Elsa Ribeiro** (3B´s) for her collaboration in the experimental work related do SEM/EDS analysis and great sense of humor. **Miguel Abreu** (UMinho) for his collaboration in the experimental work related to chemical solutions. My great friend **Felipe Duarte** (CESPU) , I am grateful for all your teachings and guidance since the beginning of my profession. In the difficult moments you were the one who strongly encouraged me to accomplish my goals. **Álvaro Gonçalves** , for the many afternoons we spent working in many of my academic presentations. To my **parents**, for all your guidance, patience and love. I dedicate this doctoral thesis to my beloved wife and dear children, who have been my source of happiness throughout my life . **Joana**, **Luisa and Henrique**. I would never done it without you.

Scientific publications by the PhD candidate

1. Article published in RevSALUS (RACS): Pinto-Borges, H., Carvalho, Óscar, Henriques, B., Silva, F., Ramos, A., & Souza, J. (2021). Desgaste das próteses da articulação temporomandibular: uma revisão narrativa. RevSALUS - Revista Científica Internacional Da Rede Académica Das Ciências Da Saúde Da Lusofonia, 3(1), 61–68. https://doi.org/10.51126/revsalus.v3i1.38

2. Article published in Metals (MDPI, Q1): Pinto-Borges, H., Carvalho, O., Henriques, B., Silva, F., Ramos, A., & Souza, J. C. M. (2021). A Preliminary Analysis of the Wear Pathways of Sliding Contacts on Temporomandibular Joint Total Joint Replacement Prostheses. Metals, 11(5), 685. https://doi.org/10.3390/met11050685

3. Article published in Tribology International (Elsevier, Q1): Pinto-Borges, H., Carvalho, O., Gomes, J., Henriques, B., Silva, F., Ramos, A., & Souza, J. C. M. (2022). Stresses, friction and wear on different materials and design for temporomandibular joint total joint replacement (TMJ TJR). Tribology International,178 (2023) 108051, https://doi.org/10.1016/j.triboint.2022.108051

.

CESPU INSTITUTO UNIVERSITÁRIO DE CIÊNCIAS DA SAÚDE

Index

Index of Figures

Index of tables

Index of abbreviation

ALTR Allergic local tissue reaction

ANSYS Analysis of systems

ASTM American Society for Testing and Materials

CAD-CAM Computer aided design and Computer aided manufacturing

CAM Cell adhesion molecules

CATIA Computer Aided Three-Dimensional Interactive Application

CD44 Cluster of differentiation 44

CoCrMo Cobalt-Chromium-Molybdenum

COF Coefficient of friction

Cp Commercially pure

DICOM Digital Imaging and Communications in Medicine

DLC Diamond-like carbon

EDS Energy dispersive spectroscopy

FDA Food and Drug Administration

FEA Finite element analysis

FEG/SEM Field Emission Guns Scanning Electron Microscope

FEM Finite element modeling

GPa Giga pascal

HXLPE Highly cross-linked polyethylene

ICAM 1 Intercellular Adhesion Molecule 1

LPTM Lateral pterygoid muscle

MPa Mega pascal

PBS Phosphate buffered saline

PMMA Polymethylmethacrylate

ROS Reactive oxygen species

SEM Scanning electron microscope

Ti6Al4V Titanium-aluminium-vanadium

TiN Titanium nitride

TJR Total joint replacement

TMD Temporomandibular disorder

TMJ Temporomandibular Joint

TMJ TJR Temporomandibular joint total joint replacement

TMJR Temporomandibular joint replacement.

TNF Tumour necrosis factor

UHMWPE Ultra-highly molecular weight polyethylene

Resumo

Recentemente vários materiais e designs biomédicos foram avaliados na tentativa de melhorar o desempenho mecânico das próteses de substituição total da articulação temporomandibular. No entanto, o desgaste do côndilo ocorre com o movimento de carga com deslizamento contra o componente da fossa, à base de polímero, levando à perda de material e libertação de detritos. O objetivo deste estudo foi avaliar o coeficiente de atrito, volume de desgaste, danos de superfície e biomecânica em relação a diferentes materiais e design de côndilos para substituição total da articulação temporomandibular aloplástica. A pesquisa bibliográfica foi realizada nas bases de dados: MEDLINE/PubMed (via National Library of Medicine) e ScienceDirect (Elsevier). Foram utilizados os termos: " prótese de articulação temporomandibular," OR "implante articulação temporomandibular" OR " "prótese de ATM" OR "implante ATM" OR "ATM alloplástica" OR "substituição ATM" OR "CoCr" AND "desgaste" OR "fricção " OR "dano de superfície" OR "detritos" OR "toxicidade". O estudo foi realizado em dois grupos de côndilos metálicos com materiais e designs diferentes, anatómicos e esféricos. Os côndilos foram preparados a partir de ligas de CoCrMo ou Ti6Al4V que foram testadas contra um polietileno de ultra-densidade molecular (UHMWPE). Testes de deslizamento recíproco foram realizados considerando o movimento da prótese; carga de 30 N, 1 Hz, deslizamento de 4 mm, durante 60 min em solução de Ringer a 37º C. As superfícies foram inspecionadas por microscopia eletrónica acoplada à espectroscopia dispersiva de energia. As tensões de Von Mises foram calculadas através de simulação 3D de elementos finitos, realizada em relação ao eixo central da prótese. Foram encontrados 165 estudos no PubMed e 3912 no ScienceDirect, sendo que 48 estudos foram selecionados para um estudo de revisão. Estudos prévios revelaram que o atrito destes dispositivos promoveu a libertação de detritos de desgaste, como partículas e iões. Os processos de desgaste dependeram dos materiais, design e estabilidade da prótese. Consequentemente, os detritos tóxicos levaram ao recrutamento de linfócitos e macrófagos, induzindo a morte celular. No presente estudo, foram registados valores médios de coeficiente de atrito variando entre 0,06 e 0,08. Relativamente ao efeito do design, os valores médios de taxa específica de desgaste das superfícies de UHMWPE foram superiores contra côndilos esféricos (5,53 x10^{-4} mm^3/Nm para CoCrMo e 4,54 x10^{-4} mm^3/Nm para Ti6Al4V). Imagens microscópicas da região central das pistas de desgaste no polietileno, revelaram deformação plástica e a existência de tribocamadas. Os valores de Von Mise encontrados nos côndilos anatómicos de CoCrMo, em torno de 25 MPa, foram menores quando comparados aos côndilos esféricos tanto para CoCrMo quanto para Ti6A4lV, aproximadamente 35 MPa e 30 MPa, respetivamente. Achados experimentais mostraram um baixo desgaste do Ti6Al4V contra superfícies de polietileno, embora a perda de volume registada para as superfícies de polietileno tenha sido menor para o côndilo anatómico. Os danos causados pela carga friccional cíclica e partículas abrasivas foram mais prejudiciais para as superfícies de CoCrMo/UHMWPE quando comparadas com o par Ti6Al4V/UHMWPE. O côndilo de formato anatómico diminuiu as tensões nas superfícies de contacto, portanto, a degradação e a perda de material foram diminuídas.

Palavras-chave: articulação temporomandibular, prótese de ATM, atrito, desgaste, biotribologia.

Abstract:

Recently several biomedical materials and designs have been assessed in attempt to improve the mechanical performance of temporomandibular joint total joint replacement (TMJ TJR) prostheses. Nevertheless, the wear of the TMJ TJR condyle occurs with sliding motion against the polymer-based fossa component during loading, leading to material loss and the release of debris. The purpose of the present study was to evaluate the coefficient of friction (COF), wear volume, surface damage, and biomechanics regarding different materials and condyle design for alloplastic temporomandibular joint total joint replacement (TMJ TJR). A search was carried out using electronic databases: MEDLINE/PubMed (via National Library of Medicine) and ScienceDirect (Elsevier). The following terms were used: "temporomandibular joint prosthesis" OR "temporomandibular joint implants" OR " "TMJ prosthesis" OR "TMJ implant" OR "alloplastic TMJ" OR “TMJR” OR “CoCr” AND “wear” OR “friction” OR “surface damage” OR “debris” OR “toxicity”. The experiment was performed regarding two groups of metallic condyle materials and two different designs, namely anatomical and spherical. Condyle specimens were prepared from CoCrMo or Ti6Al4V alloys which were assessed against ultra-highly molecular weight polyethylene (UHMWPE) samples. Reciprocating sliding tests were performed considering usual TMJ TJR joint motion; 30 N loading, 1 Hz and stroke length of 4 mm for 60 min in Ringer’s solution at 37^{o} C. Worn surfaces were inspected by scanning electron microscopy (SEM) coupled to energy dispersive spectroscopy. Von Mises stresses were calculated using a 3D finite element model (FEM) simulation performed relatively to the central axis of the TMJ TJR assembly. The search strategy yielded 165 studies on PubMed and 3912 on ScienceDirect although 48 studies were selected for a review study. Previous studies revealed that friction in TMJ TJR promoted the release of wear debris at nano and micro-scale size such as particles and ions. Friction and wear processes were dependent on the materials, design, and the stability of the TMJ TJR. As a consequence toxic debris lead to tissue reactions carried out by fibroblasts, lymphocytes, and macrophages inducing cell death. On the present study, COF mean values were recorded ranging between 0.06 and 0.08. Regarding design effect, the mean values of specific wear rate of UHMWPE surfaces were higher against spherical specimens (5.53 x10^{-4} mm^3/Nm for CoCrMo and 4.54 x10^{-4} mm^3/Nm for Ti6Al4V). SEM images of the middle region of the wear tracks on

UHMWPE revealed plastic deformation and the existence of tribolayers. The Von Mises stress values found on anatomical condyles of CoCrMo at around 25 MPa were lower when compared with the spherical-shape condyles either for CoCrMo or Ti6A4lV, approximately 35 MPa and 30 MPa, respectively. Experimental findings showed a low wear on Ti6Al4V against UHMWPE surfaces although the volume loss recorded for the UHMWPE surfaces was lower for the anatomical condyle. The damage caused by cyclic frictional loading and abrasive particles were more detrimental to the CoCrMo/UHMWPE bearing surfaces when compared with the UHMWPE/Ti6Al4V pair. The anatomical-shape condyle decreased the stresses on the bearing surfaces and therefore the degradation and loss of material was decreased.

Key words: temporomandibular joint, TMJ TJR, friction, wear, biotribology

CESPU
INSTITUTO UNIVERSITÁRIO
DE CIÊNCIAS DA SAÚDE

Introduction

The human temporomandibular joint (TMJ) is a diarthrodial system of the mandible to the temporal bone that produces sliding-hinge movements that provides the essential human functions of mastication, speech, airway support, and deglutition [1–3]. Temporomandibular joint disorders (TMD) involve muscular pain, opening mouth limitations, migraines, and bruxism that affect around 25% of the world population. In the treatment of TMD, surgical procedures of temporomandibular joint are seen as a last resort for some end-stage problems. Thus, surgical procedures for TMJ total joint replacement (TJR) are recommended for only 2-5% of TMD issues that still corresponds to a large number of patients with TMJ TJR [4,5].

On the manufacturing of TMJ devices, titanium alloys are used to promote osseointegration in the mandible ramus and articular fossa. Cobalt-Chromium (CoCr)-based alloys are used to replace the condyle that is placed in contact with a prosthetic articular fossa composed of a polymeric material such as ultra-high-molecular-weight polyethylene (UHMWPE) [4,6]. One major mechanical issue of TMJ TJR is the mismatch in physical properties (i.e., elastic modulus) of the prosthetic materials and surrounding bone structures [7,8], that can determine the stress distribution through the TMJ TJR materials towards the supporting bone [9,10]. A mechanical instability of TMJ TJR can provide a high stress concentration on materials and bone, leading to an increased wear of the bearing surfaces [11,12]. On the sliding of the TMJ TJR condyle onto the synthetic polymeric fossa, a two-body abrasion takes place on the tribological pair (i.e., CoCrMo versus UHMWPE) [6,13]. The abrasion results in the plastic deformation of the contacting surfaces depending on the normal (axial) loading magnitude and roughness (micro/nano-scale peaks dimensions) of the components [3,14,15]. Then, a rupture of intermolecular bonds take place followed by a subsurface damage caused by the movement of surface molecules under cyclic loads [16,17]. Micro-cracks and removal of material such as particles and ions occurs in the wear track leading to the release of micro- and nano-scale debris to the surrounding tissues [16–19]. Degradation debris at micro- and nano-scale dimensions do affect the cells of the surrounding tissues such as fibroblasts, mesenchymal cells, osteoblasts, lymphocytes, and macrophages. As a result, the inflammatory reaction can occur with cytokine production, cell apoptosis, and activation of osteoclasts [7,8].

The present PhD project was structured from a methodical search and selection of studies followed by an evaluation of relevant previous findings. An experimental study was designed considering the lack of outcomes on the friction and wear processes on different materials and design for TMJ TJR. The current PhD thesis is divided in five chapters as follow: **Chapter 1** deals with a literature review on the temporomandibular joint (TMJ) and related disorders (TMD), TMJ TJR, materials, biomechanics, degradation pathways, and adverse biological effects of debris. Materials and Methods is described in **Chapter 2** that starts with a systematic search and selection of studies published in literature. The preparation of condyle specimens was carried out from CoCrMo or Ti6Al4V alloys while the fossa component was manufactured from UHMWPE. The mean values of COF and wear volume were recorded on reciprocating wear sliding tests. Then, surfaces were inspected by scanning electron microscopy (SEM) coupled to energy dispersive spectroscopy (EDS). Also, the following physicochemical assays were performed: Dynamic Mechanical Analysis (DMA); nanoindentation, and Fourier transform infrared (FTIR) spectroscopy. At last, stresses on the condyle to the UHMPE was evaluated by using the finite element method (FEM). **Chapter 3** focuses on the description and discussion of results from the experimental study. Results were discussed and compared with the findings reported in literature. At last, **Chapter 4** deals with the main outcomes of the present PhD thesis while **Chapter 5** provides suggestions for future work.

Regarding the review and experimental study, four articles were prepared and submitted in indexed scientific international journals. In 2021, a narrative review entitled “Wear of temporomandibular joint prostheses” was published in RevSALUS (Ed. RACS) and then another review entitled “A Preliminary Analysis of the Wear Pathways of Sliding Contacts on Temporomandibular Joint Total Joint Replacement Prostheses” was published in Metals (Ed. MDPI). At last, the main original study entitled “Stresses, friction, and wear on different materials and design for temporomandibular joint total joint replacement (TMJ TJR” has been accepted for publication in Tribology International (Ed. Elsevier) in 2022.

Objectives

The **main goal** of the present PhD project was to evaluate the coefficient of friction, wear volume, surface damage, and biomechanics regarding different materials and condyle design for TMJ TJR prostheses.

Considering the differences in design, a **first hypothesis** was that an anatomical-shaped condyle can decrease the friction loading and wear volume of bearing surfaces in TMJ TJR. A **second hypothesis** was that CoCrMo and titanium alloys reveal different coefficient of friction and wear behavior on sliding against UHMWPE surfaces.

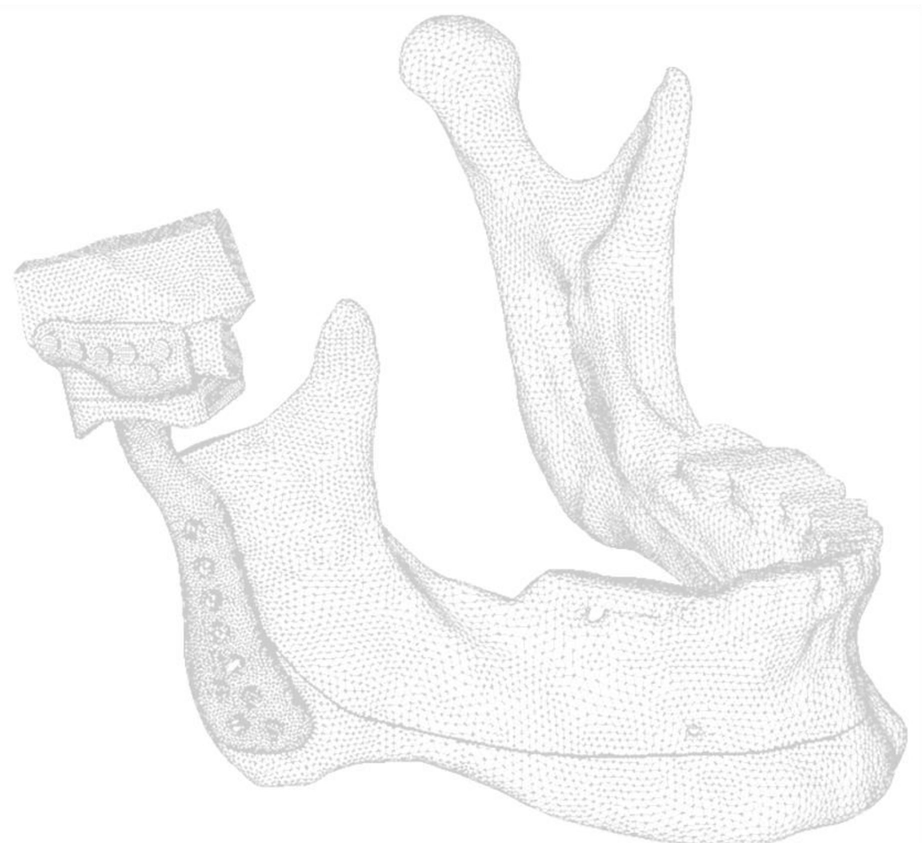

Chapter 1
Literature Review

1. Literature Review

1.1. Temporomandibular joint and related disorders

The human synovial temporomandibular joint (TMJ) has a unique capability of sliding on a hinge joint that allows movements in various vector planes involved in essential human actions such as speaking, chewing, airway support, and swallowing [20,21]. TMJ comprises the mandible condyle, fibrous articular disc, and temporal bone fossa (Figure 1). The mandibular condyle fits into the temporal bone mandibular fossa. TMJ physiologic actions occur due to the rotation motion of the condyle over the articular disc and the translation of the disc-condyle complex along the articular eminence, as seen in Figure 1 [22–24]. Mandibular rotation occurs on the inferior side of the disc, and mandibular translation occurs at the superior disc surface [24,25]. The articular disc and cartilage are adhered over the bony surfaces in the TMJ allowing for the dissipations of shearing, normal, and frictional loads generated by the functional jaw, promoting tissue remodelling [30,33]. However, high concentration of loading and therefore stresses can occur on the articular disc being transferred to the surrounding cartilage and bone structures [26]. The average of the elastic modulus in the TMJ bone structures are recorded at 25–30 GPa, while the elastic modulus of the mandibular condylar cartilage is around 5–12 GPa [26–28]. In fact, the TMJ complex is habitually under cyclic loading, more than any other joint in the body throughout life since the mouth movements of opening and closing can occur up to 2000 times per day [29]. Essential human actions such as speaking, chewing, airway support, and swallowing are supported by the shape and functioning of the TMJ.

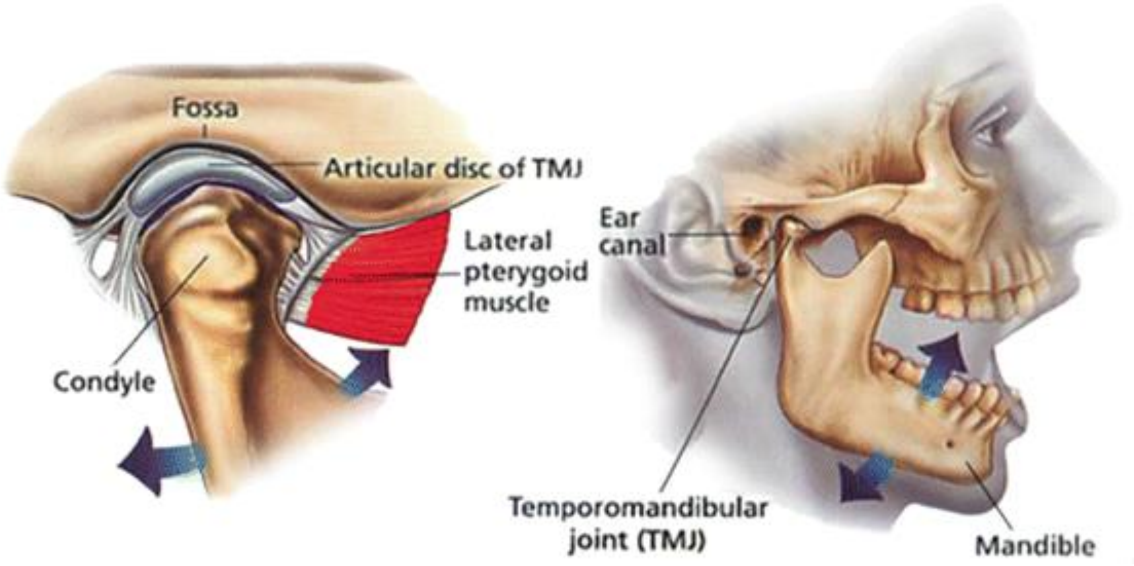

Figure 1- Schematics of the human temporomandibular joint (TMJ). Adapted from [30].

Temporomandibular disorder (TMD) is the second most common chronic musculoskeletal issue after chronic low back pain, resulting in pain and disability [31,32]. Such group of disorders muscular pain, opening mouth limitations, migraines, and sleeping issues. That can negatively affect individual's daily activities, psychosocial functioning, and quality of life [33]. Overall, the annual TMD management costs in the USA (not including imaging) has doubled to $4 billion in the last decade [31,34]. Around 25% world population is affected by some degree of TMD, although surgical procedures are recommended in only 2-5% of TMD cases [35–37]. In the USA, approximately 1 million people per year are diagnosed with a TMD but only around 3000 patients need surgical replacement of the temporomandibular joint (TMJ TJR). [3,5,38].

TMD encompasses a wide variety of clinical conditions on pain and dysfunction of the temporomandibular regions. Nowadays, the Diagnostic Criteria for Temporomandibular Disorders (DC/TMD) is widely accepted for assessment and classification of TMD [31]. According to such recent evaluation protocol, the aetiologic factors for TMD are multifactorial and can be attributed to both physical and psychosocial factors [39]. Regarding physical factors, TMD can be divided into articular disorders, and the more common (85%-90%) non articular or disorders [39,40]. Several studies reported that TMD symptoms of arthrogenous origin may be related to internal derangement of the TMJ, which can be defined as a mechanical issues of the physiologic TMJ movements [41–43]. Other causes of TMD can be unilateral posterior crossbite [44], habitual body posture during sleep that allows the ipsilateral condyle to displace posteriorly that causes anterior disc displacement [45]. TMJ adaptability to mechanical demands may be affected by age, gender, and traumatic injury [46]. A high predilection for the TMD symptoms in women compared with men has been reported in literature. Also, TMD symptoms has been often reported during the female childbearing years. Thus, studies suggested that the female sex hormones may have a role in the pathogenesis of the TMJ disorders [46]. Sex hormones are known to influence the differentiation, growth, development, and metabolism of connective tissues. A previous study reported that sex hormones affect the extracellular matrix of the TMJ disc of female and male rats [47]. Unfortunately, it is not clear yet whether the female sex hormones or the estrogen receptors are responsible for the TMD gender paradox [48].

When the TMJ functioning affects their friction free and smooth movements, a disruption of the internal aspect takes place, usually preceding disc displacement over the articular surfaces. Previous studies suggested that internal derangement precedes degenerative joint diseases, namely osteoarthritis [6,39,41,42]. High loading concentration can promote the damage of cells and tissues over functional or parafunctional movements of the jaw such as clenching or bruxism [49–51] [49,52]. The damage of extracellular and cell molecules induces the immune response leading to continuous inflammatory reactions [49]. The severity of internal derangement has been classified by Wilkes into five stages regarding the pain, mouth opening, disc location, and anatomy [53]. The Wilkes' classification (***Table 1***) ranges from painless clicking of the joint (Stage I) up to severe pain of the joint with severe degenerative bone changes (Stage V), as seen in Table 1. Wilkes' classification has served as an aid to guide treatment options in the management of arthrogenous TMD [39].

Table 1- Wilkes' staging classification of internal derangement of TMJ considering clinical, radiologic, and surgical findings. Adapted from [53].

TMD degree	Signals and symptoms
I. Early stage	Clinical: No significant mechanical symptoms other than opening reciprocal clicking; no pain or limitation of motion Radiological: Slight forward displacement; good anatomic contour of the disc; negative tomograms Anatomic pathology: Excellent anatomic form; slight anterior displacement; passive in-coordination demonstrable
II. Early intermediate stage	Clinical: One or more episodes of pain; beginning major mechanical problems consisting of mid-to-late opening loud clicking; transient catching, and locking Radiological: Slight forward displacement; beginning disc deformity of slight thickening of posterior edge; negative tomograms Anatomic pathology: Anterior disc displacement; early anatomic disc deformity; good central articulating area.
III. Intermediate stage	Clinical: Multiple episodes of pain; major mechanical symptoms consisting of locking (intermittent or fully closed); restriction of motion; difficulty with function Radiological: Anterior disc displacement with significant deformity or prolapse of disc (increase thickening of posterior edge); negative tomograms Anatomic pathology: Marked anatomic disc deformity with anterior displacement; no hard tissue changes
IV. Late intermediate stage	Clinical: Slight increase in severity over intermediate stage. Radiological: increase in severity over intermediate stage; positive tomograms showing early-to-moderate degenerative changes—flattening of eminence, deformed condylar head, sclerosis Anatomic pathology: Increase in severity over intermediate stage, hard tissue degenerative remodelling of both bearing surfaces (osteophytosis); multiple adhesions in anterior and posterior recesses; no perforation of disc or attachments
V. Last stage	Clinical**:** Characterized by crepitus; variable and episodic pain chronic restriction of motion and difficulty with function. Radiological: Disc or attachment perforation; filling defects; gross anatomic deformity of disc and hard tissues; positive tomograms with essentially degenerative arthritic changes. Anatomic pathology: Gross degenerative changes of disc and hard tissues; perforation of posterior attachment; multiple adhesions; osteophytosis; flattening of condyle and eminence; subcortical cyst formation

Most TMD cases can be improved applying non-invasive management options [6,54]. The initial management of TMD may include conservative options such as analgesics, non-steroidal anti-inflammatory drugs, anxiolytics, anti-depressants, and occlusal appliances [39]. Physiotherapeutic approaches have been suggested for management of TMD showing beneficial effects on various clinical issues in TMD [55,56]. For myogenous TMD, Botulin Toxin injection, acupuncture, and dry needling techniques have been suggested as an effective method to reduce stress in some patients [57–59]. Also shock wave therapy seems to provide positive outcomes for treatment of muscular disorders [60,61]. For arthrogenous issues which are not responsive to conservative treatment, procedures like articular injections, arthroscopy and arthrocentesis are indicated for debridement of damaged tissues (Figure 2) [62]. Also, different pharmacological agents for intra-articular injection have been proposed such as hyaluronic acid, corticosteroid, analgesics, platelet-rich plasma, and platelet-rich fibrin [63]. However, a combined therapeutical approach can be required considering the TMD degree of the patient [39].

Figure 2- Two needle arthrocentesis treatment. Adapted from [62].

Common causes for surgical procedures for TMJ TMJR are related to severe trauma or end-stage joint diseases such as ankylosis (Figure 3), degenerative diseases (i.e., osteoarthritis), tumours and congenital/developmental disorders [31,36,64]. A cone beam computed tomography image (CBCT) of a transarticular bone adhesion namely ankylosis of a TMJ is shown in Figure 3.

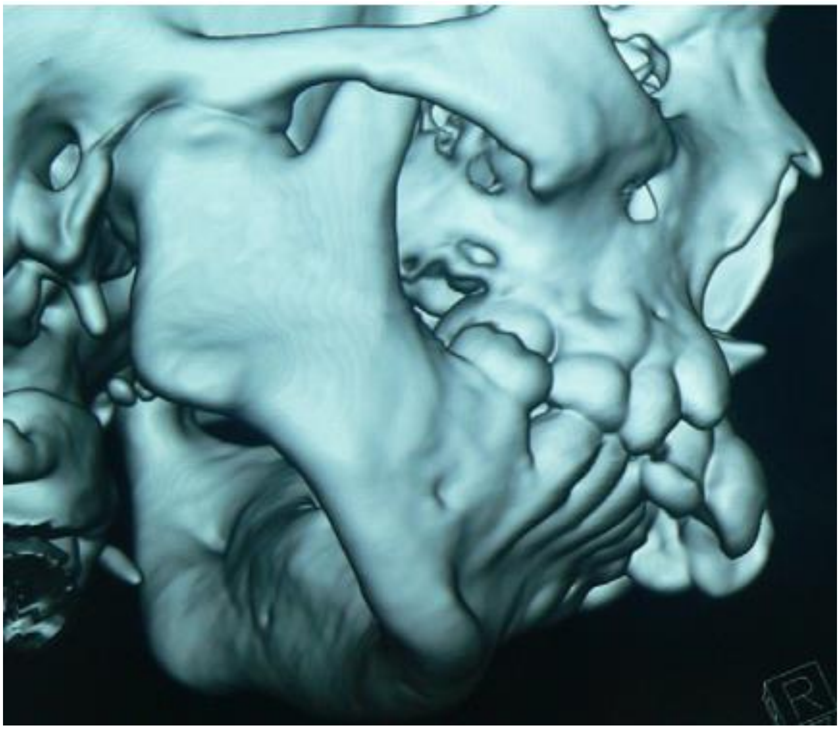

Figure 3- CBCT image on a transarticular bone adhesion (ankylosis). Adapted from [65].

1.2 Temporomandibular joint total replacement

The design process for medical devices is complex, requiring collaboration between experts in the engineering, medical, material domains and transfer of technologies and ideas throughout the manufacturing process [66,67]. Long term success of medical prostheses and devices depend not only on the design but also on the materials [68]. In 1960, Sir John Charnley reported the use of a total alloplastic prosthetic hip replacement system utilizing an ultra-high molecular weight polyethylene (UHMWPE) articulating with a stainless-steel femoral head component [6,69,70]. Modifications of such orthopaedic prosthesis device using titanium, titanium alloy and cobalt- chromium-molybdenum against the UHMWPE component, have become the first choice for achieving a low friction on orthopaedic TJR. The first total temporomandibular joint replacement (TMJ TJR) method was conceived in 1965 by Christensen and then other systems have been developed and currently applied [5,71].

Alloplastic TMJ reconstruction increased in popularity in the early 1980's due to the disadvantages in autogenous reconstruction involving longer surgery, high morbidity of the donor site, more time to heal, graft micromotion, delayed physical therapy, high relapse potential when combined with orthognathic surgery [72].

At that time, Vitek Inc. (Vitek, Houston, USA) received FDA approval for the use of their Proplast-Teflon™ within an interposition meniscus replacement after discectomy to maintain vertical dimension and prevent degenerative changes of the condyle [20,73]. Despite incomplete testing and warnings given by the supplier company that Teflon™ implants have a high degradation, 26,000 patients across North America were fitted with those implants (Figure 4) [70,74]. In the early 1990s, negative experiences with patients experiencing irreversible symptoms related to mechanical failure with the Vitek–Kent prosthesis brought discredit on all alloplastic TMJ replacements (Figure 4). In January 1991, the FDA ordered Vitek to recall the implants from the market [20,75]

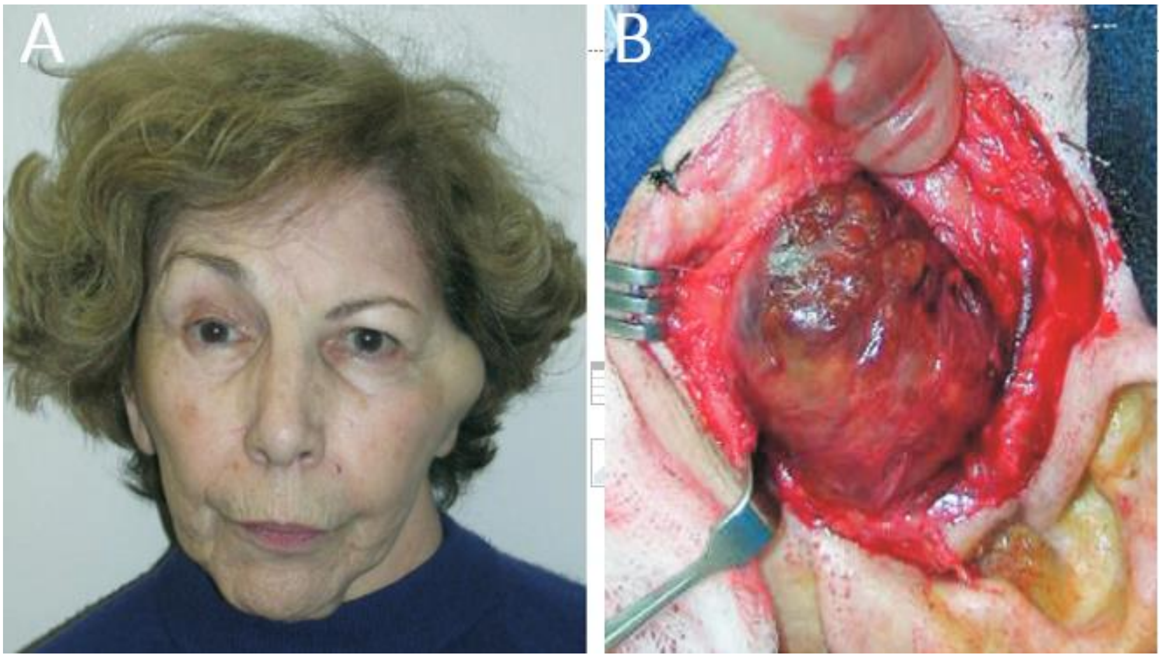

Figure 4 - Foreign Body Giant Cell Reaction to the Vitek-Kent interpositional implant. (**A**) External frontal view. (**B**) Intraoperative view. Adapted from [73]

In 1995, the TMT TJR system by Biomet was approved by the FDA for use in clinical trials. TMJ Concepts and NEXUS CMF products were also approved in 1999 and 2001, respectively. The TMJ TJR system was officially approved as a clinical device in 2005 in USA [75]. Currently, three TMJR TJR systems are approved by FDA as follow (***Fig. 5***): stock (off-the-shelf) and custom CAD/CAM, patient-matched version of the stock implant, available only in Europe (Zimmer Biomet, Warsaw, IN, USA); custom (patient-fitted) prosthesis (TMJ Concepts, Ventura, CA, USA); Christensen stock and custom prosthesis (TMJ implants Nexus CMF, Salt Lake City, UT, USA) [2,76–78].

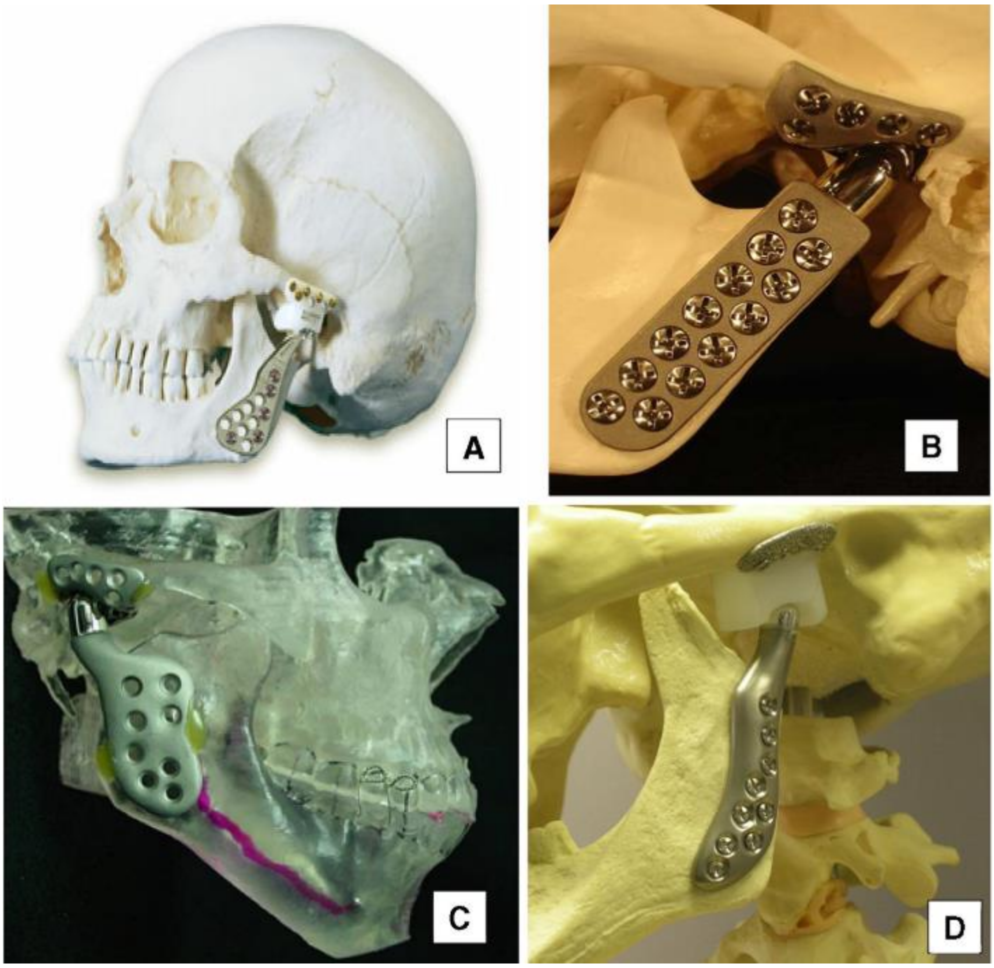

Figure 5 - Different TMJ TJRsystems. (**A)** Stock metal-on- polyethylene device (Biomet , USA); (**B)** Stock metal-on-metal device (Nexus CMF, USA); (**C**) Custom metal-on- metal device (Nexus CMF, USA); (**D)** Patient-fitted metal-on-polyethylene TMJ Concepts device (TMJ Concepts, USA). Adapted from [78]

Total stock TMJ TJR from Zimmer Biomet includes a mandibular component available in three different sizes (55, 50, and 45 mm) and a prosthetic articular fossa in different size (wide, medium, small) [79,80]. Zimmer Biomet^{TM} TMJ TJR have a CoCrMo alloy (ASTM type F799 or F1537) condyle coupled to the mandible ramus component composed of titanium grade V to promote the osseointegration process [81,82]. The fossa component consists of an ultra-high molecular density polyethylene (UHMWPE) component, without metallic support [6,13,81]). Both components are fixed using 2.0 mm self-tapping screws for the articular fossa and 2.7 mm for the mandibular component [81–83]. On standard components, the articular fossa and the mandibular ramus have to be fitted, or the prosthesis itself needs to be bent or shimmed in order to fit the implantation site [11,84,85]. Although the prosthetic articular fossa can be stabilized without the use of bone graft materials, anatomic features (i.e., deep articular fossa) can limit the fitting of the TMJ TJR prostheses [70,75,86]. Since all present stock devices do not have a posterior stop [70,87], the potential for posterior condyle dislocation can result in a perforation of the auditory canal resulting in pain malocclusion or infection . It should be of particular concern for orthognathic cases while setting the condyle into "centric" during mandibular procedures, and especially in combination with counter-clockwise mandibular rotation procedures [80,84]. The standard TMJ TJR systems usually involves a two-step protocol. On the first surgery, the ankylosed bone is removed to provide a suitable bone space for placing a spacer component. Within the second surgery, the spacer component is removed and the selected TMJ TJR prosthesis is placed [64,79,88]. In the treatment of very asymmetric patients with high mandibular angles, which the majority of patients with TMD, the placement of standard TMJ TJR prostheses becomes more challenging due to the limited choices of dimensions and design [12,88]. The benefits of standard TMJ TJR involve low cost and immediate availability [79,89,90]. Biomet/Lorenz (Zimmer Biomet, Germany) is one of the most used standard system with FDA approval [5,74,91]. In a previous clinical and radiological study of 33 patients, the VAS scale for Biomet stock prostheses between 2010 and 2016 improved for pain, diet, incisal opening, and quality of life before and after surgery of the patients [92]. Clinical studies published between 2005 and 2012 suggested a success rate of standard TMJ TJR ranging from 84 up to 91% [93].

The Christensen^{TM} prosthesis is a stock or custom [78] full metal-metal device made of cobalt chromium alloy (ASTM type F75), with a possible choice of 44 size for the temporal component, while the mandibular component is available in three sizes (55, 50, and 45 mm). The fixation is accomplished with three screws in the fossa and up to nine screws in the mandibular component [80,93]. That TMJ TJR system has not shown high failure rates in the short term [87] associated with different issues such as excessive wear, allergy to materials (i.e nickel, chromium), corrosion, chronic infection and systemic disease [80,94]. A comparative previous study reported differences between the Christensen™ and the TMJ concepts™ TMJ TJR system [95]. In another comparative in vitro study, the Zimmer Biomet™ system revealed improvements over the Christensen™ system regarding strain distribution and tensions in the opposite intact disc in unilateral cases [93].

Custom-made TMJ TJR are designed and developed according to the patient's anatomic features, requiring little or no changes on the surgical procedure [84,96]. The custom-made system had statistically significant improved outcomes compared with stock TMJ TJR systems relative to postsurgical incisal opening, pain, jaw function and diet. On custom-maded TMJ TJR, the condyle component is also composed of CoCrMo alloy while the ramus is composed of titanium alloy (e.g., Ti6Al4V). Both components are anchored using Ti6Al4V screws [6,13,71]. The length of the screws can be previously designed. The articular fossa component can consist of a commercially pure titanium (cp Ti) mesh or rough framework adhered to the UHMWPE fossa component which has a posterior stop to prevent dislocation. Additionally, Cp Ti mesh or rough framework allow the integration of bone and soft tissues [70,87]. One noteworthy benefit of custom-made TMJ TJR is related to the fitting leading to a decrease in micro-movements of components and promoting higher mechanical stability [25,97,98]. From a surgeons point of view, the use of custom-made device and virtual surgical planning reduce surgical time, and has advantages over the stock devices regarding the precision and predictability of the screws positioning, especially when jaw repositioning is required [76,89,90]. Although the long-term performance of custom-made TMJ TJR prostheses is undefined, a previous study reported a 20-year follow-up study of 56 patients (52 women and 4 men) with an average age at 38.6 $\pm$10 years who received custom-made TMJ TJR prostheses. According to the findings, there was an improvement in the function scores of incisal opening measurement, pain, and diet. None of the prostheses failed, that indicated a high long-term performance of those devices [64]. There are numerous published articles that validate the successful use of custom-made TMJ TJR prostheses with an indication of significant improvement in the incisal opening, mandibular function, and in pain levels. Thus, approximately 87% patients reported improvement in their quality of life [2,99–101].

1.3 Biomechanics of TMJ TJR

The process of designing a TMJ prothesis must take in consideration the natural features of the TMJ [24,102]. On functional movements, the mandibular condyle rotates relative to the articular disc, while the condyle-disc complex translates along the temporal eminence [22–24]. The physiologic translation movement of the TMJ was reported to be in the order of 16mm [103]. However, the translation capability of TMJ TJR is very reduced and usually it does not exceed 2 mm as a result of the design and the lacking attachment of the lateral pterygoid muscle (LPTM) to the condyle [68,103,104]. Previous studies showed that natural translation movement of the condyle can be mimicked by placing the rotation center 15 mm lower than the positioning of the condyle [103,105,106]. The rotation center can be moved vertically to correct the open bite deformity [105]. In this way, computational modelling and simulations by using the finite element method (FEM) become interestingly applied to predict the positioning and biomechanics of biomedical devices including TMJ TJR systems [25,107]. Simulation using FEM begins with the computer generation of a digital model. On modelling, the following software are usually reported in literature: CATIA V5^{TM} (Dassault Systèmes, Intrinsys, USA)[108] and SolidWorks^{TM} (Dassault Systèmes, Intrinsys, USA. The geometric models can also be acquired from CBCT images and then processing DICOM files into 3D models [4]. FEM software programs reported in previous studies were the following: MSC Marc (MSC Software) [2,12,109], ANSYS, CATIA V5[108], Abaqus (Dassault Systèmes) [87] and COMSOL Multiphysics (COMSOL Inc.) [110]. Before computational simulation, the properties of the materials, boundary conditions and loading must be defined in the model. The material properties of the device components can be established from previous in vitro studies [4,88,93,107]. The transferring of load transfer between condyle and fossa is one of the most important issues assessed on TMJ TJR by FEM [111]. Most FEM studies describe different computational parameters and therefore provide different outcomes [4]. However, there was agreement in the following issue: the implanted TMJR condyle-ramus components developed high mean stress and strain values at the posterior and lateral regions of the condyle neck and mandibular ramus. That accounted for instability and loosening of the device during vertical displacement [12,102,107,112]. The values for maximum stress in the posterior region of the condyle reported in studies are around 75MPa [12], 170 MPa [107], and 200MPa[102], while some studies have suggested that screws can become loose in posterior region [93]. In fact, stresses revealed lower magnitude on custom-made TMJ TJR condyles when compared to standard TMJ TJR ones [112]. In the physiologic TMJ, the higher stress values were reported at around 33 MPa [113] and were located in the posterior bottom of the condyle neck although did not reach the mechanical limit of human bone of the order of 130-190 MPa [114]. Regarding loading and screw fixation in the mandibular component, screws close to the condyle head revealed the highest strain values (Figure 6) [115–118].

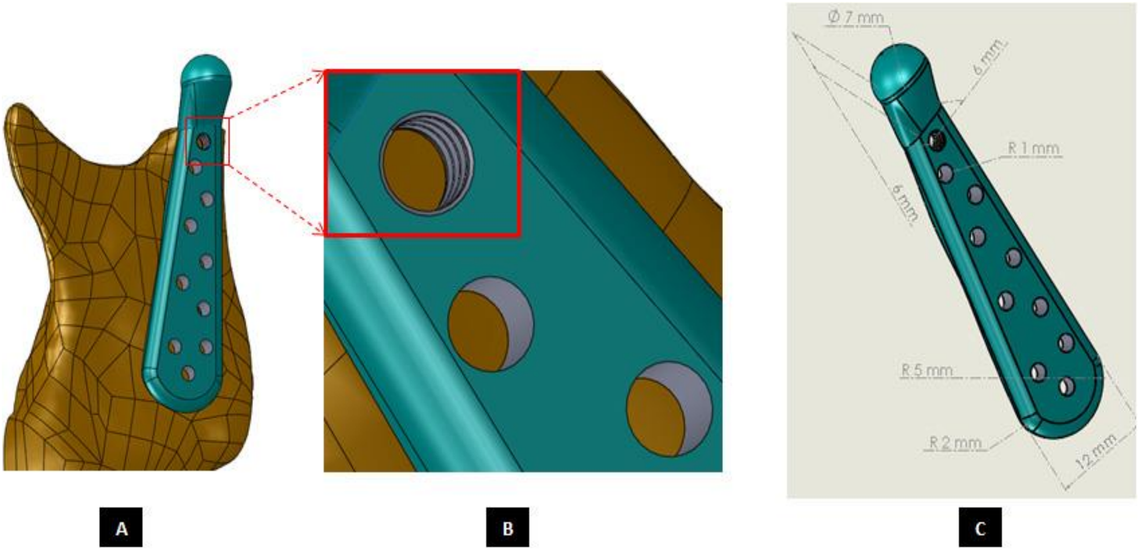

Figure 6- Schematics of the condylar/ramus component of the TMJ TJR system for left side. (**A**) Lateral view of the implant with screw holes. (**B**) Enlarged view of the screw holes, where the first superiorly located screw hole has threads to incorporate locking-plate-screw mechanism. (**C**) Image with engineering dimensions of a specific patient.

The mean values of von Mises stresses on the first fixation screws ranged from 11.8 to 236 MPa [107,119–121]. Regarding fixation, a minimum of three staggered screws has shown to be required for stable prosthetic condyle and adequate stress distribution in a TMJ TJR [87,109,120,122,123]. However evidence suggested that the positioning of the screws was more important than the number [12,120,124]. The parallel design of fixation screw positioning revealed smaller von Mises and shear stresses than a zigzag positioning design [119,120]. On the other hand, a previous study showed good results on the use of zig zag screw positioning [121]. Some studies suggested that increasing the number of condyle-ramus component fixation screws may reduce the stress magnitude on the condyle-ramus component and supporting bone [87,118]. According to the literature, mean values of von Mises and shear stress were lower for titanium based condyle-ramus screws than those recorded for CoCrMo based condyle-ramus screws [121]. The mean values of von Mises stress for the UHMWPE fossa against Ti6Al4V and CoCrMo alloys ranged from 29 and 50 MPa [125–127]. Other previous studies recorded stress values of around 16 and 31 MPa [107,128–131] while the Von Mises stress values on the TMJ condyle-ramus component during the simulated clenching were recorded between 126 and 170MPa [107,121,123,131]. Furthermore, another study reported values of around 284 MPa for the Zimmer Biomet™ microfixation on normal or maximal chewing bite [132]. Condylar heads of TMJ TJR can be designed in different shapes to offering larger bearing surface area avoiding stress concentration at small area [24,133,134] that may lead to higher wear rate of the bearing surfaces as seen in Figure 7 [6,105,134].

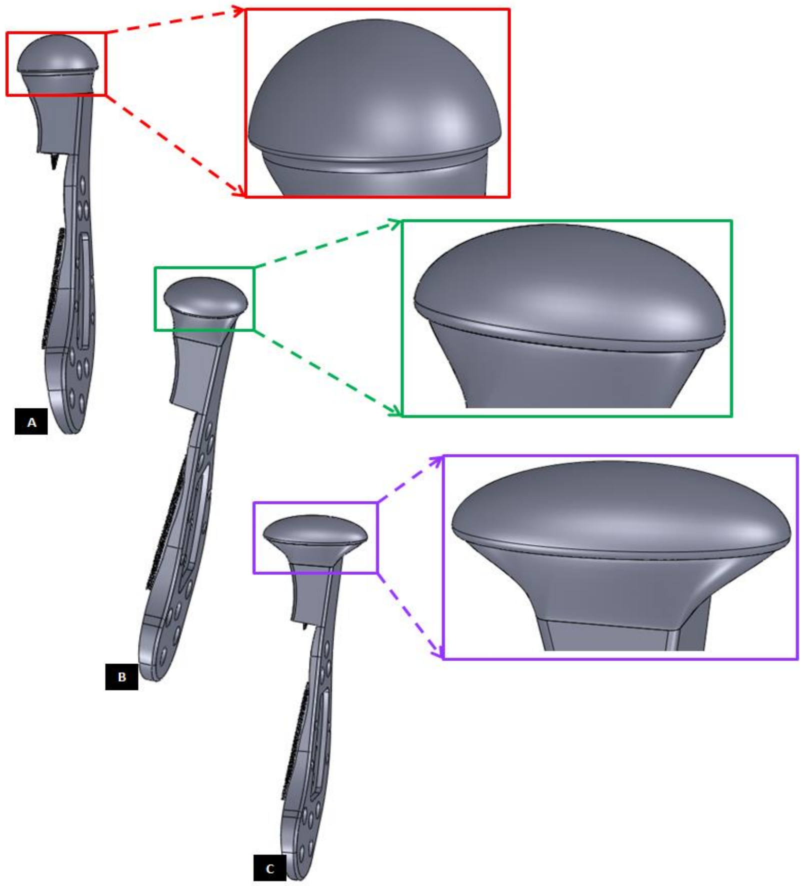

Figure 7- Schematics of different shapes of the TMJ TJR condylar heads of the condylar/ramus component. (**A**) Spherical condylar head. (**B,C**) Elliptical head of different dimensions. Adapted from [105].

On the design of the ramus of the mandibular component (Figure 8), a previous study reported that the anatomical shape of custom TMJR ramus components revealed a proper stresses distribution and higher mechanical stability when compared to a stock model [105,112,118]. Lower values of von Mises stress were reported on the custom TMJR condyle-ramus component and at the surrounding bone compared to the stock component [118,135]. Changes in condylar component thickness also influences the prosthetic stiffness and load transferring to the fixation screws [118,133,134].

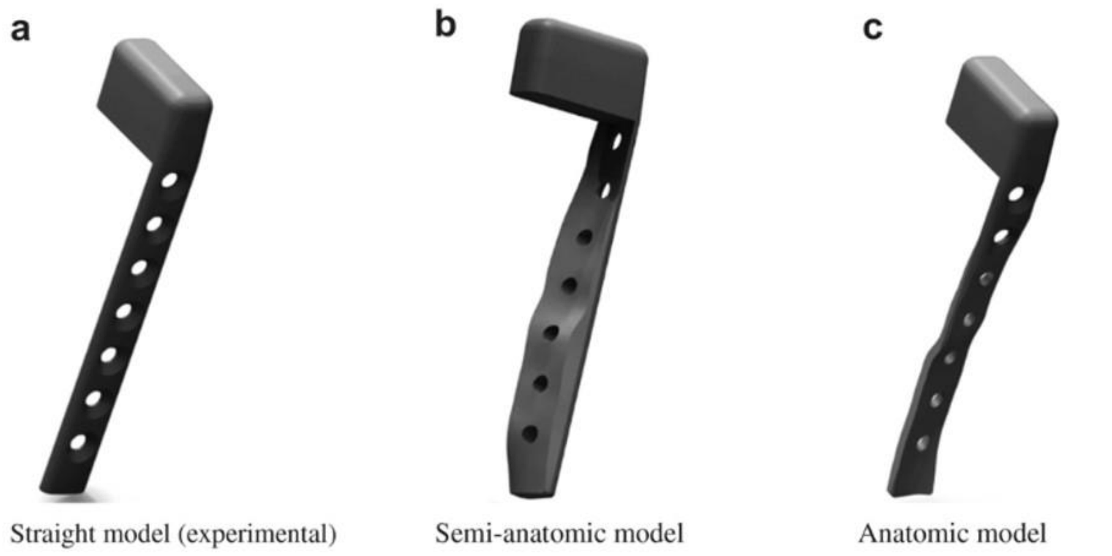

Figure 8- CAD models of different implant ramus design. (A) Straight model. (B) semi-anatomical fitting to the mandible bone with different thickness along its lenght. (C) Customized anatomical fitting and a constant thickness. Adapted from [118].

The maximum contact pressure on the condyle ramus component is achieved when the condyle rotates to its fully anterior positioning and in the posterior side of the condyle [12,87,119,120]. The maximum contact stress in the prosthetic condylar component increased from 47 MPa at 0 degrees of anterior rotation to 150 MPa at 15 degrees of anterior rotation [87]. A previous study reported the function of the natural, contralateral fibrocartilaginous articular disc was significantly altered by the presence of a TMJR device [118]. There is consensus that a healthy mandible withstands lower stresses in the articular disk, than the contra lateral side of the mandible that has undergone TMJ TJR [136], especially stock prosthetics [112]. A previous study, have reported changes in the masticatory pattern and ranges of motion in patients who underwent unilateral and bilateral TMJ TJR [137]. The dynamic simulation has shown how the load on the TMJ TJR decreases while the load on the healthy side increases with the opening of the mandible [25]. Thus, the healthy side is affected by a 15% increase in stress in the articular disk from FEM studies [2].

1.4 Wear and Degradation of TMJ TJR materials

The degradation of material used for TMJ TJR depends on a series of factors such as primary stability level, surface conditions, loading, wear resistance, and properties of the materials [3,6]. Wear is one of the most important causes of failure on bearing contact prostheses once contacting materials surfaces are subjected to complex loading and relative motion [1,103,138]. Enhancement of the mechanical properties of the components in contact with bone is still an industrial challenge and therefore ordinary materials are currently in clinical use [1,108,139]. Materials with an elastic modulus closer to that of bone are preferred over the ones with a higher elastic modulus to preventing micromotion and assuring optimum stability [6,12]. Bone has an elastic modulus of 4–30 GPa, depending on the type of bone tissue and direction of measurement. Most titanium-based alloys used in the screws have a elastic modulus of around 110 and 150GPa [6,24,91,140,141] while CoCrMo alloys revealed a higher elastic modulus of around 210 GPa [4]. The mismatch in elastic modulus leads to abrupt loading transference and concentration of stresses at prosthetic interfaces. The transference of loading through the TMJ TJR prosthesis can cause bone resorption or fibrosis if the TMJ TJR [9,12]. In fact, a high magnitude of loading at the cranium base has been recorded ranging from 60 up to 150 N in the anterior region and around 270 N in the posterior region [4,99]. In the absence of an alloplastic articular disc, there is only a small contact area between the condyle and the articular fossa. Regardless of the material, a certain load on a small area results in a high loading concentration on the bearing surfaces [142,143].

On the sliding of the metallic condyle onto the polymeric fossa, a two-body abrasion takes place on the tribological pair (i.e., CoCr versus UHMWPE) [6,13,144]. Abrasion wear can occur on both surfaces since they are rubbing away from each other by direct contact with their asperities under oscillatory loading [19,25]. The resultant plastic deformation of the contacting surfaces depends on the axial loading magnitude and roughness (micro and nano-scale) of the components [3,24]. As seen in Figure 9 and 10, the plastic deformation occurs by ploughing with the fracture (micro-cracks) regions and ejection of materials from both contacting surfaces in the wear track [16,18,19]. In fact, fatigue also occurs within the wear pathways since there is a rupture of intermolecular bonds followed by a subsurface damage caused by the movement of surface molecules under cyclic load [23,24] As a result, there is a release of metallic (oxide layer) and polymeric debris to the peri-prosthetic region [3,78,146].

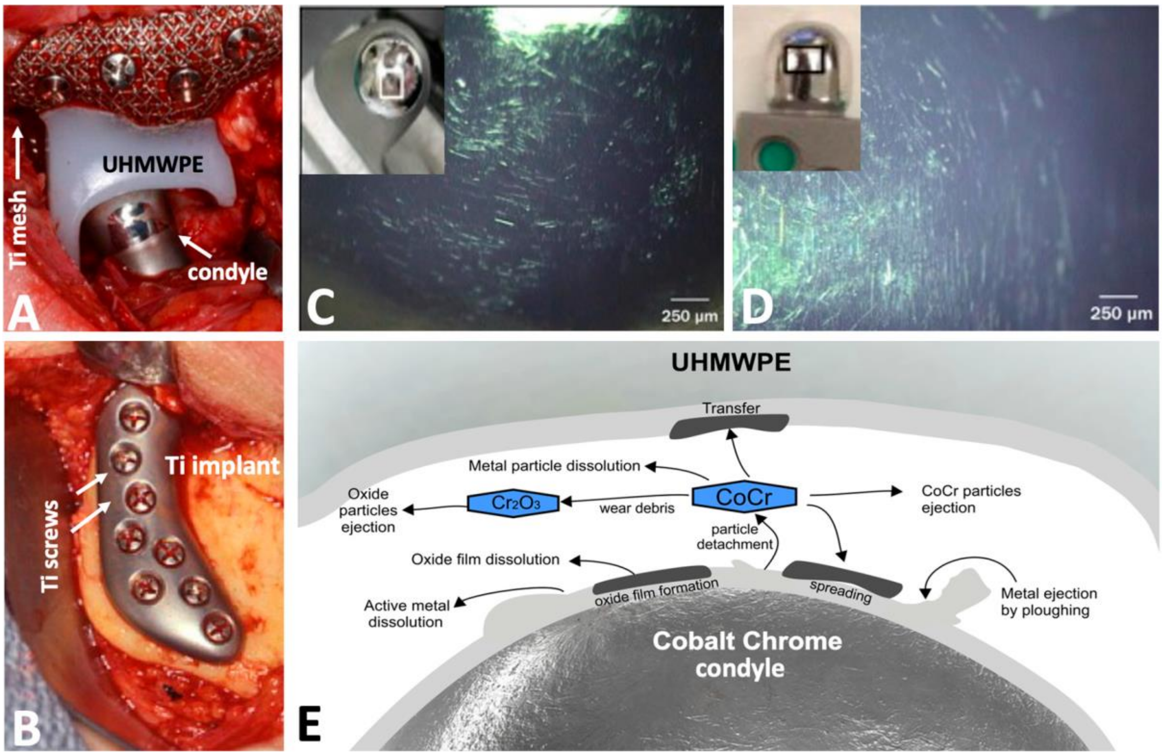

Figure 9- Images of the TMJ TJR. **(A)** condyle and **(B)** ramus implant. Microscopic images (x93.5) revealing abrasive scratches on the **(C)** custom-made and **(D)** standard condyle surfaces. Adapted from [3]. (Elsevier 2016). **(E)** Schematics of the wear pathways on CoCr-based condyle against UHMWPE fossa surfaces.

Then, abrasive particles move along the surfaces in tribological contacts, scratching away the antagonist surface. If the prosthetic contacts act as a closed tribological system, the material loss is higher, when compared to the material loss in open environment where the abrasive particles move away from the tribological contact zone [23,24]. Wear adhesion is another related pathway once wear particles can also become attached like platelet shapes to surfaces forming tribo-layers under friction [145]. However, fracture of the micro-welds resulting from adhesive wear can occur, leading to an increase in the wear rate [16,147]. Thus, hard debris such as CoCr-based particles act as third bodies in the wear pathways, leading to an increased wear rate of the surfaces as illustrated in Figure 11.

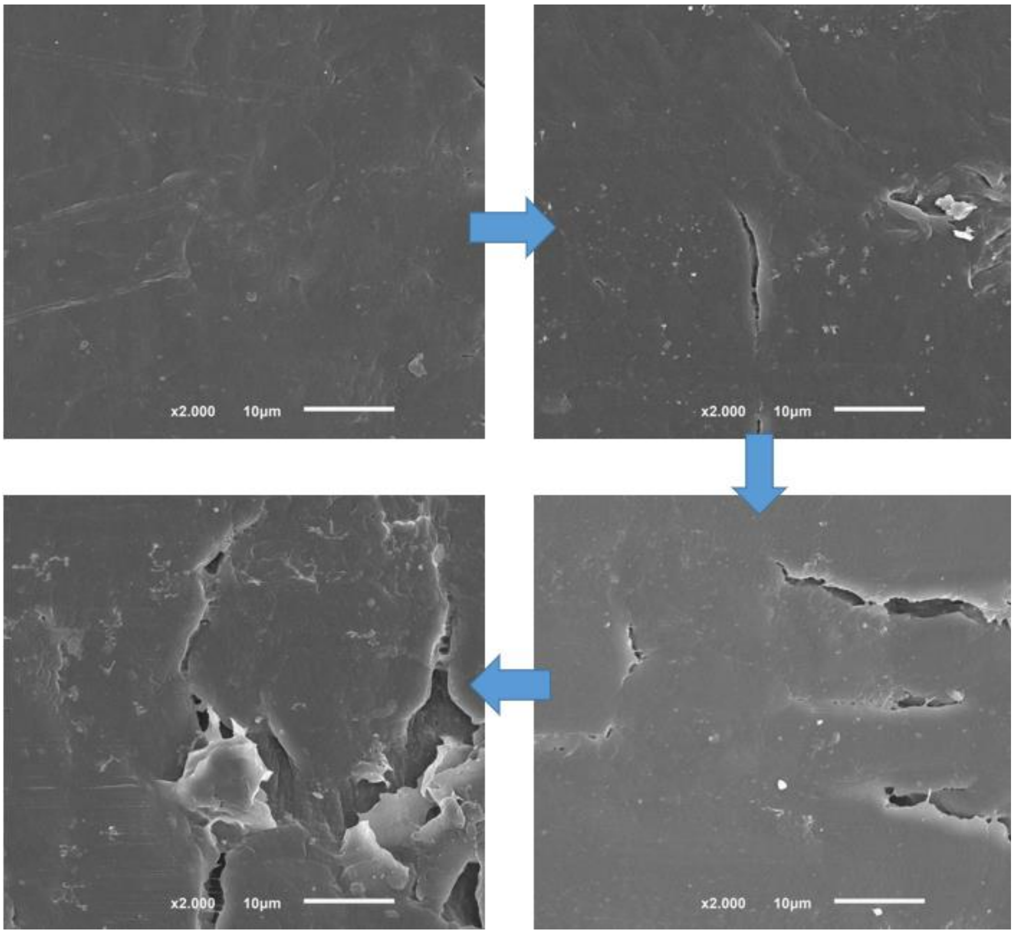

Figure 10- SEM images on worn UHMWPE surfaces. Expansion of cracks and ejection of debris.

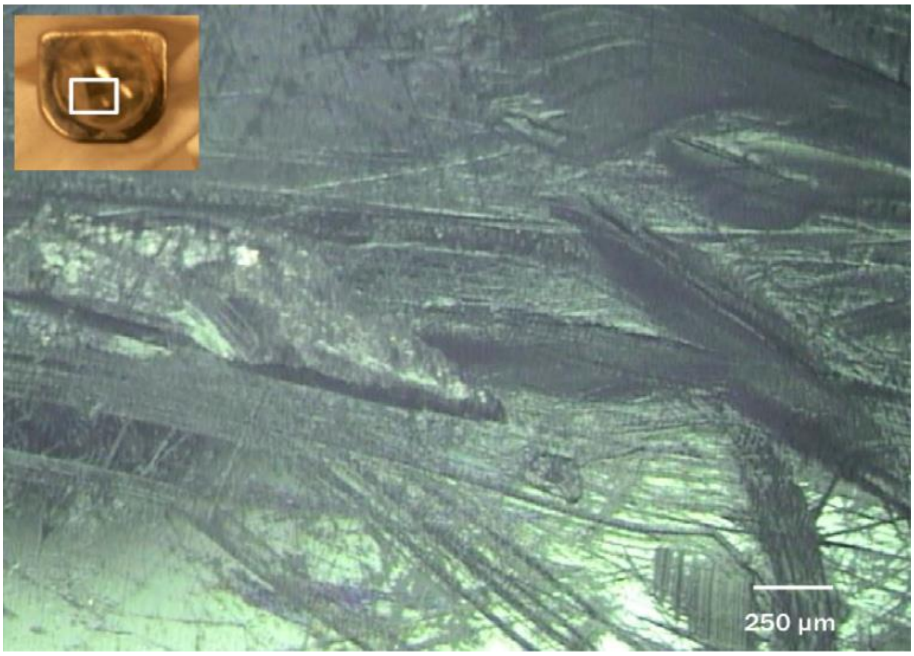

Figure 11- Microscopic image (x93.5) revealing bi-directional abrasive scratches on TMJ TJR condyle after 5 years. Adapted from [3].

Surface wear and consequent loss of contacting volume is one of the main causes of degradation of TMJ TJR prostheses [3,19]. The surrounding lubricant medium used in tribological studies also influences the wear behaviour of the contacting surfaces. In the presence of proteins, the liquid medium acts as a lubricant, decreasing the friction and consequent wear rate [26,165]. The thin oxide film (passive oxide film) composed of Cr_xO_y onto CoCr-based surfaces or Ti_xO_y on titanium-based surfaces also remain stable [6,22,23,25]. However, thin oxide films can be destroyed [149,150] under increased friction and sliding wear [3,23,153]. In acidic medium, the thin oxide film formed onto the CoCr- and titanium-based surfaces chemically interact with the H^+ and other ions (i.e., Cl^-) leading to a partial dissolution (active oxide film) [6,24,26,27]. As a result, the release of metallic ions and debris such as nano-particles exposes a fresh CoCr- or titanium-based surface that promptly reacts with the environment corresponding to an anodic partial current [6,24,26,27]. It should be emphasized that the bare metal has a high chemical reactivity to the medium once the thin protective oxide film was removed. Thus, a galvanic coupling is established during the wear process in the electrolyte, since the bare (worn area) may act as an anode or a cathode, while the peripheric area, composed of a passive layer (unworn area), acts as a cathode or an anode [22,23,24]. The current flowing between anodic and cathodic areas represents an increased corrosion rate of the metallic material. Previous studies have reported the simultaneous wear and corrosion (tribocorrosion) of CoCr- and titanium-base surfaces in different medium such as saline, artificial saliva, phosphate buffered solution (PBS), biofilms, and protein-rich serum [22,26,85,101]. Contrarily to hip and knee prostheses, only a few studies are available that describe the tribocorrosion behaviour and biological response of novel advancements in TMJ TJR materials [15,19,179,180]. Evidence of corrosion includes, pitting [153,154], presence of grains with variable size and location, indentations, and bidirectional lines (Figure 9) [3,86,180,181]. Multi-directional scratches can be seen on TMJ TJR devices before placement, indicating that those scratches were produced in the polishing protocol that was applied [157,158].

Therefore, wear properties may be improved by decreasing radial clearances, smoothening surfaces, and increasing the contact bearing area [3,31,79,108]. Designing contact surfaces is one way to reduce wear of TMJ TJR materials. A recent approach has proposed the modification of the condyle surfaces with a deposition of titanium nitride (TiN) [159] or diamond-like carbon (DLC) layer [160] , that can decrease friction and wear of the condyle component. The same approach has been utilized in the case of the condylar structure of hip TJR prostheses [13,161] In fact, veneering metallic surfaces with DLC or TiN could provide a protective barrier against corrosion and wear, increasing the long-term performance of the contacting TMJ TJR surfaces. Also, the high-strength ceramic condyles could be an alternative to avoid the corrosion issue [162,163]. However, the microstructure integrity (i.e., absence of defects) and low roughness of the modified surfaces should be controlled to promote such low friction effects. Defects such pores or rough coating surface are quite common considering the manufacturing processes. The detachment of coatings can also occur during normal and tangential loading during cyclic sliding and normal loading. As a consequence, three-body abrasion increase the wear of the bearing surfaces [163–165]. Despite UHMWPE properties, degradation by wear on UHMWPE is unavoidable, which requires the consideration of alternative polymers [13,166]. Many UHMWPE structures are sterilized by gamma irradiation at room environment. This has subsequently been shown to cause oxidative degradation of the polymer both in vitro and in vivo leading to an increased wear rate and release of polymeric debris [166,167]. Some studies have reported a lower friction when a highly cross-linked polyethylene (XLPE) counter-body was used instead of UHMWPE against CoCr-based surfaces [162,168].

1.5 Adverse biological effects of wear debris

The peri-implant environment is a complex system containing several inorganic and organic components that can have a significant impact on the biomedical materials [91]. The inherent composition of human body environment changes regarding health or pathologic state of the patient and degradation behaviour of the biomedical materials [171,172]. Previous studies have reported that the failures of the TMJ TJR structures can be related to a synergistic effect among friction, wear, and corrosion resulting in the release of metallic ions as well as metallic and polymeric debris [3,19,31] [151,169–171]. TMJ TJR debris (ceramic, metallic, and polymeric particles) and ions can accumulate around the peri-prosthetic tissues, promoting adverse local tissue reactions such as necrosis, osteolysis, and pseudo-tumors [169,170]. The presence of ions and debris into the tissues activates endothelial cells at the peri-prosthetic region causing the expression of molecules such as P-selectin, ICAM-1, CAM and CD44 [150]. In this way, immune cells (granulocytes, macrophages, monocytes and lymphocytes) are stimulated by those molecules towards the tissue interfaces [169,172]. Then, the immune cells induce the discharge of a variety of prostaglandins, degradative enzymes, growth factors, reactive oxygen species (ROS), and pro-inflammatory cytokines including TNF-a, interleukins (IL-1a, IL-1b, IL-6 and IL-8) [1,169,173]. Several studies reported that primary cytokines stimulate the release of other mediators. The consequent inflammatory cascade results in the recruitment of other types of cells and the formation of peri-implant granuloma [172,174,175]. The fusion of macrophages results in multinucleated-giant cells and osteoclasts that adhere onto the surfaces of the metallic particles [175,176]. On degradation, TMJ TJR particles can be released like granules, splinters, flakes, and needle-like shape (Figure 12) [177,178].

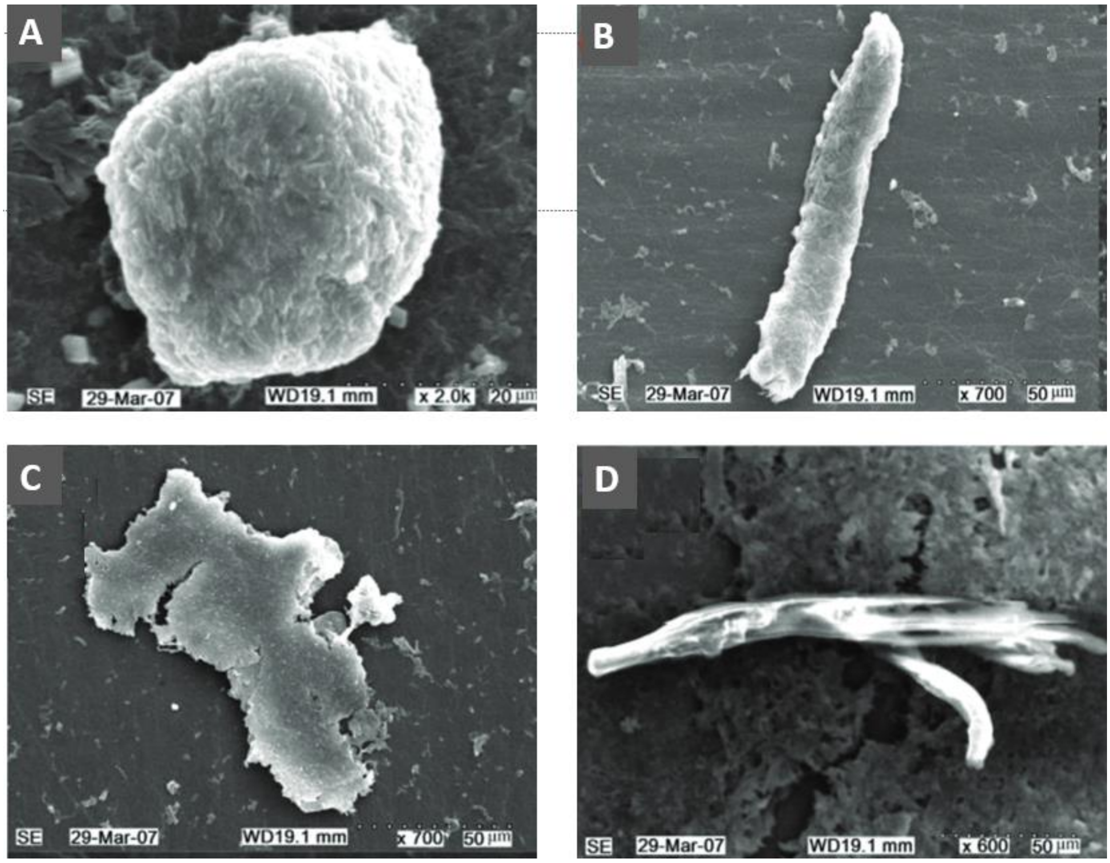

Figure 12- Different types of UHMWPE debris. (**A)** Near roundness wear debris, usually below 5 µm. (**B)** Splinter like wear debris (10-100 µm In size). (**C)** Sheet wear debris (20-50 µm). (**D)** Needle-like wear debris (~100µm). Adapted from [179].

Immediately on implant placement, synthetic materials spontaneously bind to a layer of host proteins that mediate the interaction with immune cells [180]. For instance, macrophages interact with wear particles through the layer of adsorbed serum proteins, including type I collagen, aggrecan proteoglycans, immunoglobulin, fibronectin and albumin (Figure 13) [167,181].

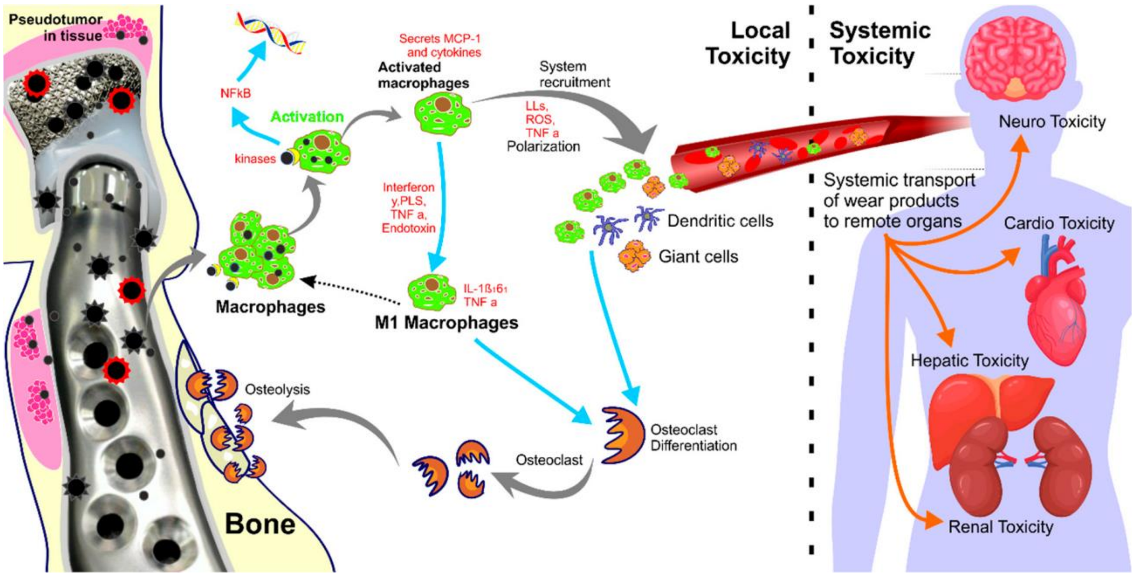

Figure 13- Schematics of the toxic effects of metallic debris released from the degradation of TMJ TJR prostheses. Adapted from [182]

UHMWPE particles in the 0.1–1.0 μm size range have been shown to a higher biologically reaction when compared with larger particles [183–185]. Submicron-scale particles have been involved in inflammatory reactions of late aseptic loosening of total joint replacements [183,186]. Regarding the differences in size, submicron and nano-scale UHMWPE particles are engulfed by macrophages that attempt to degrade the polymeric particles, although without success. The macrophages become activated and release prostaglandins, cytokines (TNF-α, IL-6, IL-1, IL-8), metalloproteinases, and lysosomal enzymes [180,183,187]. Metallic ions, submicron-, and nano-scale particles released from surface degradation are chemically active and can interact at the level of cellular organelles with potential risks of mutagenic reactions [175,188]. The biological response of cells depends on the chemical composition, size, and amount of the particles and ions [174,175]. The main CoCr-based alloys used to manufacturing the condyle have approximately 68% Co, 28% Cr, and 7% Mo, while titanium alloys (Ti grade V) have around 89% Ti, 6% Al, and 4% V. Metallic particles can be found from micro- (below 1–50 um) up to nano-scale (1–100 nm) size after tribocorrosion of a CoCr- or titanium-based condyle against a UHMWPE [175,181,186,189,190]. CoCr micro- and nano-scale particles and Co^{2+}, Cr^{3+}, Cr^{6+} ions are the main degradation products from CoCr-based alloys [3,151,190]. CoCr-based nanoparticles and Cr^{3+} ions can trespass the cell membrane by diffusion or endocytosis, generating reactive oxygen and nitrogen species and disturbing the respiratory function of the cells. Submicron- (0.1–0.99 um) and nano-scale particles are internalized by the cells via pinocytosis and phagocytosis processes of macrophages [186]. Also, the nano-scale debris and ions can reach the cell DNA inducing mutagenic reactions. The saturation of metallic debris has a negative consequence in the antioxidant mechanism of the cells causing cell wall damage and metabolism disorders [175,191] Studies have reported apoptosis and inflammatory responses in macrophages and pneumocytes when in contact with Co^{2+} and Cr^{3+} [151,175,192–194]. Additionally, Co^{2+} can influence iron metabolism by interaction with apo-transferrin that might affect the physiologic hematopoietic tissue metabolism. A previous study reported toxic concentrations for Co^{2+} at 8–10 ppm and 250–500 ppm for Cr^{3+}[195]. Other study has shown that normal levels reach 2 ppm Ti while 8.1 ppm Ti found in patient with failed titanium-based implant [176]. Recently, a retrospective study found that the presence of adverse local tissue reaction (ALTR) was associated with high levels of cobalt and chromium (6.2ppb and 3.6 ppb respectively) [170]. Such ALTRs can be source of excessive pain to the patient and mostly lead to the revision of the implant [3,196,197]. In a pilot study, Mercuri et al, [169] analysed the blood samples from patients with prosthetic devices (dental implants, TMJ TJR prosthesis, orthognathic intervention). In a total of 12 patients, 4 showed high levels of these metals in the blood. Detection limits in serum were set at 0.15 ng/mL for cobalt, 0.1ng/mL for chromium, and 0.3 ng/mL for titanium. Although there is not a consensus among studies on the amount of particles required to cause cytotoxicity, the human body contain about 10-20mg of Ti at physiologic conditions [198]. After implantation surgery, levels of metallic ions increase in serum concentration and urine [199]. Another previous study reported high titanium ion levels in patients with implants [171] . The levels of metallic ions reached a high peak for 36 months while those levels were 18 times higher for 120 months. Furthermore, systemic toxicity could take place when the debris and ions get into the bloodstream and reach lymph nodes, liver, spleen, and bone marrow [169,175,176,200,201]. A relationship between wear debris accumulation and upregulation of metalloprotein I/II has been reported that can result in the alteration of xenobiotic metabolism by liver [202,203]. Erythrocytes which are degraded by the liver contain metal that circulate throughout the body tissues and amplify the risks of genotoxicity and immunological effects [175,181]. The metallic debris can trespass different cells and tissues and can also be transferred among organs. An in vivo study found Co particles in the liver and kidney of rodents with values similar to those seen in some patients with metal implants (range:

4–38 µg/L Co in blood). Another in vivo study on rats reported metal accumulation in liver and kidney tissues after intramuscular placement of a CoCrMo implant for 9 months. Such findings suggested that metal particles and ions are released from CoCr-based implants even under non-functional conditions. In fact, TMJR TJR components (condyle, screws, fossa mesh, and ramus) are sources of metallic debris and ions. Regarding the titanium-based ramus and screws, many manufacturers use Ti6Al4V alloys due their high strength and capability of osseointegration [204]. Nevertheless, inflammatory reactions were also reported for Ti, TiO_2 particles and Ti ions as found for CoCr-based debris. Additionally, the presence of V and Al ions has been associated with potential mutagenic and carcinogenic response [175,181,186,205]. The development of biocompatible titanium alloys, without potentially toxic elements like Al or V and the surface modification methods have been the targets for recent research. Nowadays, TiZr and TiZrNbTa alloys are alternative materials to replace Ti6Al4V alloys [206,207].

Chapter 2
Materials and Methods

2. Materials and Methods

2.1. Search and selection of studies

A bibliographical search was carried out using the following electronic databases: MEDLINE/PubMed (via National Library of Medicine) and ScienceDirect (Elsevier). The present search of studies was carried out in accordance with previous integrative or systematic review articles [4,172,186,204]. The following search terms were used: "temporomandibular joint prosthesis" OR "temporomandibular joint implants" OR "alloplastic temporomandibular joint" OR "TMJ prosthesis" OR "TMJ implant" OR "alloplastic TMJ" OR “TMJR” OR “CoCr” AND “wear” OR “friction” OR “surface damage” OR “debris” OR “toxicity”. A manual search was also performed considering the references in the selected articles. The inclusion criteria involved English language articles published up to May 2021, reporting the friction and wear rate of TMJ TJR components. The eligibility inclusion criteria used for article searches also involved: meta-analyses; randomized controlled trials; and prospective cohort studies. The exclusion criteria were the following: narrative review; systematic review; papers without English abstract; case report with short follow-up period; articles assessing only other properties of TMJ TJR. Studies based on publication date were not restricted during the search process.

The articles retrieved by the search process were evaluated in three steps. Studies were primarily scanned for relevance by title, and the abstracts of those that were not excluded at this stage were assessed. The evaluation of the potentially relevant articles by review of the title and abstract were evaluated independently by two of the authors (JCMS, HPB). A final evaluation of a third author (AR) was conducted in cases of disagreement. The total of articles was compiled for each combination of key terms and therefore the duplicates were removed using Mendeley citation manager (Elsevier). Selected articles were individually read and analysed considering the purpose of this study. At last, the eligible articles received a study nomenclature label, combining first author names and year of publication. The review article variables considered for this review were the following: authors’ names; journal; publication year; purpose; wear test conditions; surface damage; coefficient of friction; wear volume; debris release. Data of the reports were harvested directly into a specific data-collection form to avoid multiple data recording regarding multiple reports within the same study (e.g., reports with different set-ups). This evaluation was individually carried out by two researchers, followed by a joint discussion to select the relevant studies.

2.2 Preparation of the specimens for wear tests

Four different groups of metallic condyle specimens and one group of polymeric flat surfaces were prepared by computer aid design and computer aid manufacturing (CAD-CAM). Pin-like condyle specimens were prepared from two different materials: CoCrMo (Wironium Extra hard^{TM}, BEGO, Germany); and Ti6Al4V (TiFast S.R.L, Italy) alloys. Additionally, two different pin-like condyle design were produced concerning the contact surface for tribological testing: anatomical- and spherical-shape condyle specimens (Figure 14 A and B). Anatomical specimens had a radius of 15 mm while spherical specimens had a radius of 4.25 mm. Anatomical specimens followed the design of a recent patent on TMJ TJR condyle [12] and the spherical specimens were representative of commercially available TMJ TJR condyle [99,208]. Polymeric cylindrical plate specimens with diameter at 15 mm and thickness at 3 mm were machined by CAD-CAM from UHMWPE rods (Garland, USA).

The surface of the CoCrMo specimens were finished by electrochemical polishing treatment in electrolytic bath (Dentaurum GmbH 7 Co., Germany) for 10 min. Ti6Al4V specimens were electrochemically polished in a solution containing 2% HF and 20% HCl for 10 min. At last, surfaces were ultrasonically cleaned in isopropyl alcohol for 10 min and then in distilled water for 10 min. Condyle specimens were divided into four groups considering the type of materials and design.

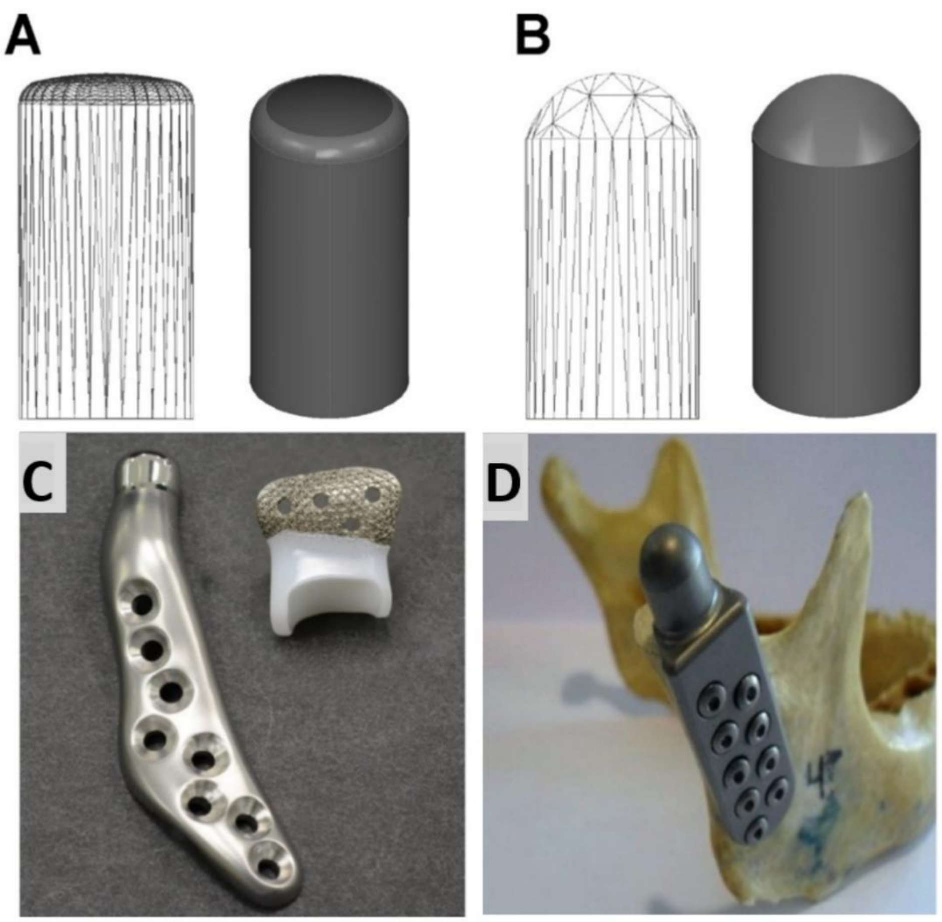

Figure 14- Design of the pin-like condyle specimens. (A, C) Anatomical-shape condyle. (B, D) Spherical-shape condyle.

The chemical composition and properties of the materials provided by manufacturers are shown in Table 2. Mean values for Young's modulus and Vicker's hardness were also recorded by nano-indentation tests and DMA while chemical analyses were performed to confirm the chemical composition of the materials.

Table 2. Chemical composition and properties of materials used for TMJ TJR. Data given by the manufacturers.

Material	Poisson's ratio	Young modulus (GPa)	Density (g/cm^3)	Hardness (Vickers)	Chemical composition (wt%)
CoCrMo	0.29	230	8.2	345	Co (61), Cr (30), Mo (5), Mn (2), Si (1)
Ti6Al4V	0.34	110	4.43	340	Ti (~89), Al (5.5-6.7), V (3.5-4.5), Fe (0.4), C (0.08), N (0.05), H (0.012), O (0.2)
UHMWPE	0.46	4.5	0.94	6.4-8.3	C_2H_4

2.3 Reciprocating sliding wear tests

Sliding tests on pin-on-plate set up (*n* = 12) were performed at a normal applied load (Fn) of 30 N and at reciprocating sliding frequency of 1 Hz with a stroke length of 4 mm (Figure 15**)**. Considering the variation of the TMJ TJR motion, normal loading was recorded ranging from 1 up to 150 N on the anterior region of the articular fossa and reaching maximum values at 270 N on the posterior region of the articular fossa while the frequency has been recorded ranging from 1 up to 10 Hz [4,6,14,78,99]. In this way, tribological parameters were chosen considering usual TMJ joint motion on low frequency and regular loading magnitude as well as following tribological parameters performed in previous studies [146,209–211].

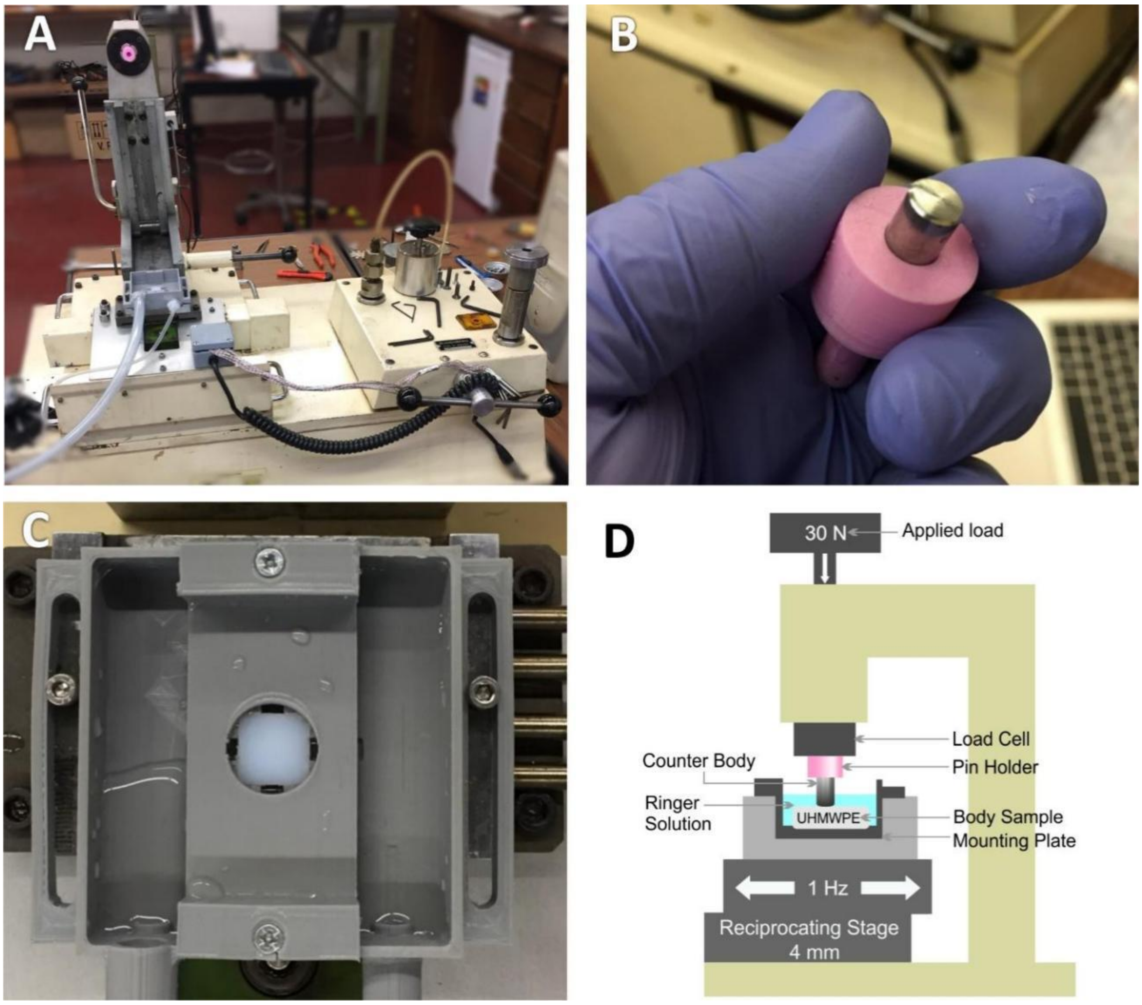

Figure 15. (A) Image of the wear test apparatus (Plint Te76/R, Phoenix Tribology ltd, UK), (B) condyle specimen coupled to a pin holder, and (C) UHMWPE plate attached to an electrolytical recipient. (D) Schematics of the wear testing set up.

Reciprocating sliding wear tests were carried out at 37°C in Ringer's solution using a wear test apparatus (Plint TE67/R, Phoenix Tribology ltd, UK) to mimic the environment surrounding the TMJ TJR. Ringer's solution comprised 8.4 g/L NaCl, 0.3 g/L KCl, 0.3 g/L $CaCl_2$, and 0.2 g/L $NaHCO_3$ dissolved in distilled water resulting in a pH at 6.4. Even though Ringer's solution did not contain protein, the electrolyte properties promoted by the presence of inorganic compounds is quite similar to that recorded for physiological body serum [14,19,212,213]. Also, other previous studies performed wear tests CoCrMo or titanium materials against UHMWPE in Ringer's solutions and therefore the tribological outcomes should be compared [212,213].

Different segments of the plots were analysed to measure the mean values of the steady-state coefficient of friction (COF) for the tribological pairs. As a result of the reciprocating sliding motion, a wear track was noticed onto the UHMWPE counterbody. The wear track was geometrically outlined to measure the contact area, pressure, and wear volume of the counterbody, assuming the mechanical and geometric integrity of the metallic pins. Mean values of bearing area and indentation depth were estimated by using the theoretical model of contact between elastic bodies as seen in Figure 16 [214,215].

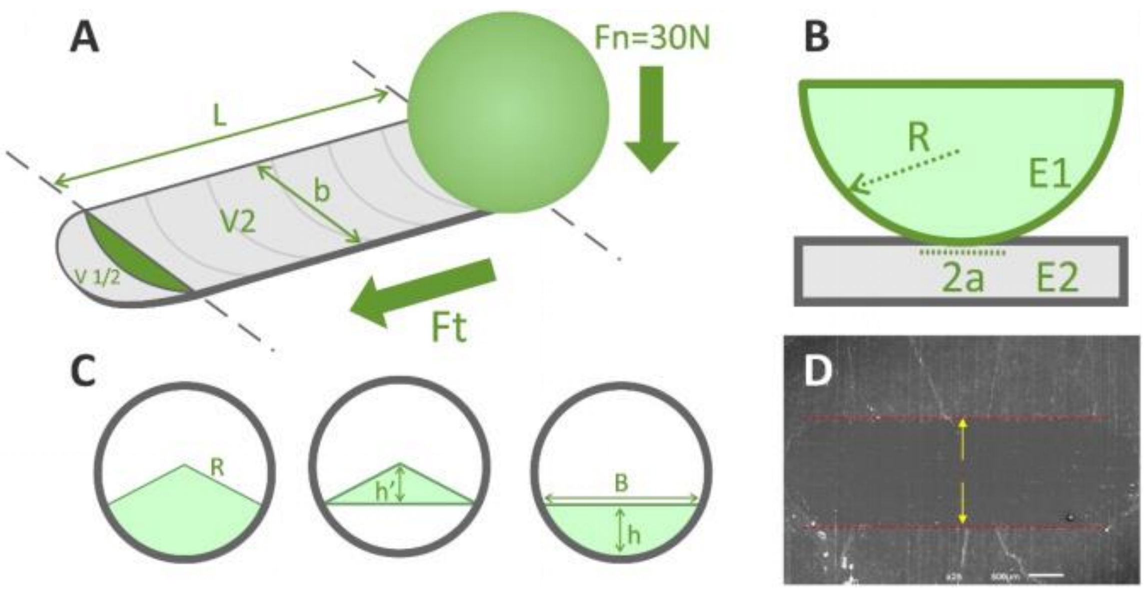

Figure 16. Wear Model Schematics of the (A,C) wear track to estimate the wear volume on the UHMWPE and (B) the theoretical model to estimate the contact pressure. (D) SEM image of the wear track over the UHMWPE surface.

After the reciprocating sliding tests, the width at the middle region of the wear track was measured and related to the condyle design (Figure 16D). The total volume loss of the wear track, ΔV, in mm^3, corresponding to the wear of the specimens was calculated using Equation (1):

$$\Delta V = L \times \left[\frac{1}{2} \times R^2 \times sin^{-1}\left(\frac{s}{R}\right) - \frac{b \times h'}{2}\right] + \frac{\pi \times h'}{64R} \qquad (1)$$

Where, L is the stroke length in mm, R is the radius of the pin-like specimens in mm, s is the half of the width of the wear track (b/2) in mm and h' is the height of the triangle in mm, as shown in (Figure 3C). The volume loss values were then converted into specific wear rate, K, in mm^3/N.m, using Equation (2):

$$K = \frac{\Delta V}{Fn \times L} \qquad (2)$$

where F_n is the applied load, and L the total sliding distance in m.

The maximum contact pressure between the pin-like specimens and the UHMWPE plate was estimated at the starting time point of the reciprocating sliding wear following the representative theoretical model shown in Figure 16B and related equations from the Hertz theory. Considering the contact between two elastic bodies, the maximum contact pressure, $(\sigma_c)_{max}$, at the starting time point of the wear test was estimated by using Equations (3-5).

$$a \cong \left(\frac{3}{2}\ \frac{RF}{E*}\right)^{1/3} \qquad (3)$$

$$\frac{1}{E_*} = \frac{1}{2}\left(\frac{1 - v_1^2}{E_1} + \frac{1 - v_2^2}{E_2}\right) \qquad (4)$$

$$(\sigma_c)_{max} \cong \frac{3}{2}\frac{F}{\pi a^2} \qquad (5)$$

where a is the radius of the contact between the sphere and plane, R is the sphere radius on indenting the specimen (Equation 3), E is the reduced elastic modulus, E_1, E_2 are the elastic modulus of two materials, and v_1, v_2 are the Poisson's ratio associated with each contacting body (Equation 4). On anatomical-shape condyle design, the contact pressure on Ti6Al4V against UHMWPE was recorded at 91.6 MPa while the contact pressure on CoCrMo against UHMWPE was recorded at 92.8 MPa. On spherical-shape condyle design, the contact pressure on Ti6Al4V against UHMWPE was recorded at 212 MPa while the contact pressure on CoCrMo against UHMWPE was recorded at 215 MPa.

2.4. Mechanical characterization

At first, the elastic modulus and Vickers' micro-hardness of the materials were evaluated by nano-indentation assays. Nano-indentation testing was carried out with the loading axis at angles of 90° relative to the surface plane of the materials. A nano-hardness tester (Nano Instruments, Inc. Knoxville; TN, USA) operated with a Berkovich diamond pyramid tip (apex angle of 143°) was used to make nanoscopic indentations in triplicate along the cross-sectioned test samples (n = 15). Loads of 1 or 20 mN were applied onto the polymeric and metallic substrates, respectively, during 15 s. Mechanical properties of the materials were recorded as a function of the position of the indenter axis relative to the surface. The shape function was determined by the Oliver & Pharr method (1992). Nanoindentation tests allow evaluating stress/strain fields induced during indentation considering the displacement axis of the indenter. Young's modulus measurements on the metallic and polymer materials were also measured by Dynamic Mechanical Analysis (DMA 242 C, Netzsch Gerätebau GmbH, Germany) using a three-point bending apparatus.

2.5. Scanning electron microscopy

The worn UHWMPE surfaces were sputter-coated with a AuPd thin film by using a sputter-coater (Cressington 108 AUTO, Germany) to provide conductive surfaces for scanning electron microscopy (SEM) analyses. SEM images were acquired on backscattered (BS) and secondary electron (SE) mode at 5–10 kV by using a SEM unit (JSM-6010 LV, JEOL, Japan). Images were recorded at magnification ranging from x25 up to x2000 for each specimen to identify the dominant wear mechanisms. The software Adobe Photoshop (Adobe Systems Software, Ireland) was used to measure the width of the wear tracks on the SEM images.

2.6. Chemical analysis

The elemental chemical analyses of the contact surfaces of the metallic condyle specimens and corresponding polymeric counterbodies were performed using energy dispersive spectroscopy (EDS, INCAx-Act, PentaFET Precision, Oxford Instruments, USA) coupled to the SEM. Infrared spectra of UHMWPE specimens were recorded on an FTL 2000 equipment (Bomem, Canada) by transmittance. All spectra were acquired on 100 × 100 μm spot size on the sample surface, on 200 scans at a 4 cm^{-1} resolution at the 700–4000 cm^{-1} region.

2.7 Finite element analysis

Specimens were modelled using CAD software (SolidWorks 2012, Dassault Systems SolidWorks Corp., Concord, MA, USA) regarding two designs: spherical- and anatomical-shape condyle (Figure 17). Pin-like condyle specimens were virtually placed at the centre of the UHMWPE. The model on spherical shape condyle corresponded to commercially available TMJ TJR condyles [99,208], while anatomical-shape condyle specimens were based on a recent patent [12,93].

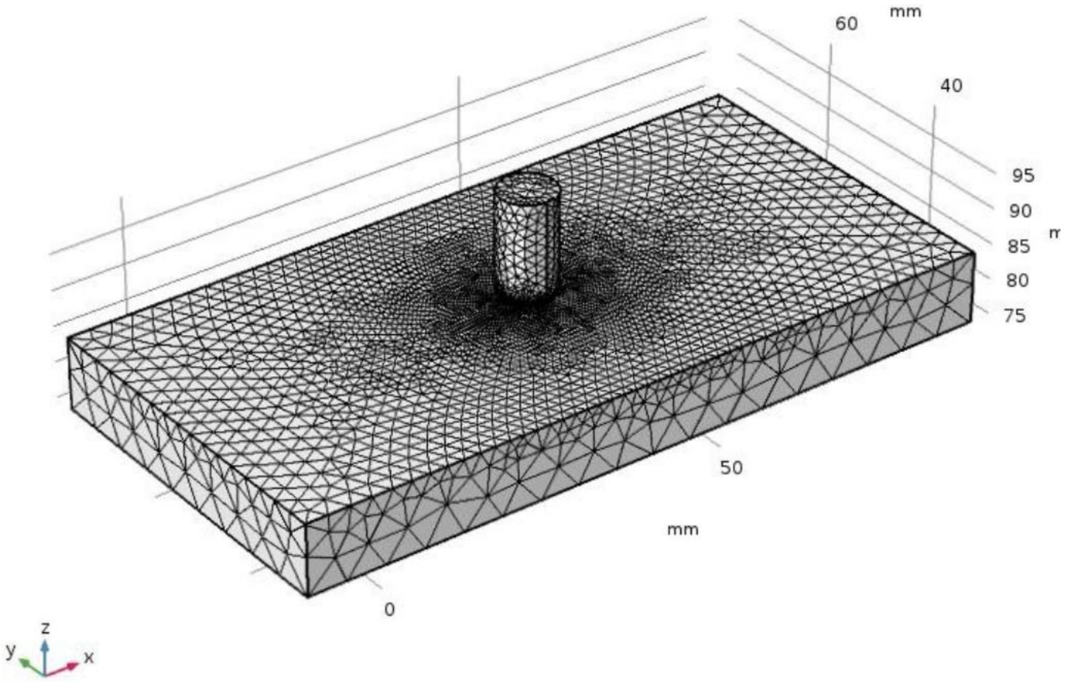

Figure 17. The finite element model mesh built of the pin-on-plate contact with free tetrahedral linear elements

In this study, the finite element analysis (FEA) was performed using COMSOL Multiphysics 5.3 (COMSOL, Sweden). Spherical- and anatomical-shape condyles were designed to assess the total displacement of the materials and the von Mises stresses through the tribological pairs. The finite element model mesh was built with free tetrahedral linear elements as shown in Figure 17. Additionally, the mesh was refined at the bearing area between the materials by increasing the tetrahedral linear elements to optimize the computational analysis. A convergence analysis was carried out to examine the sensitivity of the results to the mesh size. The number of stable mesh elements for the pairs were the following: 54717 for anatomical CoCrMo (Figure 18) and 55251 for anatomical Ti6Al4V; 75633 for spherical CoCrMo and 75430 for spherical Ti6Al4V. The properties of the materials were used on FEA. The elastic modulus of the materials acquired by nano-indentation and DMA while density and Poisson' coefficient data were given by the manufacturer. On FEA, a load of 30 N was applied vertically parallel to the long axis of the pin-like condyle towards the UHMWPE. Also, the depth of the wear track after the reciprocating wear sliding tests was considered on FEA. The von Mises stresses resultant from the loading forces were analysed considering different materials (CoCrMo and Ti6Al4V) and design (spherical and anatomical) after reciprocating wear sliding tests against UHMWPE.

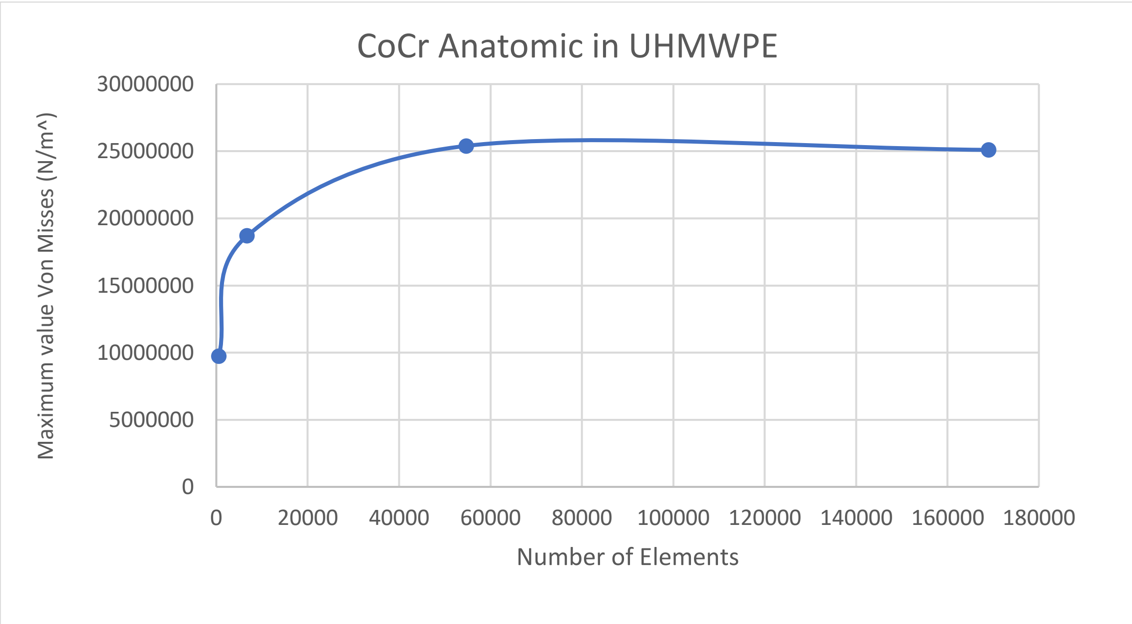

Figure 18 - Results on the converge on the number of elements for CoCrMo/UHMWPE

2.8. Statistical analysis

Results were statistically analyzed by normality test Shapiro-Wilk and two-way ANOVA to determine statistical differences in COF and wear rate values between groups. The t student test was used to compare the results regarding the type of materials and design for TMJ TJR condyle. A probability value <0.05 was considered significant. The power analysis was performed by t student test or ANOVA, to determine the number of samples for each group (n), and to reveal a test power of 100% in the present study. Statistical analyses were carried out using Origin Lab statistical software (Origin Lab, Northampton, MA, USA).

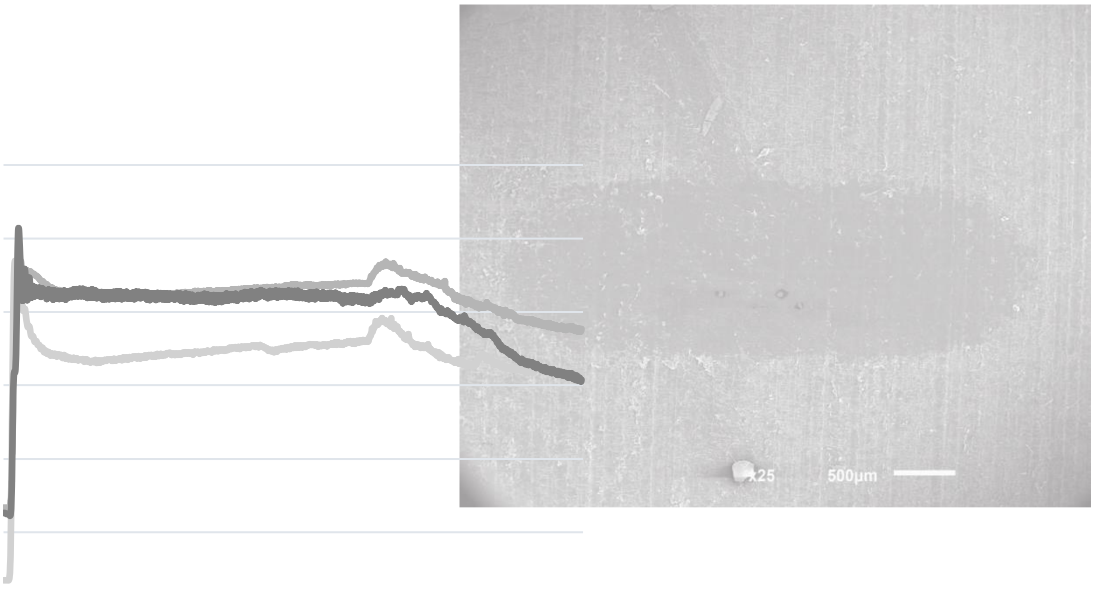

Chapter 3
Results and Discussion

3. Results and Discussion

3.1. Reciprocating wear sliding tests

On tribological tests, the ratio between the tangential and normal forces during sliding provided the coefficient of friction (COF). COF values recorded for both condyle design (CoCrMo or Ti6Al4V) against UHMWPE are shown in Figure 19. At the starting point of the sliding motion, plots revealed an increase in COF values followed by a running-in phase revealing a slightly COF stabilization. The fitting of the bearing surfaces promotes a stabilization of COF values that is considered as a steady state along the wear testing [128,145,216,217].

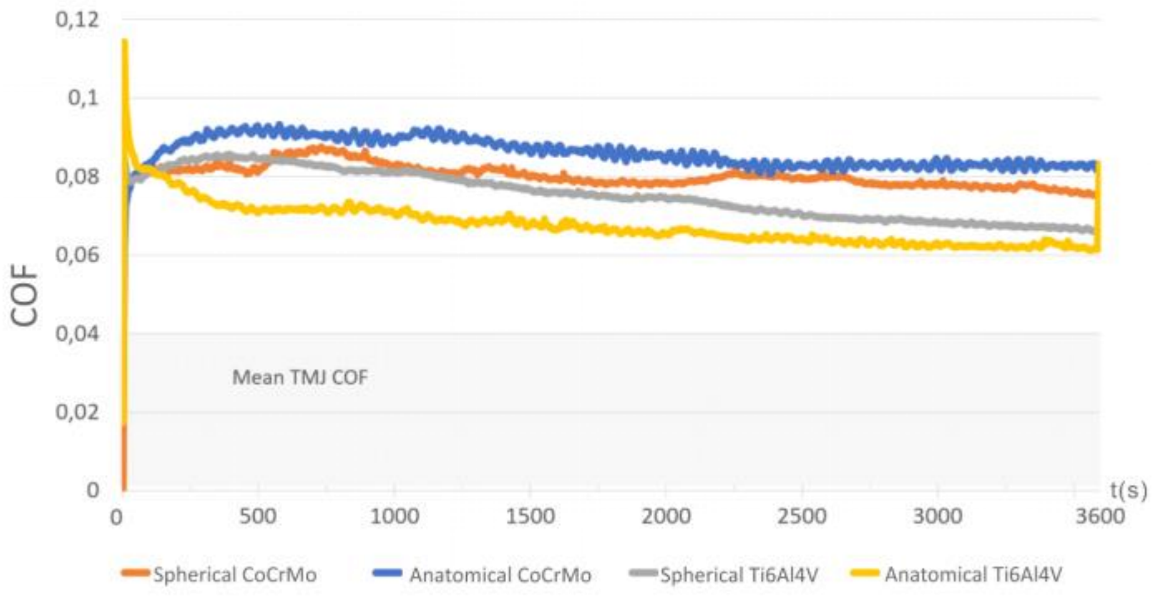

Figure 19- Evolution of the coefficient of friction (COF) with time for CoCrMo or Ti6Al4V pin-like specimens against UHMWPE flat surfaces in Ringer's solution at 37°C (FN = 30 N, L = 4mm, frequency = 1 Hz and time = 3600 seconds). COF mean values for physiologic TMJ are indicated in gray background.

On the other hand, small amplitude fluctuations of COF values can be noticed for the tribological pairs over the steady-state regime of reciprocating wear sliding (Figure 19). The frictional behaviour can be explained by the occurrence of periodic localized fractures and probable materials' adhesion phenomena. That often occur between bearing surfaces for such tribological pairs in solutions containing or not proteins. Additionally, a possible effect of formation of third bodies at the bearing surfaces corresponding to debris can also contribute to the fluctuations in COF values [14,26].

On all tribological pairs, the average steady state COF values were very close to each other as shown in Figure 20. COF mean values were recorded ranging between 0.06 and 0.08 and no statistical differences were recorded between the tribological pairs ($p < 0.05$). That validate the null hypothesises founded in this study considering the materials for TMJ TJR condyle. COF values were recorded at 0.081 for CoCrMo/UHMWPE anatomical-shape condyle and at 0.078 for CoCrMo/UHMWPE spherical-shape condyle in Ringer's solution at 37 ^{o}C. COF values for anatomical- and spherical-shape condyle composed of CoCrMo were not statistically different in this study ($p < 0.05$). On Ti6Al4V condyle surfaces against UHMWPE in Ringer's solution, COF mean values at the steady-state were recorded at 0.077 independently of the condyle design. In fact, such COF values at around 0.06-0.08 suggested a lubricant effect of the UHMWPE counterbody in Ringer's solution leading to a low friction and wear of the bearing surfaces. Indeed, UHMWPE reveal a low friction that validate its use as the first-choice material for manufacturing prosthetic articular fossa component of commercially available TMJ TJR. Nevertheless, COF values for both CoCroMo or Ti6Al4V against UHMWPE were slightly higher when compared to those reported for healthy temporomandibular joints (~ 0.001-0.04) [26,93].

In a previous study, similar steady-state COF values at 0.06 were recorded for CoCrMo against UHMWPE on 20 N loading and stroke length of 30 mm in solution containing proteins [146]. Another previous study reported steady-state COF values at around 0.055-0.075 CoCrMo against UHMWPE surfaces on 50 N loading and at a stroke length of 17.4 mm in solution containing proteins [146]. Regarding Ti6Al4V surfaces, steady-state COF values at around 0.07 were also recorded for Ti6Al4V against UHMWPE surfaces on 39 N or 20 N and at a stroke length of 4 mm in solutions containing proteins [129,218]. In the present study, COF values were quite similar to those recorded for Ti6Al4V against UHMWPE in previous studies.

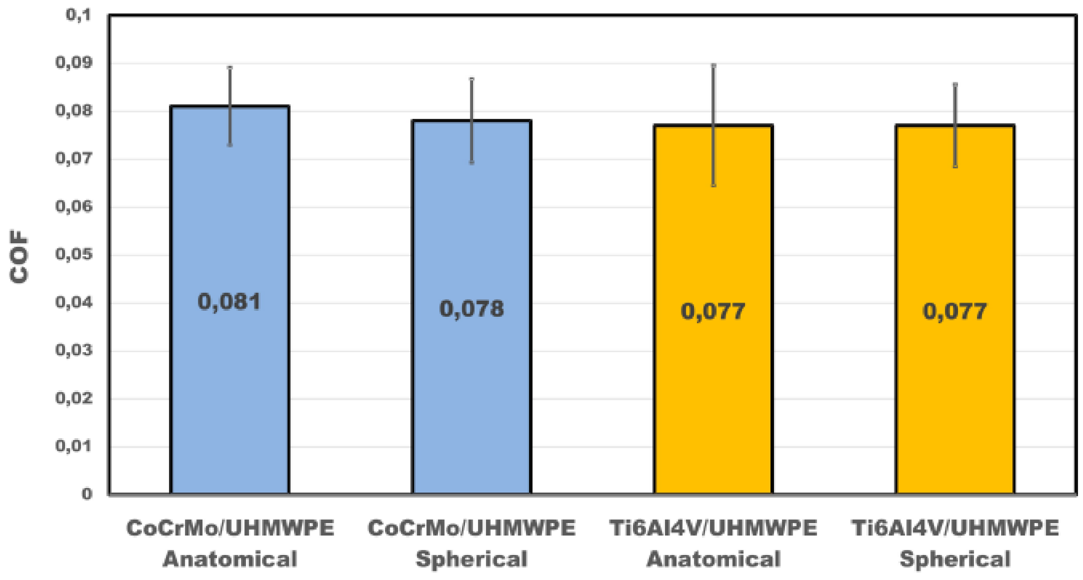

Figure 20- Steady-state coefficient of friction (COF) for CoCrMo or Ti6Al4V pin-like specimens against UHMWPE flat surfaces in Ringer's solution at 37°C (FN = 30 N, L = 4mm, frequency = 1 Hz and time = 3600 seconds).

Indeed, COF values reported in previous studies for both CoCrMo or Ti6Al4V against UHMWPE surfaces in the presence of protein-containing solutions are similar to the COF values recorded in the present study [129,146,209,218]. It reveals a low friction of the pairs of materials for both condyle design for composing the TMJ TJR. A low friction is resultant from low magnitude of tangential forces considering a constant normal loading as applied in the present study. A decrease in tangential forces over bearing surfaces of TM TJR reduces the stresses over the surfaces leading a decrease of the wear rate. Also, it decrease the amplitude of micromovements leading to a mechanical stability of the system [25]. On alloplastic materials, proteins perform a lubricant effect on the bearing surfaces since a protein-based thin film can decrease the magnitude of the tangential forces [219,220]. However, the protein-based thin films are continually detached due to the tangential forces under sliding movements. Proteins can adhere once again on the surfaces after detachment whether they were not destroyed due to the shear and compressive stresses and to an increase in temperature. That is the difference between alloplastic surfaces and biological materials since biological materials (e.g., fibrous tissues) possess the capability of self-healing by producing new proteins to maintain a long term ultra-low friction [26,93].

3.2 Wear rate and morphological aspects of the worn surfaces

Wear tracks on UHWMPE surfaces were inspected after sliding against the spherical- or anatomical pin-like condyle design. The chemical composition of UHWMPE was confirmed by FTIR and EDS. Representative SEM images of the wear tracks are shown in Figure 21. The width mean values of the wear track were significantly higher for anatomical-shape condyle specimens since the contact area increased regardless the material. The morphological aspects of the wear tracks were smoother after sliding against the anatomical-shape condyle (Figure 21 A and C).

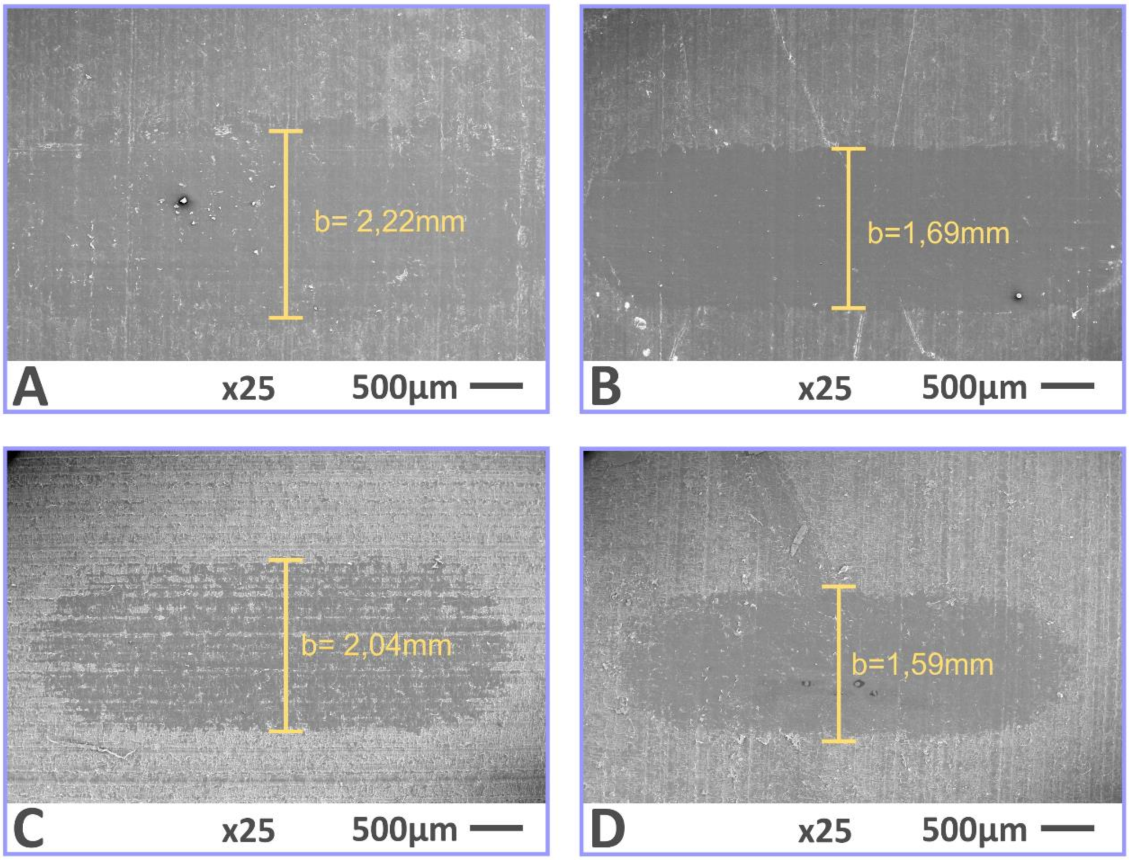

Figure 21. FEGSEM images of the worn surfaces of UHWMPE against (A) anatomical CoCrMo, (B) spherical CoCrMo, (C) anatomical Ti6Al4V, and (D) spherical Ti6Al4V. SEM images acquired on secondary electrons (SE) mode at 15 kV.

Representative SEM images of the middle region of the wear tracks on UHMWPE after sliding against Ti6Al4V or CoCrMo, are shown in Figure 22. The existence of cracks and layers of materials (tribolayers) was noticeable in the wear track. On the sliding of the condyle specimens onto the UHMWPE, a two-body abrasion occurred as noticed in Figure 21 and 22. The morphological aspects of surfaces for the tribological pairs were similar to those reported in previous studies [13,221].

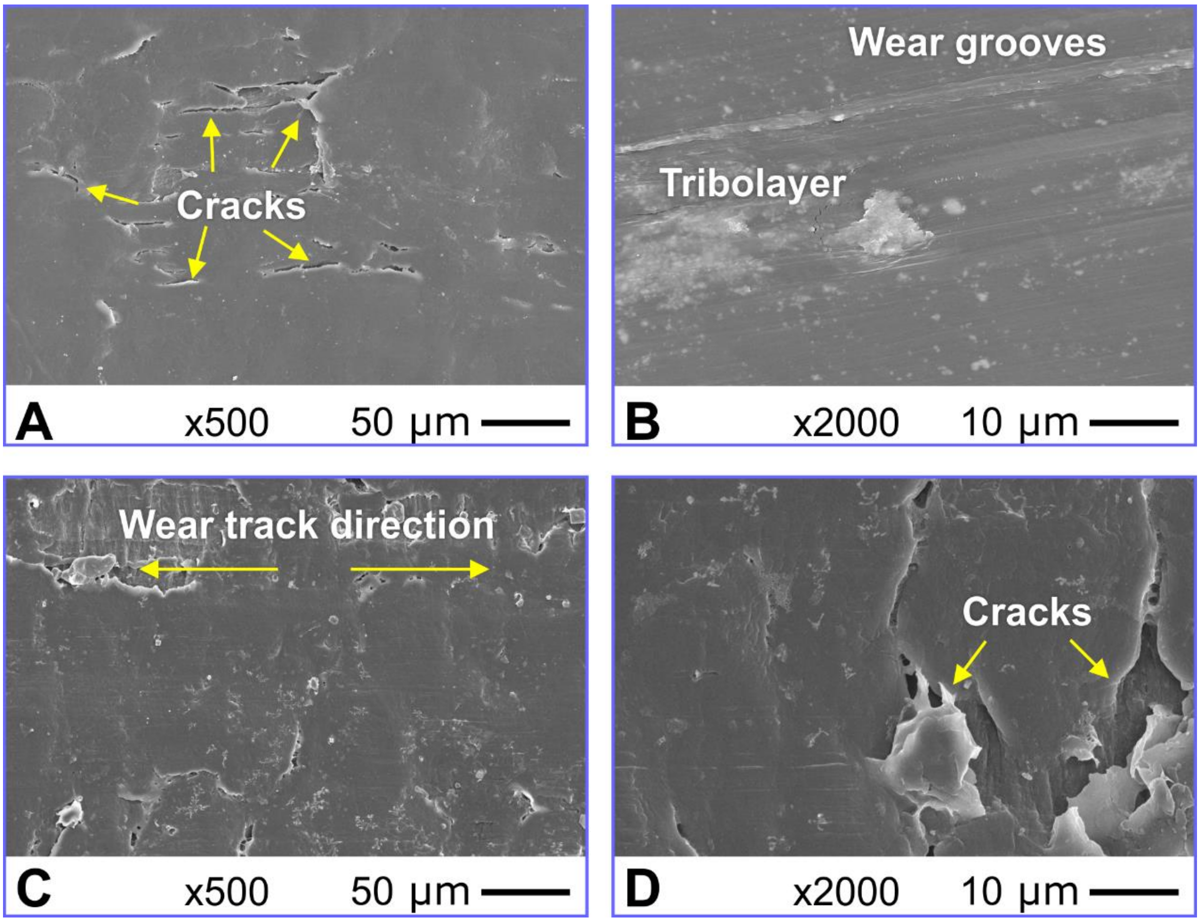

Figure 22. (A,B) Representative FEGSEM images of the middle region of the wear track on the UHMWPE, after sliding against (A,B) Ti6Al4V or (C,D) CoCrMo. (B, D) Magnification of the middle region of the wear tracks.

Abrasion wear is represented by wear grooves aligned with the sliding direction due to the effect of two-body bearing contact and the presence of hard particles detached along the wear track. Abrasion wear takes place on both surfaces since they are on rubbing against each other by direct contact with their micro- and nano-scale peaks under fluctuating and complex loading [3,145]. Plastic deformation, micro-cracks, and ploughing occurs onto the materials bearing surfaces due to abrasion, depending on the normal (axial) loading magnitude and roughness of the materials [13,19], as seen in

(Figure 22A and C). Also, a rupture of intermolecular bonds followed by a subsurface damage occurs, due to the movement of atoms and molecules under cyclic loads [145,169] as seen in Figure 22 A and C**.**

Abrasive particles move throughout the surfaces on the tribological contacts rubbing away the bearing surfaces. Then, the adhesion of detached material results occurs leading to the formation of adherent layers of damaged material, named tribolayers, as seen in Figure 22B. The material loss can become severe when the abrasive particles remain in the tribological contact region increasing the wear rate of bearing materials [3,13,222,223]. That can occur mainly in retentive regions as found around TMJR TJR. In this, a progressive damage of materials by two-body abrasion intensifies the release of abrasive loose wear particles leading to an extreme overall wear of the surfaces. Tribo-layers over the surfaces can be easily damaged or detached resulting in the further release of wear particles.

Representative SEM images of the worn surface of the pin-like condyle specimens (CoCrMo and Ti6Al4V) are shown in Figure 23. Chemical analyses performed by EDS did not detect transfer of metallic material to the UHMWPE over the wear tracks. Such findings were evaluated regarding the mechanical behaviour of the soft UHMWPE against CoCr- and titanium-based alloys considering the tribological parameters used in this study. The wear behaviour of the UHMWPE against CoCrMo or Ti6Al4V surfaces was mainly attributed to smooth abrasion of the surfaces resulting in relatively low wear. Scratches parallelly oriented along the sliding direction can be detected on the metallic worn surfaces. Black regions indicated the presence of UHMWPE debris (Figure 23 A and C) as confirmed by the presence of carbon by EDS (Figure 23 B and D).

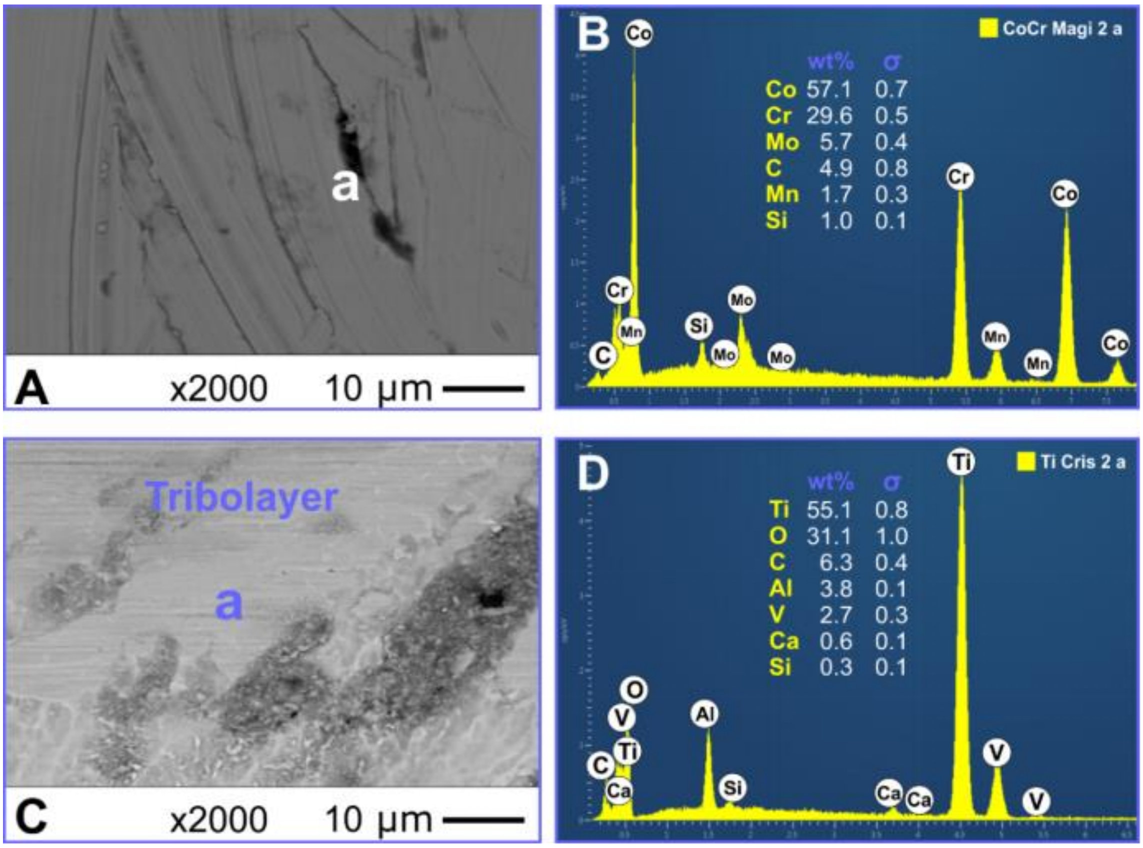

Figure 23- Representative FEGSEM images of the worn surfaces of **(A)** CoCrMo and **(C)** Ti6Al4V after sliding against UHMWPE in Ringer's solution at 37 ºC. Chemical analysis by EDS for both **(B)** CoCrMo and **(D)** Ti6Al4V worn surfaces.

Thus, the titanium oxide film formed over Ti6Al4V can protect the surface against the corrosion although the oxide film can involve other chemical elements from the surrounding medium. On reciprocating sliding motion, the titanium oxide films can be destroyed under increased friction and sliding wear as found in the present study. It should be emphasized that the bare metal has a high chemical reactivity to the medium once the thin protective oxide film was removed. On Ti6Al4V, calcium and oxygen were detected by EDS that indicate a chemical reactivity of the titanium-based surface to the surrounding environment. The destruction of the titanium oxide film is the first step in the degradation of titanium and its alloys leading to the release of Ti ions and particles composed of Ti_xO_y [7,146,158]. On CoCrMo or Ti6Al4V, a galvanic coupling arises during the wear process in the electrolyte, since the bare (worn area) may act as an anode or a cathode, while the peripheric area, composed of a oxide layer (unworn area), acts as a cathode or an anode [19]. The current flowing between anodic and cathodic areas represents an increased corrosion rate of the metallic materials. Previous studies have reported the simultaneous wear and corrosion of CoCr- and titanium-base surfaces in different medium such as saline, artificial saliva, phosphate buffered solution (PBS), biofilms, and protein rich serum [19,148,224].

In fact, UHMWPE is the major polymeric material for bearing surfaces of TMJ TJR, due to the resultant low COF values, high resilience, and high chemical stability [6,13,24,78]. However, UHMWPE has relatively low mean values of hardness, Young's modulus, and strength associated with a high magnitude of ductility leading to a plastic deformation by ploughing and material loss under reciprocating sliding motion against CoCr- or titanium-based alloys [6,24]. Several commercial brands perform the sterilization of UHMWPE by gamma irradiation that cause an oxidative degradation of the polymer resulting in damage of its physical properties. High loading and wear on contacting surfaces increase the release of debris to the surrounding tissues and consequent adverse inflammatory reactions at peri-prosthetic tissues [3,14,225]. UHMWPE submicron- and micro-scale particles can be engulfed by macrophages that attempt to degrade the polymeric particles. Macrophages interact with wear particles through the layer of adsorbed serum proteins, including type I collagen, aggrecan proteoglycans, immunoglobulin, fibronectin and albumin. Additionally, the activation of macrophages induces the release prostaglandins, cytokines (TNF-α, IL-6, IL-1, IL-8), metalloproteinases and lysosomal enzymes [58,60]. That results in the migration of inflammatory cells leading to an osteolysis process [57].

The specific wear rate of UHMWPE surfaces considering both spherical- and anatomical-shape condyle design and two different materials (CoCrMo and Ti6Al4V) are shown in Figure 24.

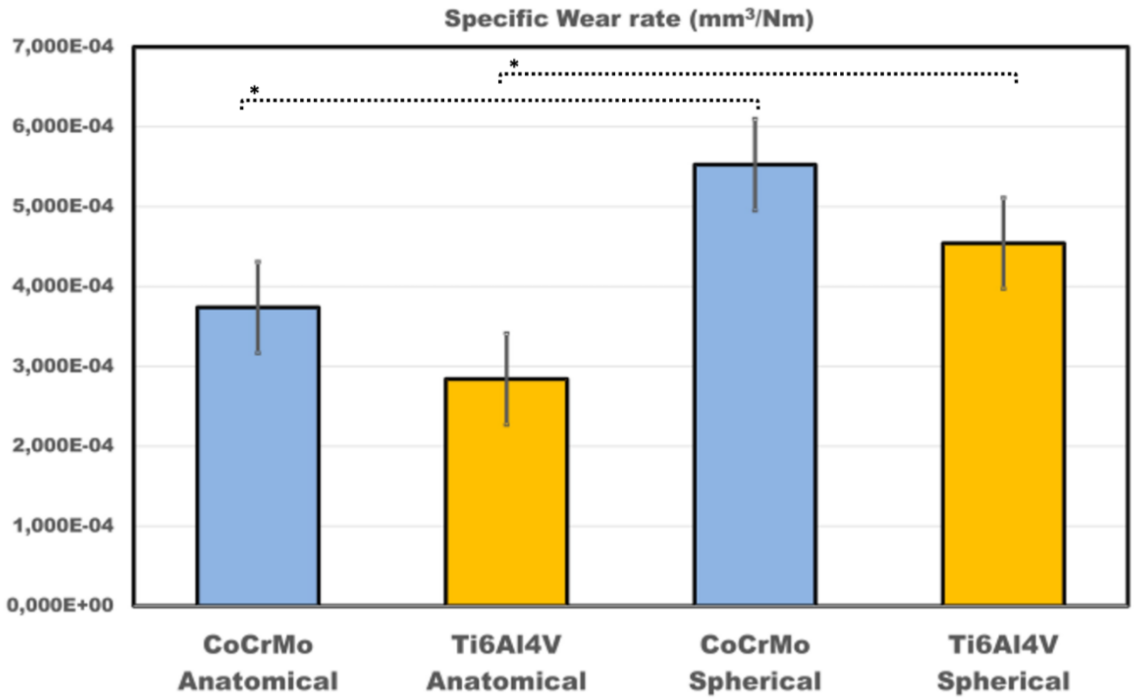

Figure 24- Specific wear rate of UHMWPE after reciprocating sliding against CoCrMo and Ti6Al4V pin-like specimens in Ringer´s solution at 37ºC (F_N = 30 N, stroke length = 4 mm , 1 Hz, 3600 seconds of sliding time). * Statistical differences detected between the tribological pairs.

Regarding the condyle design effect, the mean values of wear rate of UHMWPE surfaces were higher against the spherical-shape condyle specimens (5.53 x10^{-4} mm^3/Nm for CoCrMo and 4.54 x10^{-4} mm^3/Nm for Ti6Al4V) when compared to that one against anatomical-shape condyle specimens (3.74 x10^{-4} mm^3/Nm for CoCrMo and 2.84 x10^{-4} mm^3/Nm for Ti6Al4V). Statistical differences were recorded between spherical- and anatomical-shape condyle design regarding each type of condyle material as seen in Figure 7 ($p < 0.05$). The results rejected the null hypothesises founded in this study regarding the condyle design for TMJ TJR. Regarding the condyle materials, the highest mean values of specific wear rate of UHMWPE at around 5.53 x10^{-4} mm^3/Nm were recorded against the spherical-shape CoCrMo condyle specimens.

Other studies reported also low values of wear rate for CoCrMo against UHMWPE in distilled water [103,226]. On CoCrMo or Ti6Al4V, results of the present study are in accordance with those recorded in a previous study on the tribological behaviour against UHMWPE in diluted bovine serum (25%) [227]. However, other previous studies reported specific wear rate values of UHMWPE 2.04 x10^{-6} mm^3/Nm [228] and and 2.7

x10^{-6} mm^3/Nm [146] against CoCr-based pin-like specimens. A previous study recorded specific wear rate values for UHMWPE against CoCr-based surfaces of around 6.70 x 10^{-6} mm^3/Nm in the presence of Hyalgan solution [146] while other studies recorded values of 11 x 10^{-6} mm^3/Nm in bovine serum solution[229], 7.6x 10^{-6} mm^3 /Nm in human serum solution [218], and 4 x10^{-6} mm^3 /Nm in artificial saliva [145]. Also, different specific wear rates values were previously reported for UHMWPE against Ti6Al4V [146,229]. Thus, previous studies have shown that the use of appropriate bearing materials and design can decrease the wear rate of the materials leading to an adequate long term clinical performance of the prosthetic and implant structures [24,80].

3.3. Mechanics and finite element analyses

The mean values and standard deviation of elastic modulus and Vicker's hardness measured for the tested materials are shown in Table 3. Results were quite similar to those given by the manufacturer and therefore the experimental mean values of Young's modulus were used for finite element analysis.

Table 3- Young's modulus and Vicker's hardness of the materials

Material	Young modulus (GPa)	Hardness (Vickers)
CoCrMo	225 ±6	353 ±8
Ti6Al4V	114 ±4	342 ±7
UHMWPE	4.8 ±0.4	6.8 ±0.9

Regarding the finite element analysis performed in this study, the Von Mises stress values found on anatomical-shape condyle composed of CoCrMo at around 25 MPa were lower when compared with the values recorded for spherical-shape condyle either for CoCrMo or Ti6A4lV, approximately 35MPa and 30 MPa, respectively (Figure 25). The highest Von Mises stresses at around 35 MPa were recorded on the spherical-shape CoCrMo condyle against UHMWPE. The von Misses stress values recorded for Ti6Al4V against

UHMWPE in several studies were very similar with those ones recorded within this study since stress mean values of 32 MPa and 29 MPa were found in other previous studies [125,126]. Other previous studies recorded stress values of around 16-31 MPa [128–130]. However, higher stress values were recorded for Ti6Al4V against UHMWPE ranging from 48 up to 68 MPa in other studies [6,146,227]. Also, the Von Misses stress recorded for CoCr/UHMWPE in several studies exceed the maximum values found in this study. A previous study recorded a stress contact of 51 MPa [146] while other studies recorded stress values at around 68 MPa [227] and 75 MPa [12].

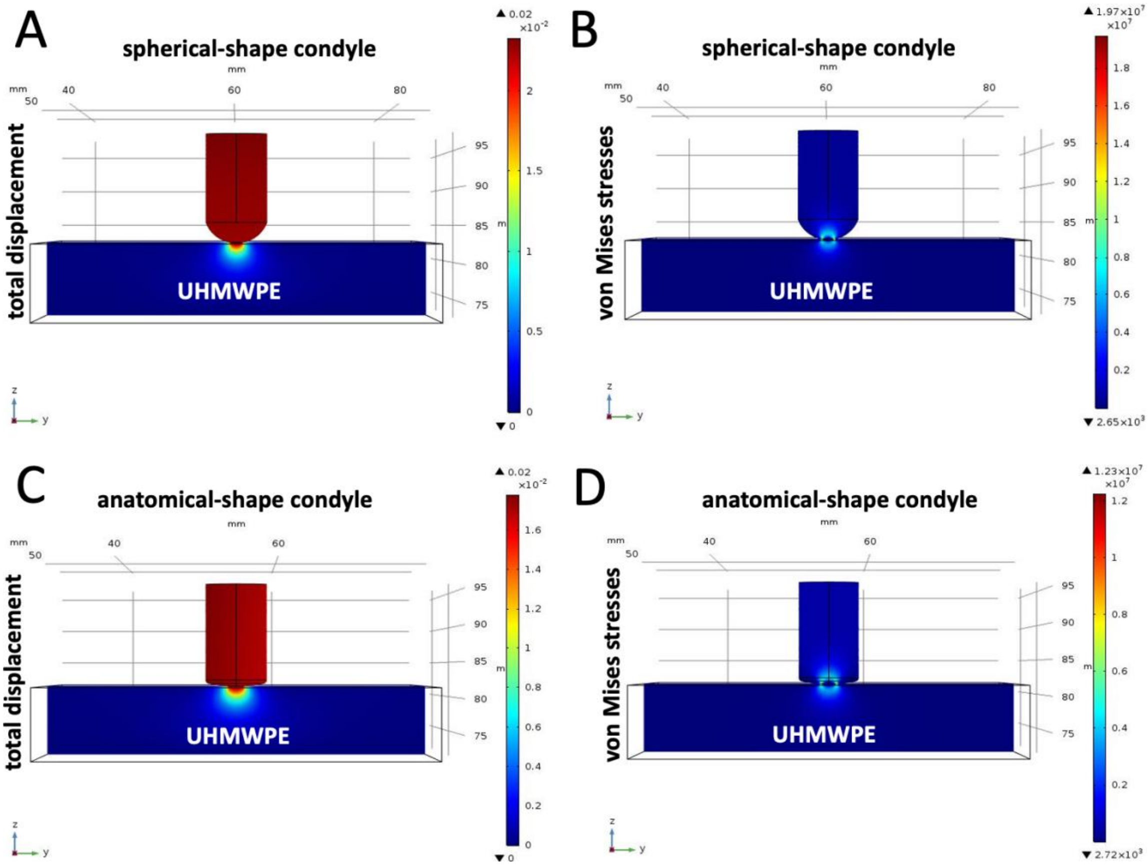

Figure 25- Total displacement for **(A)** spherical- and **(C)** anatomical-shape CoCrMo condyle against UHMWPE. Maximum Von Mises stresses for **(B)** spherical- and **(D)** anatomical-shape CoCrMo condyle against UHMWPE.

In this study, anatomical-shape CoCrMo condyle promoted a significantly decrease in the Von Mises stresses against the UHMWPE surfaces. In fact, the anatomical TMJ TJR design provided a higher bearing surface area (Figure 21) leading to lower contact stresses. That can prevent stress concentration at small bearing area which may result in increased wear rate of the materials for TMJ TJR. A previous study reported lower mean stress values around custom condyle–ramus components and surrounding bone when compared to stock condyle–ramus components and surrounding bone [112]. An increase in the bearing contact area promotes a distribution of forces on the wear track that resulted in lower values of von Mises stresses. A lower magnitude of stresses would considerably decrease the wear of the bearing surfaces. Also, UHMWPE has a low elastic modulus and high ductility leading to a high absorption of energy from the normal loading. That results in a proper distribution of forces leading to lower stress on the prosthetic fossa. The stresses on the bearing surfaces of TMJ TJR play the significant role on the wear and fracture of the materials. Regardless the material, the loading from occlusal contact or chewing is located at a small bearing area of the TMJ TJR condyle-to-fossa assembly that results in high stresses and wear rate of materials [3,169].

Over rotational movement in TMJ TJR, maximum compression forces were recorded from 90 up to 270 N, depending on patients' opening angle, loading magnitude, and action points [230]. An increase in the maximum contact pressure on the condyle–ramus component was reported when it was anteriorly rotated in the fossa component [87,120]. Indeed, a high concentration of stresses and misfit of the prosthetic joint has been reported in the literature [4]. Furthermore, patients who are in need of a TMJ TJR most likely exhibit altered TMJ function, resulting in limited movements and reduced functional loads [84]. The loading on the condyle to fossa region is resultant from the occlusal loading that differs on the posterior (molars and premolars) and anterior teeth. Also, loading on prosthetic teeth involving dental implants quite lower when compared to natural teeth of the patients. In patients with temporomandibular disorders (TMD) involving bruxism, the load magnitude from the maxillo-mandibular relationship can be higher when compared with a non-pathological condition. In TMD issues including TMJ TJR, the resultant contact pressure between condyle and articular fossa leads to higher risks of fracture and wear of the related TMJ TJR materials [3,14].

Among several methods of mechanical assessment, the finite element method (FEM) has been applied to predict displacement and stress distribution through different prosthetic design and materials [93,231]. Thus, factors related to loading, design, and materials can be evaluated before experimental mechanical assessment. FEM has become a attractive tool for studying the stress distribution on the structural materials for TMJ TJR, as well as detecting potential issues affecting the prosthetic stability, degradation, and bone remodelling [4]. Several studies have shown findings from computational simulations associated or not with experimental tests on TMJ TJR to predict the stress magnitude on their components [4,12,93,119]. The presence of different materials promotes abrupt variations of properties (hardness, elastic modulus, yield strength). Also, aspects related to the design of the TMJ TJR such as length, diameter, and shape can be optimized to decrease the stress distribution through the materials towards the bone. Some previous studies utilized similar mean loading values to evaluate the stress distribution, while other studies varied the loading to study its influence on stress distribution through materials and supporting bone tissues. Regarding the positioning of the TMJ TJR condyle, high stresses were detected when the condyle was placed at the outer and posterior regions of the mandibular ramus [12,93,183]. The Von Mises stress values on the TMJ condyle–ramus component during simulated clenching were below 160 MPa [123]. In a previous study, mean values of von Mises and shear stress were lower for titanium-based condyle–ramus components than those measured for CoCrMo-based condyle–ramus [121].

However, finite element analyses have shown limitations considering the physical properties of different materials for TMJTJR. Results acquired from FEM depends on the modeling of the prosthetics, implants, and tissues as well the parameters used for biomechanical analyses. For instance, boundary conditions on FEM varied widely among the previous studies. In most studies, constrained regions were located on the lower incisors and condyles of the models and the constraints were designed in two or three directions in each region. Generally, the z-axis was fixed for both the lower incisors and condyles, although there was variation in the x- and y-axes in the previous studies [93]. Also, the properties of soft and bone surrounding the prosthetic and implant tissues varies regarding the patients' conditions and methods used for physical characterization. Limitations on modeling tissues are well-known since the human tissues have inherent complex structures leading to variable properties. Significant dissimilarities in the physical properties of the material representing the host bone structures are shown in the literature [4]. Also, there are variations in the positioning of the muscle insertion and modelling anatomical issues. Further experimental validation of the FEM models is required for different patient conditions (e.g., bone quality, sex, age), surgical sites, and different TMJTJR design [4].

The present study has also some limitations considering experimental conditions for wear testing considering clinical situations. In fact, the friction and wear of the materials vary regarding the load, stroke length, counterbody, and environment [218]. Most studies assessed mean values for such parameters that can mimic regular TMJ TJR movements. Some studies attempt to assess similar parameters to perform a comparison of results and therefore understanding major pathways on the degradation of surfaces by wear processes. As previously mentioned, the normal loading is not a standard parameter and that can vary on the condyle-to-fossa bearing contacts. Also, the stroke length and frequency of reciprocating sliding movements depend on the mastication cycle and TMJ TJR motions. The environment surrounding the condyle-to-fossa bearing surfaces is not accurate as found at *in vivo* situations. In this study, an electrolyte containing distilled water and inorganic compounds was used to mimic the TMJ TJR surrounding electrolyte environment. Even though the test medium did not involve proteins, the coefficient of friction of the bearing surfaces was quite low when compared to results found in literature. Most of studies utilized solutions containing proteins or bovine serum medium that induce the coating of the alloplastic bearing surfaces with a protein-based thin film. However, further studies should provide detailed analyses on the removal of the protein-based thin film over the reciprocating sliding testing due to the stresses and increased temperature.

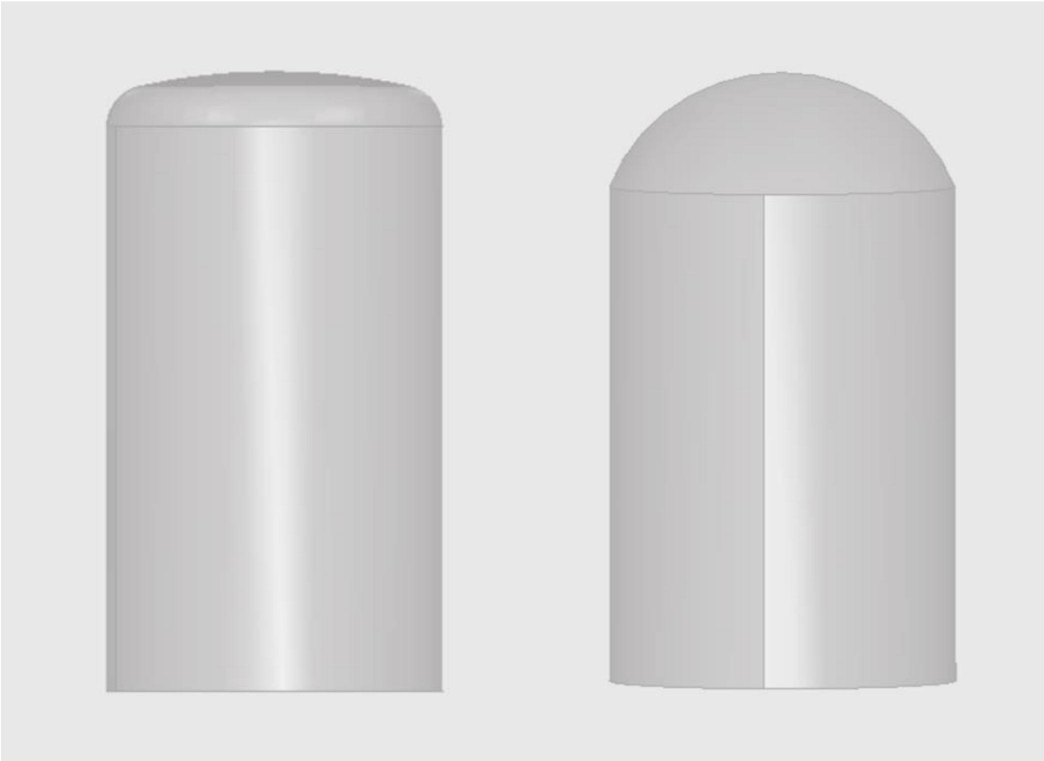

Chapter 4
Conclusions

4. Conclusions

Within the limitations of the experimental and theoretical evaluation performed in this study, the main outcomes of this work can be drawn as follow. On reciprocating sliding wear, different TMJ TJR condyle design revealed similar evolution on the coefficient of friction. However, the specific wear rate estimated for the spherical-shape condyle design was higher when compared with the wear rate values recorded for the anatomical-shape condyle design. Abrasion, detachment, and adhesion of material were identified as the dominant wear pathways for both the tribological pair of materials. Plastic deformation, micro-cracks, grooves, ejection of particles, and formation of tribolayers were detected by scanning electron microscopy. Also, the transference of the polymeric material was confirmed by chemical analyses that revealed the progressive degradation of the bearing surfaces. The damage caused by cyclic frictional loading and abrasive particles were more detrimental to the CoCrMo/UHMWPE bearing surfaces when compared with the UHMWPE/Ti6Al4V. pair. The anatomical-shape condyle decreased the stresses on the bearing surfaces and therefore the degradation and loss of material was decreased. Such results bring insights to the development of novel materials and an enhancement in the long term mechanical performance of TMJ TJR.

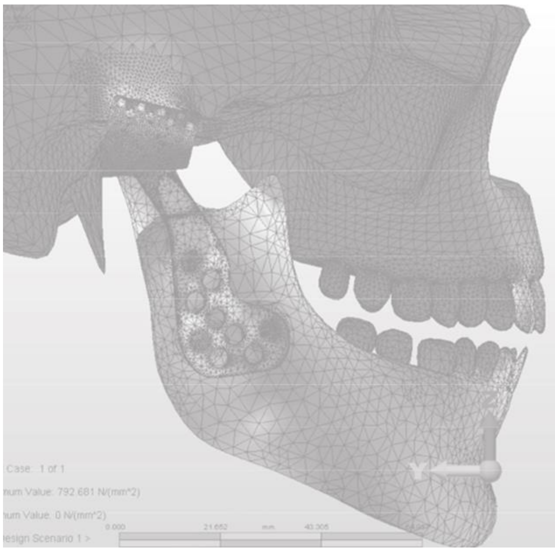

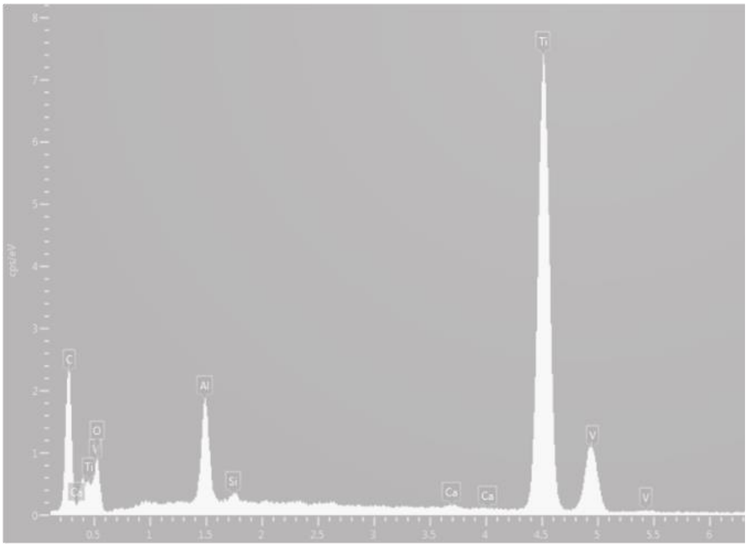

Chapter 5
Future perspectives

5. Future perspectives

While hip and Knee TJR systems are widely accepted as standard end-stage treatment options in orthopaedic surgery, the TMJ TJR system is still seen as an obscurity in the field of maxillofacial surgery, partly due to previous negative experiences with unsuitable materials or flawed mechanical design. However recent research show that the demand for use of TMJ TJR devices will increase up until 2030. The bio-mechanical behaviour of these devices can be improved by optimizing the shape of the articulating surfaces based on wear tests and confirmation of proper clinical performance on long-term follow-up studies. One of the major limitations of the existing devices is the lack of translational movement of the condyle therefore, a future TMJ TJR must allow the anterior movement of the condyle and fully opening of the mouth and also some mediolateral movement. Future studies of TMJ TJR are based on the development of design and materials in combination with tissue engineering. The development of tissues is showing promising results although further studies are required considering bone substitutes and the use of stem cells. Advancements have been made to manufacturing different alloys decreasing the risks of stress shielding, as the elastic modulus of the existent alloys is still very high comparing to the elastic modulus of the bone. The development of β-titanium alloys that contains Nb, Zr, Mo, Ta for replacing toxic alloying elements such as Al and V. Also, there is wide number of surface modification techniques to improve performance. Surface modification techniques involve altering the surface topography and/or the chemical composition of the surface by applying thin layers such as TiN or DLC coating. Hybrid materials involving metal and ceramics can also be designed for enhanced mechanical and biological outcomes. Another way to generate less wear is replacing the materials for producing the articular fossa component by using high performance polymers or composites. Finite element analysis stands out as a powerful tool for the designing of future generations of TMJ TJR using the correlations between modelling and experimental studies. A multidisciplinary approach involving medicine, dentistry, and engineering researchers should improve the knowledge on the TMJ TJR leading to the development of alternative materials and clinical procedures. Future large-scale prospective studies involving serial measurements in homogenous groups of patients may further elucidate the impact of these findings.

References

1. Anabtawi M, Beck P, Lemons J. Biocompatibility testing of simulated total joint arthoplasty articulation debris. Journal of Biomedical Materials Research - Part B Applied Biomaterials. J Biomed Mater Res B Appl Biomater; 2008;84:478–85.

2. Ramos AM, Mesnard M. The stock alloplastic temporomandibular joint implant can influence the behavior of the opposite native joint: A numerical study. Journal of Cranio-Maxillofacial Surgery. Churchill Livingstone; 2015;43:1384–91.

3. Kerwell S, Alfaro M, Pourzal R, Lundberg HJ, Liao Y, Sukotjo C, et al. Examination of failed retrieved temporomandibular joint (TMJ) implants. Acta Biomaterialia. Elsevier Ltd; 2016;32:324–35.

4. Rodrigues YL, Mathew MT, Mercuri LG, da Silva JSP, Henriques B, Souza JCM. Biomechanical simulation of temporomandibular joint replacement (TMJR) devices: a scoping review of the finite element method. International Journal of Oral and Maxillofacial Surgery. Churchill Livingstone; 2018. p. 1032–42.

5. De Meurechy N, Mommaerts MY. Alloplastic temporomandibular joint replacement systems: a systematic review of their history. International Journal of Oral and Maxillofacial Surgery. Churchill Livingstone; 2018. p. 743–54.

6. Mamidi SK, Klutcharch K, Rao S, Souza JCM, Mercuri LG, Mathew MT. Advancements in temporomandibular joint total joint replacements (TMJR). Biomedical Engineering Letters. Springer Verlag; 2019. p. 169–79.

7. Souza JCM, Barbosa SL, Ariza EA, Henriques M, Teughels W, Ponthiaux P, et al. How do titanium and Ti6Al4V corrode in fluoridated medium as found in the oral cavity? An in vitro study. Materials Science and Engineering C. Elsevier B.V.; 2015;47:384–93.

8. Santos RLP, Buciumeanu M, Silva FS, Souza JCM, Nascimento RM, Motta F V., et al. Tribological behaviour of glass-ceramics reinforced by Yttria Stabilized Zirconia. Tribology International. Elsevier; 2016;102:361–70.

9. van Loon JP, de Bont LGM, Boering G. Evaluation of temporomandibular joint prostheses. Review of the literature from 1946 to 1994 and implications for future prosthesis designs. Journal of Oral and Maxillofacial Surgery. J Oral Maxillofac Surg; 1995. p. 984–96.

10. Marwa Hattab, Ben Hassen S, Cecilia-Buenestado JA, Rodríguez-Castellón E, Ben Amor Y. Comparative Electrochemical Study of Pure Magnesium Behavior in Ringer's and Hank's Solutions. Protection of Metals and Physical Chemistry of Surfaces. Pleiades journals; 2021;57:168–80.

11. Abramowicz S, Barbick M, Rose SP, Dolwick MF. Adaptability of stock TMJ prosthesis to joints that were previously treated with custom joint prosthesis. International Journal of Oral and Maxillofacial Surgery. 2012;41:518–20.

12. Ramos A, Mesnard M. A new condyle implant design concept for an alloplastic temporomandibular joint in bone resorption cases. Journal of Cranio-Maxillofacial Surgery. Churchill Livingstone; 2016;44:1670–7.

13. Baena JC, Wu J, Peng Z. Wear performance of UHMWPE and reinforced UHMWPE composites in arthroplasty applications: A review. Lubricants. 2015;3:413–36.

14. Mathew MT, Kerwell S, Lundberg HJ, Sukotjo C, Mercuri LG. Tribocorrosion and oral and maxillofacial surgical devices. British Journal of Oral and Maxillofacial Surgery. Churchill Livingstone; 2014. p. 396–400.

15. Souza JCM, Henriques M, Teughels W, Ponthiaux P, Celis JP, Rocha LA. Wear and Corrosion Interactions on Titanium in Oral Environment: Literature Review. Journal of Bio- and Tribo-Corrosion. Springer International Publishing; 2015;1.

16. Landolt D. Corrosion and surface chemistry of metals. 1st edn. EPFL Press, Switzerland. 2007.

17. Barril S, Debaud N, Mischler S, Landolt D. A tribo-electrochemical apparatus for in vitro investigation of fretting-corrosion of metallic implant materials. Wear. Elsevier; 2002;252:744–54.

18. Souza JCM, Barbosa SL, Ariza E, Celis JP, Rocha LA. Simultaneous degradation by corrosion and wear of titanium in artificial saliva containing fluorides. Wear. 2012;292–293:82–8.

19. Alves SA, Beline T, Barão VAR, Sukotjo C, Mathew MT, Rocha LA, et al. Chapter 3 - Degradation of titanium-based implants. In: Souza JCM, Hotza D, Henriques B, Boccaccini ARBT-NB for C-M and OA, editors. Advanced Nanomaterials. Elsevier; 2018. p. 41–62.

20. Sinno H, Tahiri Y, Gilardino M, Bobyn D. Engineering alloplastic

temporomandibular joint replacements. McGill journal of medicine : MJM : an international forum for the advancement of medical sciences by students [Internet]. 2011 [cited 2020 Feb 6];13:63. Available from: http://www.ncbi.nlm.nih.gov/pubmed/22363183

21. Guarda-Nardini L, Manfredini D, Ferronato G. Temporomandibular joint total replacement prosthesis: current knowledge and considerations for the future. International Journal of Oral and Maxillofacial Surgery. Churchill Livingstone; 2008. p. 103–10.

22. Kraeima J, Merema BJ, Witjes MJH, Spijkervet FKL. Development of a patient-specific temporomandibular joint prosthesis according to the Groningen principle through a cadaver test series. Journal of Cranio-Maxillofacial Surgery. Churchill Livingstone; 2018;46:779–84.

23. Tanaka E, Kawai N, Tanaka M, Todoh M, Van Eijden T, Hanaoka K, et al. The frictional coefficient of the temporomandibular joint and its dependency on the magnitude and duration of joint loading. Journal of dental research [Internet]. J Dent Res; 2004 [cited 2022 Jul 4];83:404–7. Available from: https://pubmed.ncbi.nlm.nih.gov/15111633/

24. Van Loon JP, Verkerke GJ, De Vries MP, De Bont LGM. Design and wear testing of a temporomandibular joint prosthesis articulation. Journal of Dental Research. Intern. and American Associations for Dental Research; 2000;79:715–21.

25. Ramos A, Mesnard M. Load transfer in Christensen® TMJ in alloplastic total joint replacement for two different mouth apertures. Journal of Cranio-Maxillofacial Surgery. Churchill Livingstone; 2014;42:1442–9.

26. Tanaka E. Biomechanical and tribological properties of the temporomandibular joint. Frontiers of Oral and Maxillofacial Medicine [Internet]. AME Publishing Company; 2021 [cited 2022 Jul 4];3. Available from: https://fomm.amegroups.com/article/view/50922/html

27. Singh M, Detamore MS. Biomechanical properties of the mandibular condylar cartilage and their relevance to the TMJ disc [Internet]. Journal of Biomechanics. J Biomech; 2009 [cited 2021 Jun 12]. p. 405–17. Available from: https://pubmed.ncbi.nlm.nih.gov/19200995/

28. Tanaka E, Kawai N, Hanaoka K, Van Eijden T, Sasaki A, Aoyama J, et al. Shear properties of the temporomandibular joint disc in relation to compressive and shear strain. Journal of Dental Research [Internet]. SAGE Publications Inc.; 2004 [cited 2021 Jun

12];83:476–9. Available from: https://journals.sagepub.com/doi/abs/10.1177/154405910408300608

29. Guarda-Nardini L, Manfredini D, Ferronato G. Total temporomandibular joint replacement: A clinical case with a proposal for post-surgical rehabilitation. Journal of Cranio-Maxillofacial Surgery. Churchill Livingstone; 2008;36:403–9.

30. Muhandiram J, Wang B, Chizari M. Dynamic Simulation of the Temporomandibular Joint. Transactions on Engineering Technologies [Internet]. Springer, Dordrecht; 2015 [cited 2022 Aug 9];697–705. Available from: https://link.springer.com/chapter/10.1007/978-94-017-9804-4_49

31. Schiffman E, Ohrbach R, Truelove E, Look J, Anderson G, Goulet J-P, et al. Diagnostic Criteria for Temporomandibular Disorders (DC/TMD) for Clinical and Research Applications: Recommendations of the International RDC/TMD Consortium Network * and Orofacial Pain Special Interest Group † HHS Public Access. J Oral Facial Pain Headache. 2014;28:6–27.

32. Bormane DDS, Kakkeri RB. Detection of Temporomandibular Joint Disorder Using Surface Electromypgraphy by Supervised Classification Models. Materials Today: Proceedings. Elsevier; 2021;

33. Ahmad M, Schiffman EL. Temporomandibular Joint Disorders and Orofacial Pain. Dental Clinics of North America. W.B. Saunders; 2016;60:105–24.

34. Peck CC, Goulet JP, Lobbezoo F, Schiffman EL, Alstergren P, Anderson GC, et al. Expanding the taxonomy of the diagnostic criteria for temporomandibular disorders. Journal of Oral Rehabilitation. 2014;41:2–23.

35. Onoriobe U, Miloro M, Sukotjo C, Mercuri LG, Lotesto A, Eke R. How Many Temporomandibular Joint Total Joint Alloplastic Implants Will Be Placed in the United States in 2030? Journal of Oral and Maxillofacial Surgery. W.B. Saunders; 2016;74:1531–8.

36. Mercuri LG. Temporomandibular Joint Disorder Management in Oral and Maxillofacial Surgery. Journal of oral and maxillofacial surgery : official journal of the American Association of Oral and Maxillofacial Surgeons [Internet]. J Oral Maxillofac Surg; 2017 [cited 2022 Jan 29];75:927–30. Available from: https://pubmed.ncbi.nlm.nih.gov/27889533/

37. Mercuri LG. Total joint reconstruction--autologous or alloplastic. Oral and maxillofacial surgery clinics of North America [Internet]. Oral Maxillofac Surg Clin North Am; 2006 [cited 2022 Jan 29];18:399–410. Available from: https://pubmed.ncbi.nlm.nih.gov/18088840/

38. Gakhal MK, Gupta B, Sidebottom AJ. Analysis of outcomes after revision replacement of failed total temporomandibular joint prostheses. British Journal of Oral and Maxillofacial Surgery. Churchill Livingstone; 2020;58:220–4.

39. Li DTS, Leung YY. Temporomandibular disorders: Current concepts and controversies in diagnosis and management. Diagnostics. MDPI; 2021;11.

40. Liu F, Steinkeler A. Epidemiology, diagnosis, and treatment of temporomandibular disorders. Dental Clinics of North America. W.B. Saunders; 2013;57:465–79.

41. Stegenga B, De Bont LGM, Boering G, Van Willigen JD. Tissue responses to degenerative changes in the temporomandibular joint: a review. Journal of oral and maxillofacial surgery : official journal of the American Association of Oral and Maxillofacial Surgeons [Internet]. J Oral Maxillofac Surg; 1991 [cited 2022 Jun 24];49:1079–88. Available from: https://pubmed.ncbi.nlm.nih.gov/1890521/

42. Lai L, Huang C, Zhou F, Xia F, Xiong G. Finite elements analysis of the temporomandibular joint disc in patients with intra-articular disorders. BMC Oral Health [Internet]. BioMed Central Ltd.; 2020 [cited 2022 Jul 4];20:1–8. Available from: https://bmcoralhealth.biomedcentral.com/articles/10.1186/s12903-020-01074-x

43. Ingawalé S, Goswami T. Temporomandibular Joint: Disorders, Treatments, and Biomechanics.

44. Pellizoni SEP, Salioni MAC, Juliano Y, Guimarães AS, Alonso LG. Temporomandibular joint disc position and configuration in children with functional unilateral posterior crossbite: a magnetic resonance imaging evaluation. American journal of orthodontics and dentofacial orthopedics : official publication of the American Association of Orthodontists, its constituent societies, and the American Board of Orthodontics [Internet]. Am J Orthod Dentofacial Orthop; 2006 [cited 2022 Aug 12];129:785–93. Available from: https://pubmed.ncbi.nlm.nih.gov/16769497/

45. Hibi H, Ueda M. Body posture during sleep and disc displacement in the temporomandibular joint: a pilot study. Journal of oral rehabilitation [Internet]. J Oral Rehabil; 2005 [cited 2022 Aug 12];32:85–9. Available from: https://pubmed.ncbi.

nlm.nih.gov/15641972/

46. Milam SB, Schmitz JP. Molecular biology of temporomandibular joint disorders: Proposed mechanisms of disease. Journal of Oral and Maxillofacial Surgery [Internet]. Elsevier; 1995 [cited 2022 Aug 12];53:1448–54. Available from: http://www.joms.org/article/0278239195906754/fulltext

47. Abubaker AO, Hebda PC, Gunsolley JN. Effects of sex hormones on protein and collagen content of the ternporomandibular joint disc of the rat. Journal of Oral and Maxillofacial Surgery [Internet]. W.B. Saunders; 1996 [cited 2022 Aug 12];54:721–7. Available from: http://www.joms.org/article/S0278239196906904/fulltext

48. Detamore MS, Athanasiou KA, Mao J. A call to action for bioengineers and dental professionals: Directives for the future of TMJ bioengineering. Annals of Biomedical Engineering [Internet]. Springer; 2007 [cited 2022 Aug 12];35:1301–11. Available from: https://link.springer.com/article/10.1007/s10439-007-9298-6

49. Milam SB, Zardeneta G, Schmitz JP. Oxidative stress and degenerative temporomandibular joint disease: A proposed hypothesis. Journal of Oral and Maxillofacial Surgery [Internet]. Elsevier; 1998 [cited 2022 Aug 12];56:214–23. Available from: http://www.joms.org/article/S0278239198908722/fulltext

50. Zardeneta G, Milam SB, Schmitz JP. Presence of denatured hemoglobin deposits in diseased temporomandibular joints. Journal of Oral and Maxillofacial Surgery [Internet]. W.B. Saunders; 1997 [cited 2022 Aug 13];55:1242–8. Available from: http://www.joms.org/article/S0278239197901762/fulltext

51. Zardeneta G, Milam SB, Schmitz JP. Iron-dependent generation of free radicals: Plausible mechanisms in the progressive deterioration of the temporomandibular joint. Journal of Oral and Maxillofacial Surgery [Internet]. W.B. Saunders; 2000 [cited 2022 Aug 13];58:302–8. Available from: http://www.joms.org/article/S0278239100900600/fulltext

52. Milam SB. The process of lubrication impairment and its involvement in temporomandibular joint disc displacement: A theoretical concept: Discussion. Journal of Oral and Maxillofacial Surgery [Internet]. W.B. Saunders; 2001 [cited 2022 Aug 12];59:45. Available from: http://www.joms.org/article/S0278239101829347/fulltext

53. Wilkes CH. Internal Derangements of the Temporomandibular Joint: Pathological Variations. Archives of Otolaryngology–Head & Neck Surgery [Internet]. American

Medical Association; 1989 [cited 2022 Jun 22];115:469–77. Available from: https://jamanetwork.com/journals/jamaotolaryngology/fullarticle/617527

54. Scrivani SJ, Keith DA, Kaban LB. Temporomandibular disorders. The New England journal of medicine [Internet]. N Engl J Med; 2008 [cited 2022 Jun 24];359:2693–705. Available from: https://pubmed.ncbi.nlm.nih.gov/19092154/

55. La Touche R, París-Alemany A, Von Piekartz H, Mannheimer JS, Fernández-Carnero J, Rocabado M. The influence of cranio-cervical posture on maximal mouth opening and pressure pain threshold in patients with myofascial temporomandibular pain disorders. Clinical Journal of Pain. Lippincott Williams and Wilkins; 2011;27:48–55.

56. Shimada A, Ishigaki S, Matsuka Y, Komiyama O, Torisu T, Oono Y, et al. Effects of exercise therapy on painful temporomandibular disorders. Journal of Oral Rehabilitation. Blackwell Publishing Ltd; 2019;46:475–81.

57. Özden MC, Atalay B, Özden AV, Çankaya AB, Kolay E, Yıldırım S. Efficacy of dry needling in patients with myofascial temporomandibular disorders related to the masseter muscle. Cranio : the journal of craniomandibular practice [Internet]. Cranio; 2020 [cited 2022 Jun 24];38. Available from: https://pubmed.ncbi.nlm.nih.gov/30296920/

58. Kütük SG, Özkan Y, Kütük M, Özdaş T. Comparison of the efficacies of dry needling and botox methods in the treatment of myofascial pain syndrome affecting the temporomandibular joint. Journal of Craniofacial Surgery [Internet]. Lippincott Williams and Wilkins; 2019 [cited 2022 Jun 24];30:1556–9. Available from: https://journals.lww.com/jcraniofacialsurgery/Fulltext/2019/07000/Comparison_of_the_Efficacies_of_Dry_Needling_and.58.aspx

59. Dietrich L, Rodrigues IVS, De Assis Costa MDM, Carvalho RF, Da Silva GR. Acupuncture in Temporomandibular Disorders Painful Symptomatology: An Evidence-Based Case Report. European journal of dentistry [Internet]. Eur J Dent; 2020 [cited 2022 Jun 24];14:692–6. Available from: https://pubmed.ncbi.nlm.nih.gov/33003235/

60. Li W, Wu J. Treatment of Temporomandibular Joint Disorders by Ultrashort Wave and Extracorporeal Shock Wave: A Comparative Study. Medical science monitor : international medical journal of experimental and clinical research [Internet]. Med Sci Monit; 2020 [cited 2022 Jun 24];26. Available from: https://pubmed.ncbi.nlm.nih.gov/32564051/

61. Kraus M, Reinhart E, Krause H, Reuther J. [Low energy extracorporeal shockwave

therapy (ESWT) for treatment of myogelosis of the masseter muscle]. Mund-, Kiefer- und Gesichtschirurgie : MKG [Internet]. Mund Kiefer Gesichtschir; 1999 [cited 2022 Jun 24];3:20–3. Available from: https://pubmed.ncbi.nlm.nih.gov/10077963/

62. Guarda-Nardini L, Manfredini D, Ferronato G. Arthrocentesis of the temporomandibular joint: a proposal for a single-needle technique. Oral surgery, oral medicine, oral pathology, oral radiology, and endodontics [Internet]. Oral Surg Oral Med Oral Pathol Oral Radiol Endod; 2008 [cited 2022 Aug 9];106:483–6. Available from: https://pubmed.ncbi.nlm.nih.gov/18424123/

63. Al-Moraissi EA, Wolford LM, Ellis E, Neff A. The hierarchy of different treatments for arthrogenous temporomandibular disorders: A network meta-analysis of randomized clinical trials. Journal of Cranio-Maxillofacial Surgery. Churchill Livingstone; 2020;48:9–23.

64. Wolford L, Movahed R, Teschke M, Fimmers R, Havard D, Schneiderman E. Temporomandibular joint ankylosis can be successfully treated with TMJ concepts patient-fitted total joint prosthesis and autogenous fat grafts. Journal of Oral and Maxillofacial Surgery. W.B. Saunders; 2016;74:1215–27.

65. Arakeri G, Kusanale A, Zaki GA, Brennan PA. Pathogenesis of post-traumatic ankylosis of the temporomandibular joint: a critical review. British Journal of Oral and Maxillofacial Surgery [Internet]. Elsevier; 2012 [cited 2022 Aug 9];50:8–12. Available from: http://www.bjoms.com/article/S0266435610003050/fulltext

66. Hagedorn TJ, Grosse IR, Krishnamurty S. A concept ideation framework for medical device design. Journal of Biomedical Informatics. Academic Press; 2015;55:218–30.

67. Ramos A, Mesnard M, Relvas C, Completo A, Simões JA. Implant fixation of novel and commercial TMJ implants. Computer methods in biomechanics and biomedical engineering [Internet]. 2012 [cited 2021 Mar 30];15 Suppl 1:324–5. Available from: http://www.tandfonline.com/doi/abs/10.1080/10255842.2012.713600

68. Sonnenburg I, Sonnenburg M. Total condylar prosthesisfor alloplastic jaw articulation replacement. Journal of Maxillofacial Surgery. Churchill Livingstone; 1985;13:131–5.

69. Mercuri LG. Osteoarthritis, Osteoarthrosis, and Idiopathic Condylar Resorption. Oral and Maxillofacial Surgery Clinics of North America. Elsevier; 2008;20:169–83.

70. Mercuri LG. Alloplastic temporomandibular joint replacement: Rationale for the use

of custom devices. International Journal of Oral and Maxillofacial Surgery. Churchill Livingstone; 2012. p. 1033–40.

71. Elledge R, Mercuri LG, Attard A, Green J, Speculand B. Review of emerging temporomandibular joint total joint replacement systems. British Journal of Oral and Maxillofacial Surgery. Churchill Livingstone; 2019. p. 722–8.

72. Mercuri LG. Costochondral Graft Versus Total Alloplastic Joint for Temporomandibular Joint Reconstruction. Oral and Maxillofacial Surgery Clinics of North America. W.B. Saunders; 2018. p. 335–42.

73. Lypka M, Yamashita DDR. Exuberant Foreign Body Giant Cell Reaction to a Teflon/Proplast Temporomandibular Joint Implant: Report of a Case. Journal of Oral and Maxillofacial Surgery [Internet]. Elsevier; 2007 [cited 2022 Aug 9];65:1680–4. Available from: http://www.joms.org/article/S0278239106018866/fulltext

74. Driemel O, Braun S, Müller-Richter UDA, Behr M, Reichert TE, Kunkel M, et al. Historical development of alloplastic temporomandibular joint replacement after 1945 and state of the art. International Journal of Oral and Maxillofacial Surgery. 2009. p. 909–20.

75. Yoda T, Ogi N, Yoshitake H, Kawakami T, Takagi R, Murakami K, et al. Clinical guidelines for total temporomandibular joint replacement. The Japanese Dental Science Review [Internet]. Elsevier; 2020 [cited 2022 Jun 28];56:77. Available from: /pmc/articles/PMC7310689/

76. Gerbino G, Zavattero E, Bosco G, Berrone S, Ramieri G. Temporomandibular joint reconstruction with stock and custom-made devices: Indications and results of a 14-year experience. Journal of Cranio-Maxillofacial Surgery. Churchill Livingstone; 2017;45:1710–5.

77. Sidebottom AJ, Gruber E. One-year prospective outcome analysis and complications following total replacement of the temporomandibular joint with the TMJ Concepts system. British Journal of Oral and Maxillofacial Surgery. Churchill Livingstone; 2013;51:620–4.

78. Mercuri LG, Mathew MT, Kerwell S, Lundberg H, Sukotjo C. Temporomandibular Joint Replacement Device Research Wear and Corrosion Technology Transfer from Orthopedics. Journal of Bio- and Tribo-Corrosion. Springer International Publishing; 2015;1.

79. Lee S-H, Ryu D-J, Kim H-S, Kim H-G, Huh J-K. Alloplastic total temporomandibular joint replacement using stock prosthesis: a one-year follow-up report of two cases. Journal of the Korean Association of Oral and Maxillofacial Surgeons. The Korean Association of Oral and Maxillofacial Surgeons (KAMJE); 2013;39:297.

80. Gonzalez-Perez LM, Gonzalez-Perez-Somarriba B, Centeno G, Vallellano C, Montes-Carmona JF, Torres-Carranza E, et al. Prospective study of five-year outcomes and postoperative complications after total temporomandibular joint replacement with two stock prosthetic systems. British Journal of Oral and Maxillofacial Surgery. Churchill Livingstone; 2020;58:69–74.

81. Kanatsios S, Breik O, Dimitroulis G. Biomet stock temporomandibular joint prosthesis: Long-term outcomes of the use of titanium condyles secured with four or five condylar fixation screws. Journal of Cranio-Maxillofacial Surgery. Churchill Livingstone; 2018;46:1697–702.

82. Giannakopoulos HE, Sinn DP, Quinn PD. Biomet microfixation temporomandibular joint replacement system: A 3-year follow-up study of patients treated during 1995 to 2005. Journal of Oral and Maxillofacial Surgery. W.B. Saunders; 2012;70:787–94.

83. Ferreira FM, Cunali RS, Bonotto D, Farias AC de, Cunali PA. Total temporomandibular joint alloplastic reconstruction. Revista Dor. GN1 Genesis Network; 2014;15.

84. Mercuri LG. The role of custom-made prosthesis for temporomandibular joint replacement. Revista Espanola de Cirugia Oral y Maxilofacial. No longer published by Elsevier; 2013;35:1–10.

85. Johnson NR, Roberts MJ, Doi SA, Batstone MD. Total temporomandibular joint replacement prostheses: a systematic review and bias-adjusted meta-analysis. International Journal of Oral and Maxillofacial Surgery. Churchill Livingstone; 2017. p. 86–92.

86. Zou L, Zhang L, He D, Yang C, Zhao J, Ellis E. Clinical and Radiologic Follow-Up of Zimmer Biomet Stock Total Temporomandibular Joint Replacement After Surgical Modifications. Journal of Oral and Maxillofacial Surgery. W.B. Saunders; 2018;76:2518–24.

87. Ackland DC, Moskaljuk A, Hart C, Vee Sin Lee P, Dimitroulis G. Prosthesis Loading after Temporomandibular Joint Replacement Surgery: A Musculoskeletal Modeling

Study. Journal of Biomechanical Engineering. American Society of Mechanical Engineers (ASME); 2015;137.

88. Hu Y, Zhang L, He D, Yang C, Chen M, Zhang S, et al. Simultaneous treatment of temporomandibular joint ankylosis with severe mandibular deficiency by standard TMJ prosthesis. Scientific Reports [Internet]. 2017 [cited 2020 Feb 6];7:45271. Available from: http://www.embase.com/search/results?subaction=viewrecord&from=export&id=L625216354

89. Rhee S-H, Baek S-H, Park S-H, Kim J-C, Jeong C-G, Choi J-Y. Total joint reconstruction using computer-assisted surgery with stock prostheses for a patient with bilateral TMJ ankylosis. Maxillofacial Plastic and Reconstructive Surgery. Springer Science and Business Media LLC; 2019;41.

90. Moreira CVA, Serra AVP, Silva LOR, Fernandes ACF, de Azevedo RA. Total bilateral TMJ reconstruction for pain and dysfunction: Case report. International Journal of Surgery Case Reports. Elsevier Ltd; 2018;42:138–44.

91. De Meurechy N, Braem A, Mommaerts MY. Biomaterials in temporomandibular joint replacement: current status and future perspectives—a narrative review. International Journal of Oral and Maxillofacial Surgery. Churchill Livingstone; 2018. p. 518–33.

92. Zhao J, Zou L, He D, Ellis E. Comparison of bone adaptation after modification in biomet standard alloplastic temporomandibular joint prostheses. Journal of Cranio-Maxillofacial Surgery. Churchill Livingstone; 2018;46:1707–11.

93. Ramos A, Mesnard M. Christensen vs Biomet Microfixation alloplastic TMJ implant: Are there improvements? A numerical study. Journal of Cranio-Maxillofacial Surgery. Churchill Livingstone; 2015;43:1398–403.

94. Kanatas AN, Needs C, Smith AB, Moran A, Jenkins G, Worrall SF. Short-term outcomes using the Christensen patient-specific temporomandibular joint implant system: a prospective study. British Journal of Oral and Maxillofacial Surgery. Churchill Livingstone; 2012;50:149–53.

95. Wolford LM, Dingwerth DJ, Talwar RM, Pitta MC. Comparison of 2 temporomandibular joint total joint prosthesis systems. Journal of Oral and Maxillofacial Surgery. W.B. Saunders; 2003. p. 685–90.

96. Siegmund BJ, Winter K, Meyer-Marcotty P, Rustemeyer J. Reconstruction of the temporomandibular joint: a comparison between prefabricated and customized alloplastic prosthetic total joint systems. International Journal of Oral and Maxillofacial Surgery. Churchill Livingstone; 2019;48:1066–71.

97. Alves a C, Oliveira F, Wenger F, Ponthiaux P, Celis J-P, Rocha L a. Tribocorrosion behaviour of anodic treated titanium surfaces intended for dental implants. Journal of Physics D: Applied Physics. 2013;46:404001.

98. Thiem DGE, Al-Nawas B, Kämmerer PW. Technical report and rare case description-patient-specific spacer made of bone cement for the revision of a PSI-TMJ fossa after screw fracture. Journal of surgical case reports [Internet]. J Surg Case Rep; 2021 [cited 2022 Jul 20];2021. Available from: https://pubmed.ncbi.nlm.nih.gov/34804477/

99. Wolford LM, Mercuri LG, Schneiderman ED, Movahed R, Allen W. Twenty-year follow-up study on a patient-fitted temporomandibular joint prosthesis: The Techmedica/TMJ Concepts device. Journal of Oral and Maxillofacial Surgery. W.B. Saunders; 2015;73:952–60.

100. Ettinger KS, Arce K, Fillmore WJ, Van Ess JM, Yetzer JG, Viozzi CF. Does the Amount of Screw Fixation Utilized for the Condylar Component of the TMJ Concepts Total Temporomandibular Joint Reconstruction Predispose to Hardware Loss or Postoperative Complications? Journal of Oral and Maxillofacial Surgery. W.B. Saunders; 2016;74:1741–50.

101. Park J-H, Jo E, Cho H, Kim HJ. Temporomandibular joint reconstruction with alloplastic prosthesis: the outcomes of four cases. Maxillofacial Plastic and Reconstructive Surgery. Springer Science and Business Media LLC; 2017;39.

102. Ding R, Hua J, Qin H, He D. Biomechanical analysis of a temporomandibular joint prosthesis for lateral pterygoid muscle reattachment. Oral Surgery, Oral Medicine, Oral Pathology and Oral Radiology. Mosby; 2022;

103. Van Loon JP, Verkerke GJ, De Bont LGM, Liem RSB. Wear-testing of a temporomandibular joint prosthesis: UHMWPE and PTFE against a metal ball, in water and in serum. Biomaterials. Elsevier Science Ltd; 1999;20:1471–8.

104. Wolford LM. Temporomandibular joint devices: Treatment factors and outcomes. Oral Surgery, Oral Medicine, Oral Pathology, Oral Radiology, and Endodontics. Mosby Inc.; 1997;83:143–9.

105. Ingawale SM, Goswami T. Design and Finite Element Analysis of Patient-Specific Total Temporomandibular Joint Implants. 2022;

106. van Loon JP, de Bont LGM, Stegenga B, Spijkervet FKL, Verkerke GJ. Groningen temporomandibular joint prosthesis. Development and first clinical application. International journal of oral and maxillofacial surgery [Internet]. Blackwell Munksgaard; 2002 [cited 2020 Mar 26];31:44–52. Available from: http://www.ncbi.nlm.nih.gov/pubmed/11936399

107. Chen X, Wang Y, Mao Y, Zhou Z, Zheng J, Zhen J, et al. Biomechanical evaluation of Chinese customized three-dimensionally printed total temporomandibular joint prostheses: A finite element analysis. Journal of Cranio-Maxillofacial Surgery. Churchill Livingstone; 2018;46:1561–8.

108. Ramos A, Duarte RJ, Mesnard M. Prediction at long-term condyle screw fixation of temporomandibular joint implant: A numerical study. Journal of Cranio-Maxillofacial Surgery. Churchill Livingstone; 2015;43:469–74.

109. Mesnard M, Ramos A. Experimental and numerical predictions of Biomet® alloplastic implant in a cadaveric mandibular ramus. Journal of Cranio-Maxillofacial Surgery. Churchill Livingstone; 2016;44:608–15.

110. Mahdian N, Dostálová T, Daněk J, Nedoma J, Kohout J, Hubáček M, et al. 3D reconstruction of TMJ after resection of the cyst and the stress–strain analyses. Computer Methods and Programs in Biomedicine. Elsevier; 2013;110:279–89.

111. Mercuri LG. Alloplastic temporomandibular joint reconstruction. Oral Surgery, Oral Medicine, Oral Pathology, Oral Radiology, and Endodontics. Mosby Inc.; 1998. p. 631–7.

112. Ramos A, Mesnard M. Comparison of load transfers in TMJ replacement using a standard and a custom-made temporal component. Journal of Cranio-Maxillofacial Surgery. 2014;42:1766–72.

113. Gregolin RF, Zavaglia CADC, Tokimatsu RC, Pereira JA. Biomechanical Stress and Strain Analysis of Mandibular Human Region from Computed Tomography to Custom Implant Development. Advances in Materials Science and Engineering. Hindawi Limited; 2017;2017.

114. Turner CH, Burr DB. Basic biomechanical measurements of bone: A tutorial. Bone.

Elsevier; 1993;14:595–608.

115. Ramos A, Gonzalez-Perez LM, Infante-Cossio P, Mesnard M. Ex-vivo and in vitro validation of an innovative mandibular condyle implant concept. Journal of Cranio-Maxillofacial Surgery. Churchill Livingstone; 2019;47:112–9.

116. Gonzalez-Perez LM, Fakih-Gomez N, Gonzalez-Perez-Somarriba B, Centeno G, Montes-Carmona JF. Two-year prospective study of outcomes following total temporomandibular joint replacement. International Journal of Oral and Maxillofacial Surgery. Churchill Livingstone; 2016;45:78–84.

117. Mesnard M, Ramos A, Simões JA. Influences of implant condyle geometry on bone and screw strains in a temporomandibular implant. Journal of Cranio-Maxillofacial Surgery. Churchill Livingstone; 2014;42:194–200.

118. Ramos A, Completo A, Relvas C, Mesnard M, Simões JA. Straight, semi-anatomic and anatomic TMJ implants: The influence of condylar geometry and bone fixation screws. Journal of Cranio-Maxillofacial Surgery. Churchill Livingstone; 2011;39:343–50.

119. Ramos A, Mesnard M, Relvas C, Completo A, Simões JA. Theoretical assessment of an intramedullary condylar component versus screw fixation for the condylar component of a hemiarthroplasty alloplastic TMJ replacement system. Journal of Cranio-Maxillofacial Surgery. Churchill Livingstone; 2014;42:169–74.

120. Hsu JT, Huang HL, Tsai MT, Fuh LJ, Tu MG. Effect of screw fixation on temporomandibular joint condylar prosthesis. Journal of Oral and Maxillofacial Surgery [Internet]. J Oral Maxillofac Surg; 2011 [cited 2021 Jun 12];69:1320–8. Available from: https://pubmed.ncbi.nlm.nih.gov/21216062/

121. Kashi A, Chowdhury AR, Saha S. Finite element analysis of a TMJ implant. Journal of Dental Research [Internet]. SAGE Publications; 2010 [cited 2022 Aug 12];89:241–5. Available from: https://journals.sagepub.com/doi/10.1177/0022034509357716

122. Van Loon JP, De Bont LGM, Spijkervet FKL, Verkerke GJ, Liem RSB. A short-term study in sheep with the Groningen temporomandibular joint prosthesis. International Journal of Oral and Maxillofacial Surgery. Blackwell Munksgaard; 2000;29:315–24.

123. Huang HL, Su KC, Fuh LJ, Chen MYC, Wu J, Tsai MT, et al. Biomechanical analysis of a temporomandibular joint condylar prosthesis during various clenching tasks.

Journal of Cranio-Maxillofacial Surgery. Churchill Livingstone; 2015;43:1194–201.

124. Hsu JT, Lai KA, Chen Q, Zobitz ME, Huang HL, An KN, et al. The relation between micromotion and screw fixation in acetabular cup. Computer methods and programs in biomedicine [Internet]. Comput Methods Programs Biomed; 2006 [cited 2022 Aug 13];84:34–41. Available from: https://pubmed.ncbi.nlm.nih.gov/16971018/

125. Cornwall GB, Bryant JT, Hansson CM. The effect of kinematic conditions on the wear of ultra-high molecular weight polyethylene (UHMWPE) in orthopaedic bearing applications. Proceedings of the Institution of Mechanical Engineers Part H, Journal of engineering in medicine [Internet]. Proc Inst Mech Eng H; 2001 [cited 2022 Mar 20];215:95–106. Available from: https://pubmed.ncbi.nlm.nih.gov/11323990/

126. Fouad H. In vitro evaluation of Stiffness Graded artificial hip joint femur head in terms of joint stresses distributions and dimensions: Finite element study. Journal of Materials Science: Materials in Medicine. 2011;22:1589–98.

127. Xu X, Luo D, Guo C, Rong Q. A custom-made temporomandibular joint prosthesis for fabrication by selective laser melting: Finite element analysis. Medical Engineering and Physics. Elsevier Ltd; 2017;46:1–11.

128. Ruggiero A, D'Amato R, Gómez E, Merola M. Experimental comparison on tribological pairs UHMWPE/TIAL6V4 alloy, UHMWPE/AISI316L austenitic stainless and UHMWPE/AL2O3 ceramic, under dry and lubricated conditions. Tribology International. Elsevier; 2016;96:349–60.

129. Ruggiero A, D'amato R, Gómez E. Experimental analysis of tribological behavior of UHMWPE against AISI420C and against TiAl6V4 alloy under dry and lubricated conditions. 2015 [cited 2022 Feb 5]; Available from: http://dx.doi.org/10.1016/j.triboint.2015.06.005

130. Berni M, Lopomo N, Marchiori G, Gambardella A, Boi M, Bianchi M, et al. Tribological characterization of zirconia coatings deposited on Ti6Al4V components for orthopedic applications. Materials Science & Engineering C [Internet]. 2016 [cited 2022 Feb 2];62:643–55. Available from: http://dx.doi.org/10.1016/j.msec.2016.02.014

131. Huys SEF, Pastor-Alonso D, Theuns P, van Lenthe GH, Vander Sloten J, Mommaerts MY. A novel 3D-printed, patient-specific alloplastic temporomandibular joint replacement allowing enthesis reconstruction: A finite element analysis. Annals of 3D Printed Medicine. Elsevier BV; 2022;6:100058.

132. Ackland DC, Robinson D, Redhead M, Lee PVS, Moskaljuk A, Dimitroulis G. A personalized 3D-printed prosthetic joint replacement for the human temporomandibular joint: From implant design to implantation. Journal of the Mechanical Behavior of Biomedical Materials. Elsevier Ltd; 2017;69:404–11.

133. Ackland D, Robinson D, Lee PVS, Dimitroulis G. Design and clinical outcome of a novel 3D-printed prosthetic joint replacement for the human temporomandibular joint. Clinical Biomechanics. Elsevier; 2018;56:52–60.

134. Mesnard M, Ramos A. Towards a rigorous approach to designing a TemporoMandibular joint prosthesis. From clinical challenge to numerical prototype. Procedia CIRP. Elsevier B.V.; 2013. p. 141–6.

135. Mesnard M, Ramos A, Simões JA. Influences of implant condyle geometry on bone and screw strains in a temporomandibular implant. Journal of Cranio-Maxillofacial Surgery. Churchill Livingstone; 2014;42:194–200.

136. Bekcioglu B, Bulut E, Bas B. The Effects of Unilateral Alloplastic Temporomandibular Joint Replacement on the Opposite-Side Natural Joint: A Finite-Element Analysis. Journal of Oral and Maxillofacial Surgery [Internet]. W.B. Saunders; 2017 [cited 2022 Aug 14];75:2316–22. Available from: http://www.joms.org/article/S0278239117305463/fulltext

137. Voiner J, Yu J, Deitrich P, Chafin C, Giannakopoulos H. Analysis of mandibular motion following unilateral and bilateral alloplastic TMJ reconstruction. International Journal of Oral and Maxillofacial Surgery. Churchill Livingstone; 2011;40:569–71.

138. Mercuri LG. The use of alloplastic prostheses for temporomandibular joint reconstruction. Journal of Oral and Maxillofacial Surgery. W.B. Saunders; 2000;58:70–5.

139. Wyles CC, Paradise CR, Masters TL, Patel R, van Wijnen AJ, Abdel MP, et al. Cobalt and Chromium Ion Release in Metal-on-Polyethylene and Ceramic-on-Polyethylene THA: A Simulator Study With Cellular and Microbiological Correlations. Journal of Arthroplasty. Churchill Livingstone Inc.; 2019;

140. Sampaio M, Buciumeanu M, Henriques B, Silva FS, Souza JCM, Gomes JR. Tribocorrosion behavior of veneering biomedical PEEK to Ti6Al4V structures. Journal of the Mechanical Behavior of Biomedical Materials [Internet]. Elsevier Ltd; 2016 [cited 2021 Feb 21];54:123–30. Available from: https://linkinghub.elsevier.com/retrieve/

pii/S175161611500346X

141. Souza JCM, Correia MST, Oliveira MN, Silva FS, Henriques B, Novaes de Oliveira AP, et al. PEEK-matrix composites containing different content of natural silica fibers or particulate lithium-zirconium silicate glass fillers: Coefficient of friction and wear volume measurements. Biotribology. Elsevier Ltd; 2020;24.

142. Rostoker W, Galante JO. Contact pressure dependence of wear rates of ultra high molecular weight polyethylene. Journal of biomedical materials research [Internet]. J Biomed Mater Res; 1979 [cited 2022 Aug 14];13:957–64. Available from: https://pubmed.ncbi.nlm.nih.gov/511863/

143. Rose RM, Goldfarb H V., Ellis E, Crugnola AM. On the pressure dependence of the wear of ultrahigh molecular weight polyethylene. Wear. Elsevier; 1983;92:99–111.

144. Kato K. Classification of wear mechanisms/models. Proceedings of the Institution of Mechanical Engineers, Part J: Journal of Engineering Tribology. 2002;216:349–56.

145. Buciumeanu M, Bagheri A, Souza JCM, Silva FS, Henriques B. Tribocorrosion behavior of hot pressed CoCrMo alloys in artificial saliva. Tribology International. Elsevier Ltd; 2016;97:423–30.

146. Guezmil M, Bensalah W, Mezlini S. Tribological behavior of UHMWPE against TiAl6V4 and CoCr28Mo alloys under dry and lubricated conditions. Journal of the Mechanical Behavior of Biomedical Materials. Elsevier Ltd; 2016;63:375–85.

147. Mathew MT, Nagelli C, Pourzal R, Fischer A, Laurent MP, Jacobs JJ, et al. Tribolayer Formation in a Metal-on-Metal (MoM) Hip Joint: An Electrochemical Investigation. Journal of the mechanical behavior of biomedical materials [Internet]. NIH Public Access; 2014 [cited 2022 Feb 27];29:199–212. Available from: /pmc/articles/PMC3882021/

148. Souza JCM, Henriques M, Oliveira R, Teughels W, Celis J-P, Rocha L a. Do oral biofilms influence the wear and corrosion behavior of titanium? Biofouling. 2010;26:471–8.

149. Xu W, Yu F, Yang L, Zhang B, Hou B, Li Y. Accelerated corrosion of 316L stainless steel in simulated body fluids in the presence of H 2 O 2 and albumin. Materials science & engineering C, Materials for biological applications [Internet]. Mater Sci Eng C Mater Biol Appl; 2018 [cited 2022 Aug 17];92:11–9. Available from:

https://pubmed.ncbi.nlm.nih.gov/30184732/

150. Zhu W, Zhang R, Liu S, Tian J, Lv X, Yu F, et al. The effect of nanoparticles of cobalt–chromium on human aortic endothelial cells in vitro. Journal of Applied Toxicology. John Wiley and Sons Ltd; 2021;41:1966–79.

151. Mercuri LG, Urban RM, Hall DJ, Mathew MT. Adverse Local Tissue Responses to Failed Temporomandibular Joint Implants. Journal of Oral and Maxillofacial Surgery. W.B. Saunders; 2017;75:2076–84.

152. Fu S, Meng H, Freer F, Kwon J, Shelton JC, Knight MM. Sub-toxic levels of Co2+ are anti-inflammatory and protect cartilage from degradation caused by IL-1β. Clinical Biomechanics [Internet]. Elsevier Ltd; 2020 [cited 2021 Feb 14];79:104924. Available from: https://linkinghub.elsevier.com/retrieve/pii/S0268003319304139

153. Halwani DO, Anderson PG, Brott BC, Anayiotos AS, Lemons JE. The role of vascular calcification in inducing fatigue and fracture of coronary stents. Journal of biomedical materials research Part B, Applied biomaterials [Internet]. J Biomed Mater Res B Appl Biomater; 2012 [cited 2022 Aug 17];100:292–304. Available from: https://pubmed.ncbi.nlm.nih.gov/21953795/

154. Halwani DO, Anderson PG, Brott BC, Anayiotos AS, Lemons JE. Clinical device-related article surface characterization of explanted endovascular stents: evidence of in vivo corrosion. Journal of biomedical materials research Part B, Applied biomaterials [Internet]. J Biomed Mater Res B Appl Biomater; 2010 [cited 2022 Aug 17];95:225–38. Available from: https://pubmed.ncbi.nlm.nih.gov/20737558/

155. Mathew MT, Ariza E, Rocha LA, Vaz F, Fernandes AC, Stack MM. Tribocorrosion behaviour of TiCxOy thin films in bio-fluids. Electrochimica Acta. Pergamon; 2010;56:929–37.

156. Mathew MT, Jacobs JJ, Wimmer MA. Wear-corrosion synergism in a cocrmo hip bearing alloy is influenced by proteins. Clinical Orthopaedics and Related Research [Internet]. Springer New York LLC; 2012 [cited 2022 Aug 15];470:3109–17. Available from: https://journals.lww.com/clinorthop/Fulltext/2012/11000/Wear_Corrosion_Synergism_in_a_CoCrMo_Hip_Bearing.21.aspx

157. De Meurechy N, Aktan MK, Boeckmans B, Huys S, Verwilghen DR, Braem A, et al. Surface wear in a custom manufactured temporomandibular joint prosthesis. Journal

of biomedical materials research Part B, Applied biomaterials [Internet]. J Biomed Mater Res B Appl Biomater; 2022 [cited 2022 Jul 20];110:1425–38. Available from: https://pubmed.ncbi.nlm.nih.gov/35088936/

158. Zhang Y, Li J, Che S. Electropolishing mechanism of Ti-6Al-4V alloy fabricated by selective laser melting. International Journal of Electrochemical Science. 2018;13:4792–807.

159. Saravanan I, Perumal AE, Issac RF. Wear study of cross linked UHMWPE hybrid composite-TiN interface. Surfaces and Interfaces. Elsevier B.V.; 2016;4:42–50.

160. Łępicka M, Grądzka-Dahlke M, Zaborowska I, Górski G, Mosdorf R. Recurrence analysis of coefficient of friction oscillations in DLC-coated and non-coated Ti6Al4V titanium alloy. Tribology International. Elsevier; 2022;165:107342.

161. Silva A de M, Figueiredo VMG de, Prado RF do, Santanta-Melo G de F, Ankha M del VEA, de Vasconcellos LMR, et al. Diamond-like carbon films over reconstructive TMJ prosthetic materials: Effects in the cytotoxicity, chemical and mechanical properties. Journal of Oral Biology and Craniofacial Research. Elsevier B.V.; 2019;9:201–7.

162. Teeter MG, MacLean CJ, Somerville LE, Howard JL, McCalden RW, Lanting BA, et al. Wear performance of cobalt chromium, ceramic, and oxidized zirconium on highly crosslinked polyethylene at mid-term follow-up. Journal of orthopaedics [Internet]. Reed Elsevier India Pvt. Ltd.; 2018 [cited 2020 Mar 28];15:620–3. Available from: http://www.ncbi.nlm.nih.gov/pubmed/29881207

163. Gang S, Fengzhou F, Chengwei K. Tribological Performance of Bioimplants: A Comprehensive Review. Nanotechnology and Precision Engineering. No longer published by Elsevier; 2018;1:107–22.

164. Rothammer B, Neusser K, Marian M, Bartz M, Krauß S, Böhm T, et al. Amorphous Carbon Coatings for Total Knee Replacements-Part I: Deposition, Cytocompatibility, Chemical and Mechanical Properties. Polymers [Internet]. Polymers (Basel); 2021 [cited 2022 Jul 20];13. Available from: https://pubmed.ncbi.nlm.nih.gov/34208302/

165. Escudeiro A, Wimmer MA, Polcar T, Cavaleiro A. Tribological behavior of uncoated and DLC-coated CoCr and Ti-alloys in contact with UHMWPE and PEEK counterbodies. Tribology International. Elsevier Ltd; 2015;89:97–104.

166. Patil NA, Njuguna J, Kandasubramanian B. UHMWPE for biomedical applications:

Performance and functionalization. European Polymer Journal. Elsevier Ltd; 2020. p. 109529.

167. Lei P, Dai Z, Zhang YS, Liu H, Niu W, Li K, et al. Macrophage inhibits the osteogenesis of fibroblasts in ultrahigh molecular weight polyethylene (UHMWPE) wear particle-induced osteolysis. Journal of orthopaedic surgery and research. 2019;14:80.

168. McCalden RW, MacDonald SJ, Rorabeck CH, Bourne RB, Chess DG, Charron KD. Wear rate of highly cross-linked polyethylene in total hip arthroplasty. A randomized controlled trial. The Journal of bone and joint surgery American volume. United States; 2009;91:773–82.

169. Mercuri LG, Miloro M, Skipor AK, Bijukumar D, Sukotjo C, Mathew MT. Serum Metal Levels in Maxillofacial Reconstructive Surgery Patients: A Pilot Study. Journal of Oral and Maxillofacial Surgery. W.B. Saunders; 2018;76:2074–80.

170. Snyder MJ, Weber MA, Kromka JJ, Sims MM, Smith CN, Daji A V., et al. Predictors of Adverse Local Tissue Reaction in a High-Risk Population. Arthroplasty Today. Elsevier; 2022;13:125–9.

171. Levine BR, Hsu AR, Skipor AK, Hallab NJ, Paprosky WG, Galante JO, et al. Ten-year outcome of serum metal ion levels after primary total hip arthroplasty: a concise follow-up of a previous report*. The Journal of bone and joint surgery American volume [Internet]. J Bone Joint Surg Am; 2013 [cited 2022 Aug 16];95:512–8. Available from: https://pubmed.ncbi.nlm.nih.gov/23515985/

172. Noronha Oliveira M, Schunemann WVH, Mathew MT, Henriques B, Magini RS, Teughels W, et al. Can degradation products released from dental implants affect peri-implant tissues? Journal of Periodontal Research [Internet]. 2018 [cited 2020 Feb 6];53:1–11. Available from: http://doi.wiley.com/10.1111/jre.12479

173. Xu J, Yang J, Nyga A, Ehteramyan M, Moraga A, Wu Y, et al. Cobalt (II) ions and nanoparticles induce macrophage retention by ROS-mediated down-regulation of RhoA expression. Acta Biomaterialia. Acta Materialia Inc; 2018;72:434–46.

174. Reddy A, Caicedo MS, Samelko L, Jacobs JJ, Hallab NJ. Implant debris particle size affects serum protein adsorption which may contribute to particle size-based bioreactivity differences. Journal of long-term effects of medical implants [Internet]. 2014 [cited 2020 Feb 6];24:77–88. Available from: http://www.ncbi.nlm.nih.gov/pubmed/24941408

175. Bijukumar DR, Segu A, Souza JCM, Li XJ, Barba M, Mercuri LG, et al. Systemic and local toxicity of metal debris released from hip prostheses: A review of experimental approaches [Internet]. Nanomedicine: Nanotechnology, Biology, and Medicine. Elsevier Inc.; 2018 [cited 2021 Feb 17]. p. 951–63. Available from: https://linkinghub.elsevier.com/retrieve/pii/S1549963418300108

176. Apaza-Bedoya K, Bijukumar D, Benfatti CAM, Mathew MT, da Silva JSP, Souza JCM. Adverse local and systemic effect of nanoparticles released from oral and cranio-maxillofacial implants. Nanostructured Biomaterials for Cranio-Maxillofacial and Oral Applications. Elsevier Inc.; 2018. p. 63–79.

177. Wang A, Essner A, Stark C, Dumbleton JH. Comparison of the size and morphology of UHMWPE wear debris produced by a hip joint simulator under serum and water lubricated conditions. Biomaterials. Elsevier Science Ltd; 1996;17:865–71.

178. Savio JA, Overcamp LM, Black J. Size and shape of biomaterial wear debris. Clinical Materials. 1994;15:101–47.

179. Zhang D, Liu H, Wang J, Sheng C, Li Z. Wear Mechanism of Artificial Joint Failure Using Wear Debris Analysis. Journal of Nanoscience and Nanotechnology [Internet]. 2018 [cited 2022 Feb 1];18:6805–14. Available from: www.aspbs.com/jnn

180. Zaveri TD, Dolgova N V., Lewis JS, Hamaker K, Clare-Salzler MJ, Keselowsky BG. Macrophage integrins modulate response to ultra-high molecular weight polyethylene particles and direct particle-induced osteolysis. Biomaterials [Internet]. Biomaterials; 2017 [cited 2022 Jul 4];115:128–40. Available from: https://pubmed.ncbi.nlm.nih.gov/27889664/

181. Apaza-Bedoya K, Tarce M, Benfatti CAM, Henriques B, Mathew MT, Teughels W, et al. Synergistic interactions between corrosion and wear at titanium-based dental implant connections: A scoping review [Internet]. Journal of Periodontal Research. Blackwell Munksgaard; 2017 [cited 2021 Apr 27]. p. 946–54. Available from: https://pubmed.ncbi.nlm.nih.gov/28612506/

182. Pinto-Borges H, Carvalho O, Henriques B, Silva F, Ramos A, Souza JCM. A preliminary analysis of the wear pathways of sliding contacts on temporomandibular joint total joint replacement prostheses. Metals. 2021;11.

183. Liu A, Richards L, Bladen CL, Ingham E, Fisher J, Tipper JL. The biological response to nanometre-sized polymer particles. Acta biomaterialia. 2015;23:38–51.

184. Endo M, Tipper JL, Barton DC, Stone MH, Ingham E, Fisher J. Comparison of wear, wear debris and functional biological activity of moderately crosslinked and non-crosslinked polyethylenes in hip prostheses. Proceedings of the Institution of Mechanical Engineers, Part H: Journal of Engineering in Medicine. 2002;216:111–22.

185. Howling GI, Barnett PI, Tipper JL, Stone MH, Fisher J, Ingham E. Quantitative characterization of polyethylene debris isolated from periprosthetic tissue in early failure knee implants and early and late failure charnley hip implants. Journal of Biomedical Materials Research [Internet]. 2001 [cited 2021 Mar 30];58:415–20. Available from: http://doi.wiley.com/10.1002/jbm.1036

186. Messous R, Henriques B, Bousbaa H, Silva FS, Teughels W, Souza JCM. Cytotoxic effects of submicron- and nano-scale titanium debris released from dental implants: an integrative review. Clinical oral investigations. Germany; 2021;

187. Kaufman AM, Alabre CI, Rubash HE, Shanbhag AS. Human macrophage response to UHMWPE, TiAlV, CoCr, and alumina particles: Analysis of multiple cytokines using protein arrays. Journal of Biomedical Materials Research - Part A. J Biomed Mater Res A; 2008;84:464–74.

188. Ribeiro AR, Gemini-Piperni S, Travassos R, Lemgruber L, Silva RC, Rossi AL, et al. Trojan-Like Internalization of Anatase Titanium Dioxide Nanoparticles by Human Osteoblast Cells. Scientific Reports. Nature Publishing Group; 2016;6.

189. Royhman D, Radhakrishnan R, Yuan JC-C, Mathew MT, Mercuri LG, Sukotjo C. An electrochemical investigation of TMJ implant metal alloys in an artificial joint fluid environment: the influence of pH variation. Journal of cranio-maxillo-facial surgery : official publication of the European Association for Cranio-Maxillo-Facial Surgery [Internet]. Churchill Livingstone; 2014 [cited 2020 Mar 20];42:1052–61. Available from: http://www.ncbi.nlm.nih.gov/pubmed/24548869

190. Pourzal R, Catelas I, Theissmann R, Kaddick C, Fischer A. Characterization of wear particles generated from CoCrMo alloy under sliding wear conditions. Wear. 2011;271:1658–66.

191. Drynda A, Ren Q, Buchhorn GH, Lohmann CH. The induction of CXCR4 expression in human osteoblast-like cells (MG63) by CoCr particles is regulated by the PLC-DAG-PKC pathway. Journal of Biomedical Materials Research - Part B Applied Biomaterials. John Wiley and Sons Inc.; 2017;105:2326–32.

192. Posada OM, Gilmour D, Tate RJ, Grant MH. CoCr wear particles generated from CoCr alloy metal-on-metal hip replacements, and cobalt ions stimulate apoptosis and expression of general toxicology-related genes in monocyte-like U937 cells. Toxicology and Applied Pharmacology. Academic Press Inc.; 2014;281:125–35.

193. Pemmari A, Leppänen T, Paukkeri EL, Eskelinen A, Moilanen T, Moilanen E. Gene expression in adverse reaction to metal debris around metal-on-metal arthroplasty: An RNA-Seq-based study. Journal of Trace Elements in Medicine and Biology. Elsevier GmbH; 2018;48:149–56.

194. Roesems G, Hoet PHM, Dinsdale D, Demedts M, Nemery B. In Vitro Cytotoxicity of Various Forms of Cobalt for Rat Alveolar Macrophages and Type II Pneumocytes. Toxicology and Applied Pharmacology. Academic Press; 2000;162:2–9.

195. Catelas I, Petit A, Vali H, Fragiskatos C, Meilleur R, Zukor DJ, et al. Quantitative analysis of macrophage apoptosis vs. necrosis induced by cobalt and chromium ions in vitro. Biomaterials. 2005;26:2441—2453.

196. Langton DJ, Jameson SS, Joyce TJ, Gandhi JN, Sidaginamale R, Mereddy P, et al. Accelerating failure rate of the ASR total hip replacement. The Journal of bone and joint surgery British volume [Internet]. J Bone Joint Surg Br; 2011 [cited 2022 Aug 16];93:1011–6. Available from: https://pubmed.ncbi.nlm.nih.gov/21768621/

197. Langton DJ, Joyce TJ, Jameson SS, Lord J, Van Orsouw M, Holland JP, et al. Adverse reaction to metal debris following hip resurfacing: the influence of component type, orientation and volumetric wear. The Journal of bone and joint surgery British volume [Internet]. J Bone Joint Surg Br; 2011 [cited 2022 Aug 16];93:164–71. Available from: https://pubmed.ncbi.nlm.nih.gov/21282753/

198. Curtin JP, Wang M. Are clinical findings of systemic titanium dispersion following implantation explained by available in vitro evidence? An evidence-based analysis [Internet]. Journal of Biological Inorganic Chemistry. Springer Verlag; 2017 [cited 2022 Aug 16]. p. 799–806. Available from: https://link.springer.com/article/10.1007/s00775-017-1464-1

199. Jacobs JJ, Skipor AK, Patterson LM, Hallab NJ, Paprosky WG, Black J, et al. Metal release in patients who have had a primary total hip arthroplasty. A prospective, controlled, longitudinal study. The Journal of bone and joint surgery American volume [Internet]. J Bone Joint Surg Am; 1998 [cited 2022 Aug 16];80:1447–58. Available from:

https://pubmed.ncbi.nlm.nih.gov/9801213/

200. Shah KM, Dunning MJ, Gartland A, Wilkinson JM. Distinct Concentration-Dependent Molecular Pathways Regulate Bone Cell Responses to Cobalt and Chromium Exposure from Joint Replacement Prostheses. International journal of molecular sciences [Internet]. Int J Mol Sci; 2021 [cited 2022 Jul 20];22. Available from: https://pubmed.ncbi.nlm.nih.gov/34069294/

201. Gómez-Arnaiz S, Tate RJ, Grant MH. Cobalt Neurotoxicity: Transcriptional Effect of Elevated Cobalt Blood Levels in the Rodent Brain. Toxics [Internet]. Toxics; 2022 [cited 2022 Jul 20];10. Available from: https://pubmed.ncbi.nlm.nih.gov/35202246/

202. Urban RM, Jacobs JJ, Tomlinson MJ, Gavrilovic J, Black J, Peoc'h M. Dissemination of wear particles to the liver, spleen, and abdominal lymph nodes of patients with hip or knee replacement. The Journal of bone and joint surgery. 2000;82:457.

203. Jakobsen SS, Danscher G, Stoltenberg M, Larsen A, Bruun JM, Mygind T, et al. Cobalt-chromium-molybdenum alloy causes metal accumulation and metallothionein up-regulation in rat liver and kidney. Basic & clinical pharmacology & toxicology. England; 2007;101:441–6.

204. Souza JCM, Sordi MB, Kanazawa M, Ravindran S, Henriques B, Silva FS, et al. Nano-scale modification of titanium implant surfaces to enhance osseointegration. Acta Biomaterialia. Acta Materialia Inc; 2019. p. 112–31.

205. Tkachenko S, Datskevich O, Kulak L, Jacobson S, Engqvist H, Persson C. Wear and friction properties of experimental Ti-Si-Zr alloys for biomedical applications. Journal of the Mechanical Behavior of Biomedical Materials. Elsevier Ltd; 2014;39:61–72.

206. Mu J, Wang H, Qin B, Zhang Y, Chen L, Zeng C. Improved wear and corrosion resistance of biological compatible TiZrNb films on biomedical Ti6Al4V substrates by optimizing sputtering power. Surface and Coatings Technology. Elsevier B.V.; 2021;428.

207. Wu J, Tan X, An X, Zhang J, Guo Y, Liu J, et al. Development of biomedical Ti-Nb-Zr-Mn alloys with enhanced mechanical properties and corrosion resistance. Materials Today Communications. Elsevier Ltd; 2022;30.

208. O'Connor RC, Saleem S, Sidebottom AJ. Prospective outcome analysis of total replacement of the temporomandibular joint with the TMJ Concepts system in patients

with inflammatory arthritic diseases. British Journal of Oral and Maxillofacial Surgery. Churchill Livingstone; 2016;54:604–9.

209. Alvarez E, Vinciguerra J, Desjardins JD. The effect of a novel CoCr electropolishing technique on CoCr-UHMWPE bearing frictional performance for total joint replacements. Tribology International. Elsevier; 2012;47:204–11.

210. Geringer J, Macdonald DD. Friction/fretting-corrosion mechanisms: Current trends and outlooks for implants. Materials Letters. 2014;134:152–7.

211. Kim K, Geringer J, Pellier J, MacDonald DD. Fretting corrosion damage of total hip prosthesis: Friction coefficient and damage rate constant approach. Tribology International. 2013;60:10–8.

212. Yildiz F, Yetim AF, Alsaran A, Efeoglu I. Wear and corrosion behaviour of various surface treated medical grade titanium alloy in bio-simulated environment. Wear. 2009;267:695–701.

213. Cimpean A, Vasilescu E, Drob P, Cinca I, Vasilescu C, Anastasescu M, et al. Enhancement of the electrochemical behaviour and biological performance of Ti-25Ta-5Zr alloy by thermo-mechanical processing. Materials science & engineering C, Materials for biological applications. Netherlands; 2014;38:127–42.

214. Silva CS, Henriques B, Novaes OA, Silva FS, Gomes J, Souza JCM. Micro-scale abrasion and sliding wear of zirconium-lithium silicate glass-ceramic and polymer-infiltrated ceramic network used in dentistry. Wear. 2020;203214.

215. Sampaio M, Buciumeanu M, Askari E, Flores P, Souza JCMM, Gomes JR, et al. Effects of poly-ether-ether ketone (PEEK) veneer thickness on the reciprocating friction and wear behavior of PEEK/Ti6Al4V structures in artificial saliva. Wear. Elsevier; 2016;368–369:84–91.

216. Wang S, Liu Y, Zhang C, Liao Z, Liu W. The improvement of wettability, biotribological behavior and corrosion resistance of titanium alloy pretreated by thermal oxidation. Tribology International. Elsevier; 2014;79:174–82.

217. Alvarez-Vera M, Ortega JA, Ortega-Ramos IA, Hdz-García HM, Muñoz-Arroyo R, Díaz-Guillén JC, et al. Tribological and microstructural characterization of laser microtextured CoCr alloy tested against UHMWPE for biomedical applications. Wear. Elsevier Ltd; 2021;477.

218. Hussain O, Ahmad B, Saleem S. Analysis of tribological behavior of medical-grade UHMW polyethylene under dry and lubricated conditions with human body fluids using Taguchi and GRA techniques: https://doi.org/101177/0892705720941907 [Internet]. SAGE PublicationsSage UK: London, England; 2020 [cited 2022 Feb 6]; Available from: https://journals.sagepub.com/doi/abs/10.1177/0892705720941907

219. Prado AM, Pereira J, Henriques B, Benfatti CA, Magini RS, Lopez-Lopez J, et al. Biofilm Affecting the Mechanical Integrity of Implant-Abutment Joints. The International journal of prosthodontics. 2016;29:381–3.

220. Souza JCM, Henriques M, Oliveira R, Teughels W, Celis J-P, Rocha L a. Biofilms inducing ultra-low friction on titanium. Journal of dental research. 2010;89:1470–5.

221. Henry A, Inverso G, Granquist EJ. Revision temporomandibular joint arthroplasty for the treatment of acquired metal allergy and review of the literature. International Journal of Oral and Maxillofacial Surgery. Churchill Livingstone; 2020;49:356–60.

222. Halim T, Clarke IC, Burgett-Moreno MD, Donaldson TK, Savisaar C, Bowsher JG. A simulator study of adverse wear with metal and cement debris contamination in metal-on-metal hip bearings. Bone and Joint Research. British Editorial Society of Bone and Joint Surgery; 2015;4:29–37.

223. Wimmer MA, Sprecher C, Hauert R, Täger G, Fischer A. Tribochemical reaction on metal-on-metal hip joint bearings: A comparison between in-vitro and in-vivo results. Wear. Elsevier; 2003;255:1007–14.

224. Saikko V. Effect of contact pressure on wear and friction of ultra-high molecular weight polyethylene in multidirectional sliding. Proceedings of the Institution of Mechanical Engineers Part H, Journal of engineering in medicine [Internet]. Proc Inst Mech Eng H; 2006 [cited 2022 Feb 5];220:723–31. Available from: https://pubmed.ncbi.nlm.nih.gov/17117762/

225. Gruber EA, McCullough J, Sidebottom AJ. Medium-term outcomes and complications after total replacement of the temporomandibular joint. Prospective outcome analysis after 3 and 5 years. British Journal of Oral and Maxillofacial Surgery. Churchill Livingstone; 2015;53:412–5.

226. Saikko V. Effect of Lubricant Protein Concentration on the Wear of Ultra-High Molecular Weight Polyethylene Sliding Against a CoCr Counterface. Journal of Tribology [Internet]. American Society of Mechanical Engineers Digital Collection; 2003

[cited 2022 Jul 10];125:638–42. Available from: https://asmedigitalcollection.asme.org/tribology/article/125/3/638/463963/Effect-of-Lubricant-Protein-Concentration-on-the

227. Geringer J, Tatkiewicz W, Rouchouse G. Wear behavior of PAEK, poly(aryl-ether-ketone), under physiological conditions, outlooks for performing these materials in the field of hip prosthesis. Wear [Internet]. 2011 [cited 2022 Mar 13];271:2793–803. Available from: https://hal.archives-ouvertes.fr/hal-00620860

228. Saikko V. In vitro wear simulation on the RandomPOD wear testing system as a screening method for bearing materials intended for total knee arthroplasty. Journal of biomechanics [Internet]. J Biomech; 2014 [cited 2022 Mar 20];47:2774–8. Available from: https://pubmed.ncbi.nlm.nih.gov/24835561/

229. Xiong D, Yang Y, Deng Y. Bio-tribological properties of UHMWPE against surface modified titanium alloy. Surface and Coatings Technology. 2013;228.

230. Sonnenburg I, Sonnenburg M. Total condylar prosthesisfor alloplastic jaw articulation replacement. Journal of Maxillofacial Surgery. 1985;13:131–5.

231. Ramos AM, Mesnard M. The stock alloplastic temporomandibular joint implant can influence the behavior of the opposite native joint: A numerical study. Journal of Cranio-Maxillofacial Surgery. Churchill Livingstone; 2015;43:1384–91.